SPATIAL ESTIMATION OF FUTURE TEMPERATURE CHANGES OVER AFRICA

BY

WISEMAN SINOTHI MKHONZA

B.A.(Hons)(UZ), STD

A dissertation submitted to the Faculty of Arts in fulfilment of the requirements for the degree of **Master of Arts (M.A.)** in the Department of Geographical and Environmental Sciences at the University of Zululand.

Supervisor	: Prof B. E. Kelbe (Hydrology Department)
Administrative Supervisor	: Prof L. M. Magi (Geographical and Environmental Science Department)
Date submitted	: January 1995

APPROVED:

Prof B.E. Kelbe

(Supervisor)

Prof L.M. Magi

(Administrative Supervisor)

Prof P. van Rensburg

(External examiner)

DECLARATION

I, **Wiseman Sinothi Mkhonza**, hereby declare that the dissertation "***Spatial Estimation of Future Temperature Changes over Africa***" is my own original work, both in conception and execution, unless stated or indicated to the contrary in the text; that the opinions expressed and conclusions reached are not to be regarded as reflecting the views of persons, institutions and/or organisations reflected in the acknowledgement; and that this study is not submitted concurrently for any other degree.

Signed: _____

W.S. Mkhonza

Date: 31 / 01 / 1995

This work is dedicated to my mother Thobekile and my daughter Thandeka.

TABLE OF CONTENTS

CHAPTER 4: ANALYSIS OF TEMPERATURE DATA SERIES

CHAPTER 5: CLIMATIC TEMPERATURE CHANGES FOR DIFFERENT REGIONS IN AFRICA: AN OBSERVATIONAL ANALYSIS

CHAPTER 6: METEOROLOGICAL IMPLICATIONS OF RESULTS

LIST OF FIGURES

LIST OF TABLES

SUMMARY

Climate has been changing since time immemorial. However, these long-term changes are very important because of some of the consequences to mankind. Because the changes are small ones in relation to daily experiences, many people find it difficult to perceive and accept these changes. This might cause doubts in the minds of many people in the proclaimed global warming which now occupies numerous agenda of institutions and organisations concerned with the future planning and management of our planet. The first chapters of this thesis review the theories of climate change and attempts to determine temperature change predictions specifically for Africa.

This study neither proclaims nor disclaims this notion of global warming. Instead, it restricts itself to estimating the spatio-temporal patterns of temperature changes for Africa from an observational perspective. Analysis of recognised records of annual surface air temperature for numerous weather stations in Africa were obtained and used to derive models of the station temperature changes over the past four decades. These models were used to predict temperature changes up to the year 2000.

The individual station predictions were used to derive spatial estimates of temperature change using the IDRISI - Geographic Information Systems (GIS) provided by the Clarke University through the International Geosphere-Biosphere Program (IGBP): Global Change Database Project (GCDP): Pilot Project for Africa. The spatial extent of temperature changes was derived using Theissen polygon approximation.

The derived models of climatic temperature change for various stations indicated that 58% of the African main land will not experience temperature change greater than half of a degree(-0.45° to 0.45°C) by the year 2000. There was an even spread (52% and 48%) of the stations showing decreasing and increasing temperature trends, respectively. However, 30% of all the stations showed large

increasing (0.46° to 2.45°C) temperatures, while fewer stations (12%) showed decreasing (-3.02° to -0.46°C) temperatures.

The spatial pattern of temperature changes were derived and an attempt was made to compare features of the climate with specific patterns of temperature change. The North-west and Zaire Air Boundaries, which are zones of moisture discontinuity during the month of July, were compared to regional patterns of increasing temperature trends.

Attempts to relate predicted temperature changes with rainfall and monthly temperatures showed no significant correlation.

Stations with short records and large cyclic variability tend to produce unstable models and the implications of these trends were discussed.

OPSOMMING

Klimaatsveranderinge vind sedert die vroegste tye op 'n gereelde basis plaas. Hierdie langtermyn veranderinge is egter baie belangrik aangesien dit vir die mensdom sekere implikasies inhou. Aangesien die veranderinge oor die kort termyn baie klein is, is mens nie altyd van hierdie veranderinge bewus nie. Die persepsie dat die wêreld warmer word, soos beweer deur 'n hele aantal instansies wat besorg is oor die toekomstige bestuur en beplanning van omgewingsbeheer, word nie ook nie deur almal geglo nie. Die eerste hoofstukke in hierdie tesis gee 'n teorioorsig oor klimaatsveranderinge en vorige navorsing wat gedoen is oor die bepaling van temperatuursveranderinge met spesifieke verwysing na Afrika.

Hierdie studie probeer egter nie bewyse vind vir wêreldwye verwarming of afkoeling nie, maar beperk tot empiriese ruimtelike en temporale temperatuursveranderinge oor Afrika. Analises van jaarlikse oppervlakte temperature by 'n groot aantal weerstasies in Afrika is gebruik om modelle te ontwikkel om die veranderinge in temperatuur oor vier dekades te beskryf. Hierdie modelle is ook gebruik om die veranderinge tot die jaar 2000 te voorspel.

Ruimtelke estimasies van temperatuursveranderinge is gedoen met behulp van IDRISI (Geografiese Inligting Stelsel verskaf deur die Clarke Universiteit vir die Internasionale Geo- en Biosferiese databasis projek oor wêreldwye klimaatsveranderinge met 'n loodsprogram vir Afrika) soos aangedui deur die modelvoorspellings vir individuele stasies. Thiessenpoligoon benaderings is gebruik om hierdie ruimtelike temperatuursveranderinge te bereken.

Die modelle wat afgelei is om die temperatuursveranderinge vir verskillende stasies aan te dui, het getoon dat 58% van die Afrika kontinent geen temperatuursverandering meer as 'n halwe graad (-0.45 tot 0.45°C) tot die jaar 2000 sal ondervind nie. 'n Groot toename in temperatuur (0.46 tot 2.45°C) is deur 30% van die stasies aangetoon, terwyl 'n kleiner persentasie (12%) gewys het op 'n verlaging (-3.02 tot 0.46°C) in temperatuur.

'n Poging is aangewend om die die verskillende klimaatskenmerke met ruimtelike patrone, soos aangedui deur die temperatuursveranderinge, te vergelyk. Regionale patrone wat op 'n verhoging in temperatuur dui is met die Noordwestelike en Zaïriese laagdrukzones vergelyk wat gedurende Julie plaasvind en 'n atmosferiese vog diskontinuiteitszone veroorsaak.

Pogings om voorspelde temperatuursveranderinge met reënval en maandelikse temperature te vergelyk het geen beduidende korrelasie opgelewer nie.

Die implikasie van onstabiele modelle wat veroorsaak is deur stasies met data wat oor kort periodes geneem is en dui op groot sikliese temperatuurswisselinge, is ook bespreek.

ACKNOWLEDGMENTS

A scientific study of this nature is an undertaking few students can easily accomplish without the joint effort and cooperation of a number of people and organisation. Henceforth, I wish to express my indebtedness and sincere gratitude to the following persons and institutions:

* My supervisor, Prof B.E. Kelbe, the Head of Department of Hydrology at the University of Zululand, who contributed considerably through his fatherly attitude towards and overwhelming concern about my accomplishing this study.

* Other Hydrology Department staff members: Mr Anton P. Verwey and Mrs Nina Snyman.

* The International Geosphere-Biosphere Program (IGBP), who in collaboration with the World Data Center-A (WDC-A) for Solid Earth Geophysics, supplied their Global Change Data Base.

* Clarke University for freely distributing their IDRISI GIS programme.

* My family and friends for their support, and finally,

* My external examiner, Prof Piet van Rensburg of the Department of Geography of the Rand Afrikaans University (RAU), for his constructive criticisms which improved this thesis.

CHAPTER 1

INTRODUCTION

1.1. INTRODUCTION

The scientific community is in a dilemma about the extent and cause of global climatic change. Centuries ago, the world experienced freezing conditions during the mini-ice age and now is concerned about an approaching warming catastrophe (Abrahamson, 1989). The claims (scientific or otherwise) of global climatic change, particularly the increase in temperature, have been attributed by many scientists (Leggett, 1990; Abrahamson, 1989; Boyle and Ardill, 1989; Houghton and Jenkins, 1990; and Laurmann, 1989) to be a consequence of anthropogenic effects. These claims have been heeded by some policy makers who have banned the use of certain substances (such as hydrofluorocarbons in aerosols) in their countries (Timberlake, 1989). These decisions to ban substances have had enormous economic consequences which emphasize the importance some countries have shown for these claims of climatic change.

Despite the scientific evidence accumulating, there are numerous uncertainties about climatic temperature changes throughout the world. One of these uncertainties relates to the spatial extent of climatic temperature changes at continental and regional scales.

1.2. BACKGROUND OF THE PROBLEM

Claims of global warming have been ascribed to the changing atmospheric concentrations of chlorofluorocarbons (CFCs), tropospheric ozone (O_3) and particularly the greenhouse gases (GHGs) comprising carbon dioxide (CO_2), methane (CH_4), and nitrous oxide (NO_2). Henderson-Sellers and McGuffie (1987), Singer (1989), Abrahamson (1989), and Bach, *et.al* (1983) have all

suggested that global temperatures will increase by 1.5° to 4.5°C (0.25° to 0.75°C/decade) due to the doubling in the CO_2 concentrations in the atmosphere by the middle of the 21st century.

The extent to which this postulated global warming is valid and real at regional and continental scales is a matter of great concern. Results of work presented at the Villach (Austria) Conference in 1985 and Toronto (Canada) Conference in 1988 by Abrahamson (1989), indicated varying degrees of temperature change for different climatic regions of the world. Claims were made that semi-arid and tropical regional temperatures are expected to increase by 0.35°C by the year 2050 (0.06°C/decade) while the high latitude areas of the globe may experience 0.8° to 5°C (0.13° to 0.8°C/decade) changes in temperature by the middle of the next century. Since the bulk of Africa is between the tropics, this claim would imply that this continent could be expected to have an increase in temperatures of about 0.35°C (0.06°C/decade) by the year 2050.

Global warming can have disastrous consequences for numerous aspects of the environment. It has been claimed that it will threaten global security (Gleik, 1989), disrupt the world economy (Weiss, 1989), and disturb the natural environment (Oppenheimer, 1989) through features such as rising sea levels, altered precipitation patterns and changed frequencies of climatic extremes induced by the "heat trap" effects of GHGs. Depletion of the ozone layer and long-range transport of toxic chemicals and acidifying substances (Abrahamson, 1989) are also considered to have an effect on the natural environment. These changes, in return, have been postulated (Abrahamson, 1989 and Gleik, 1989) to imperil human health, diminish global food sources through increased soil erosion and to cause greater uncertainties in agricultural food production, (particularly for many of the more vulnerable regions). They are also expected to change the distribution and seasonal availability of fresh water resources, increase political instability (particularly the potential for international conflict), accelerate the extinction of animals and plant species upon which human survival depends, and lastly, alter productivity as well as biological activity of natural and managed

ecosystems (Woodwell, 1989).

Boyle and Ardill (1989), Gliek (1989) and Abrahamson (1989) warn that unless action is taken now by the countries of the world, these problems will become progressively more serious, more difficult to reverse and more costly to address. Hence, there was a call by the Toronto Conference of 1988 (Abrahamson, 1989) for governments, international bodies, industries, educational institutions, non-government organisations and individual to take urgent action to counter the ongoing degradation of the atmosphere which is leading to global warming. These claims are supported by calls to devote research to understand how climatic changes, on a regional scale, are related to an overall global change of climate and to develop and support cooperative projects to allow developing nations to participate in the international mitigation, monitoring, research and analyses efforts which are related to the changing atmosphere (Abrahamson, 1989).

1.3. PURPOSE OF THE STUDY

The main objectives of this study were:

1. to assess climate temperature changes that have occurred in Africa during the recent historical period,

2. to model trends in temperatures which can be used to project the temperatures of the near future for the different regions of Africa, and

3. to create maps that will show near future temperature changes for different regions of Africa.

1.4. DELIMITATIONS AND RESEARCH STRATEGIES

This study focused on the spatial estimation of climatic temperature changes for Africa, through the use of the IDRISI Geographical Information Systems (GIS).The approach was to classify Africa into identifiable regions with distinct climates. The spatial extent of each climatic zone was identified and the climatic trends, particularly those associated with temperature change within each zone, were determined from an extensive survey of the literature and historical climatic data. Where there has been no identified investigations for or within a specific region in Africa, it was necessary to identify similar climatic zones in other parts of the world where climatic trends have been identified. These trends were then extrapolated from these climatic regions to the related zone in Africa.

Temperature trends were also determined from available climatic data. The spatial temperature fields of Africa for 1989 were provided, by the World Data Centre-A (WDC-A), for Solid Earth Geophysics operated by the National Oceanic and Atmospheric Administration (NOAA), USA, in collaboration with the International Geosphere-Biosphere Program (IGBP), as part of the Global Change Database Project (GCDP): Pilot Project for Africa who also provided the IDRISI Geographic Information System (GIS) as developed by the Graduate School of Geography of Clark University. Historical surface air temperature data for numerous weather stations in Africa were obtained from the University of East Anglia (World Climate Disc, 1990). The study used this data to investigate the spatial extend and magnitude of any linear or cyclic trends in the temperature fields for Africa for the period of historical record. Identified temperature trends were examined as suitable models for application to extrapolate the temperature fields into the immediate future (year 2000).

CHAPTER 2

THE PHYSICAL BACKGROUND

2.1. INTRODUCTION

The total area of the African continent is approximately 30 million km^2 and comprises approximately twenty percent of the earth's land surface (Pritchard, 1982; Griffiths, 1972; and Lewis and Berry, 1988). Seventy five percent of this continent lies between the Tropics of Cancer and Capricon under a tropical climate. The rest of the continent lies in the mid-latitudes and has extra-tropical climates. This relative location of the continent has a dominant influence on the spatial temperature patterns. The variations in spatial temperature patterns are also influenced by altitude, relief, coastal alignment, and ocean currents. The purpose of this chapter is to define the spatial extent of regional classification of the African climates as each region may experience different climatic trends.

2.2. SIZE AND LOCATION OF AFRICA

Africa constitutes the second largest landmass on this planet after Euratia (Europe and Asia) (Figure 2.1 and 2.2). This huge area stretches approximately 8 000 km from north to south and 7 200 km from east from west. The most northerly and southerly latitudes are 34°51'N (west of Cape Blanc in Tunisia) and 35°15'S (Cape Agulhas, South Africa), respectively. The greatest length from east to west goes from 51°25'E (Ras Hafun) to 17°32'W (Cape Verde).

2.3. RELIEF OF AFRICA

The African continental physiography is characterised by a plateau, higher in the east and south, and lower in the west and north (Figure 2.3). The high plateaux regions include the Ethiopian highlands, East African Highlands, and the Drakensberg Mountains. The highest peak along the eastern plateaux is Mt

reaches an elevation of about 3 350 m. The high elevations in the western and northern parts of the continent includes the Atlas, the Ahaggar and the Tibesti Mountains.

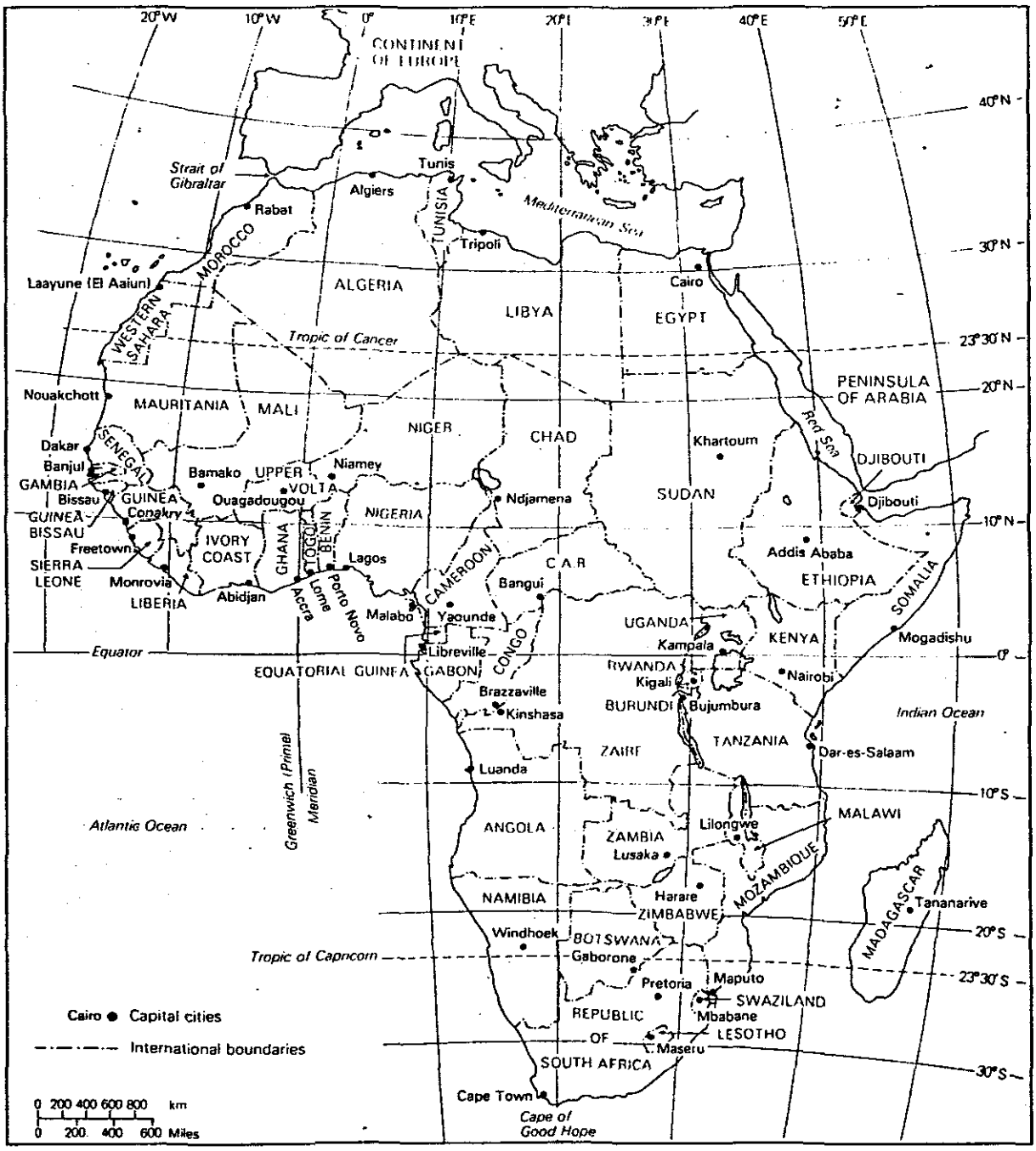

Figure 2.1: Position and size of Africa. (from Senior and Okunrotifa, 1983)

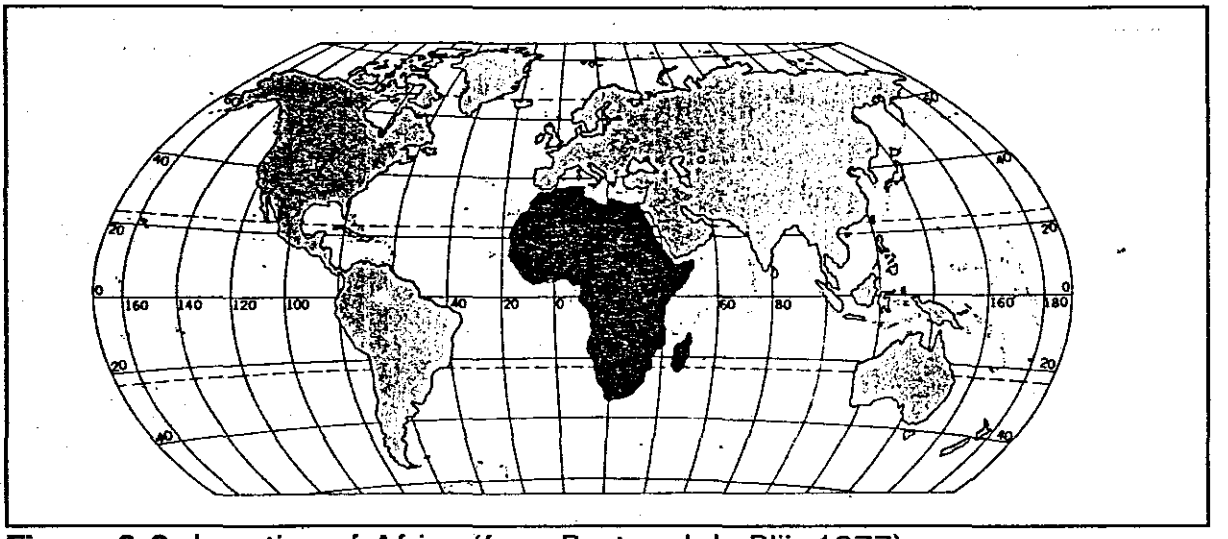

Figure 2.2: Location of Africa (from Best and de Blij, 1977)

One of the most striking features of Africa's physiography is a number of broad, shallow, saucer-like basins separated by plateau level drainage divides (Figure 2.4). The most prominent of these are Zaïre, Kalahari, Sudan, Chad, and El Djouf basins. The smaller ones include Senegal, Gabes, Libya, and Victoria.

Another spectacular relief feature of Africa is the Great Rift Valley System (Figure 2.5). This system extends over 9 600 km from Ethiopia to South Africa. It begins near Beira (Zimbabwe Highlands) and extends northwards through Lake Malawi, dividing itself into eastern and western segments through East Africa, and extending through the heart of Ethiopia and the Red Sea. Associated with the Great Rift Valley System are the lakes of East Africa which include Lake Malawi, Lake Tanganyika, Lake Victoria, and several other small ones (Figure 2.5).

2.4. CLIMATE OF AFRICA

2.4.1. TEMPERATURE

Seventy five percent of Africa lies within the tropics. Consequently one may associate this continent with high tropical temperatures and humidities. Temperature is a measure of energy storage. If climatic temperature change is significant in a region, it may also be observable in

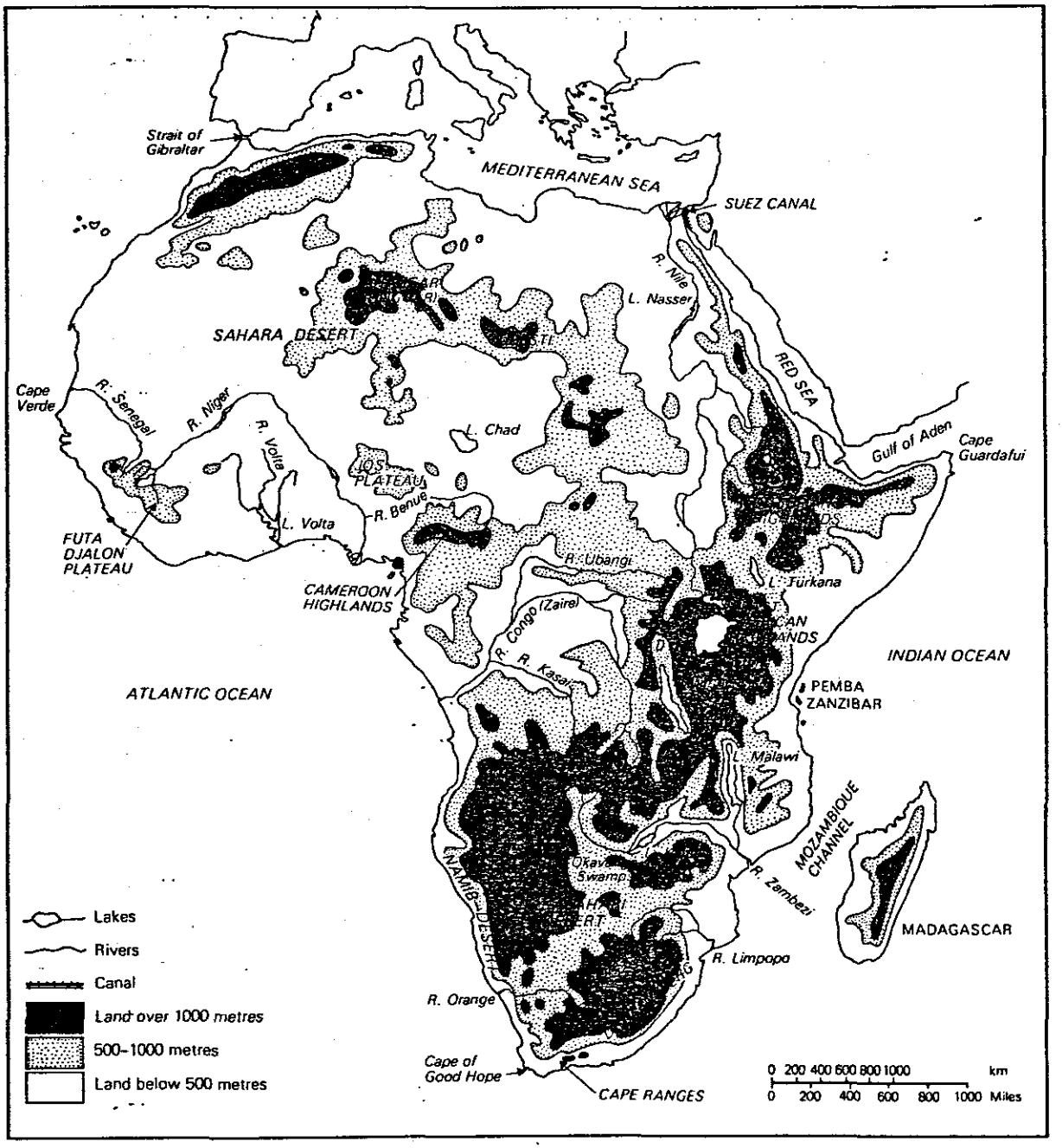

Figure 2.3: Africa - relief and drainage (from Senior and Okunrotifa, 1983)

other meteorological factors which are also affected by the energy changes (e.g. rainfall).

Legates and Wilmott (1989) have compiled average monthly air temperature maps for Africa from multiple sources. These were

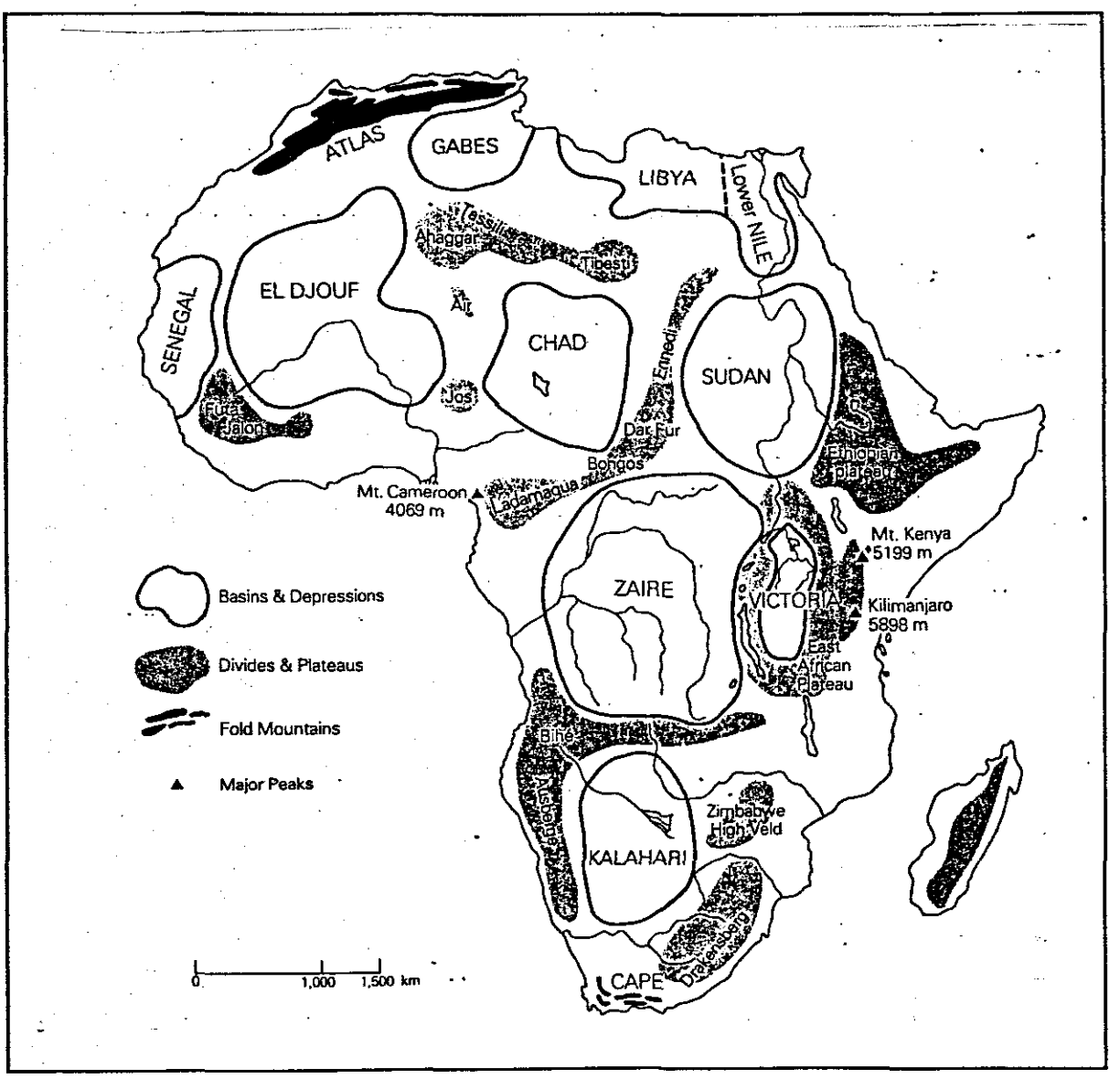

Figure 2.4: Africa - structural basins and their divides (from Pitchard, 1982)

obtained through the Global Change Database Project: Pilot Project for Africa as rasterised images for the IDRISI GIS. The mean January (southern hemisphere summer) and mean July (northern hemisphere summer) temperatures (at 0.6° grid resolution) are shown in Figures 2.6 and 2.7. These temperature patterns show relationship with the seasonal general circulation. The increase in temperatures occurring in the southern hemisphere during the summer months are reversed during the winter months. This scenario is reversed in the northern

hemisphere.

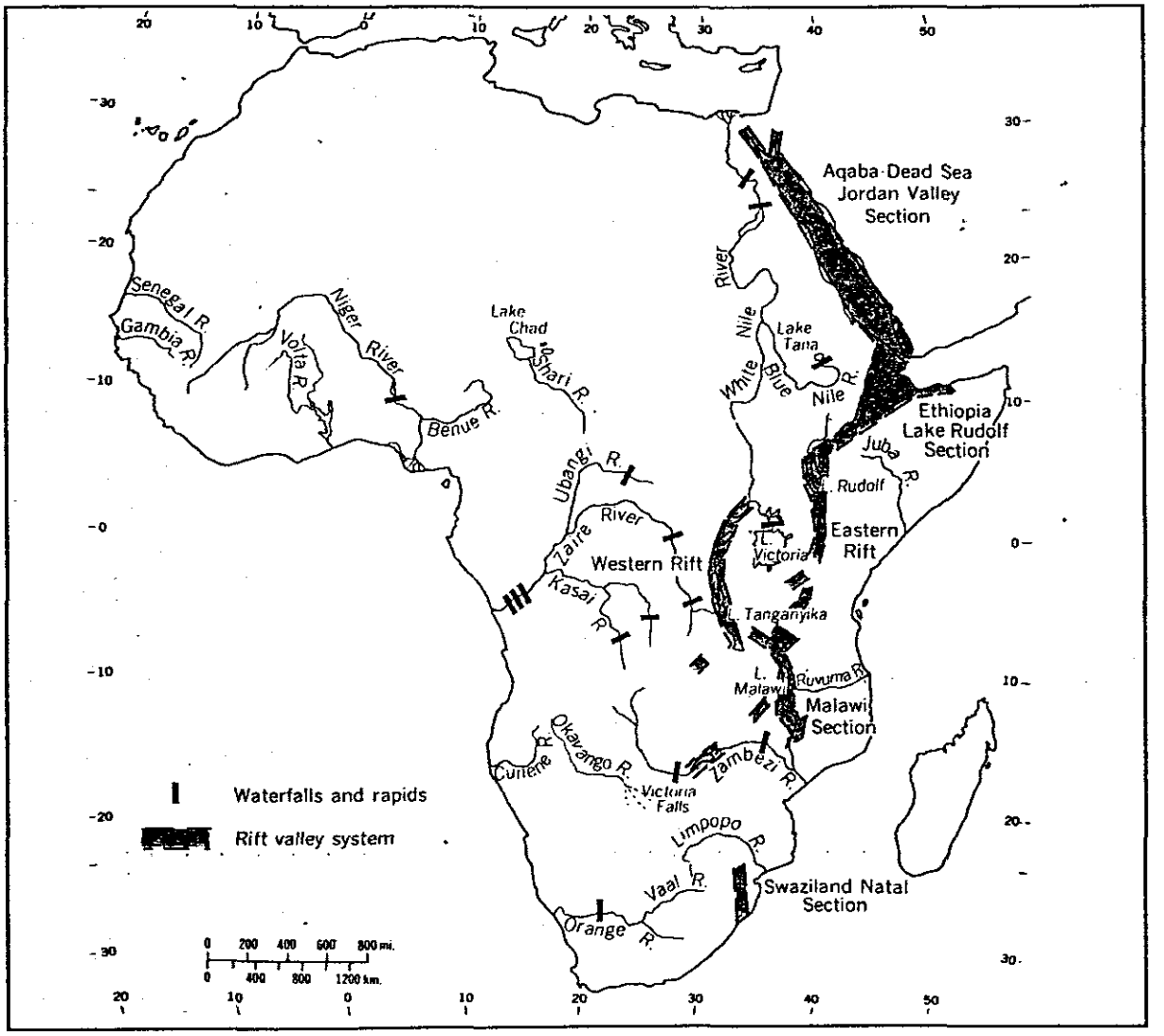

Figure 2.5: Rift valleys and rivers (from Best and de Blij, 1977)

2.4.2. RAINFALL

The mean annual rainfall (MAR) distribution for Africa is shown in Figure 2.8. The mean annual rainfall is highest in the Equatorial region from the East African and Ethiopian Highlands through Zaïre and along the Southern coast of West Africa. The lowest MARs are experienced in the Kalahari and Sahara deserts and parts of Somalia and Ethiopia. These patterns are a direct consequence of the global circulation patterns,

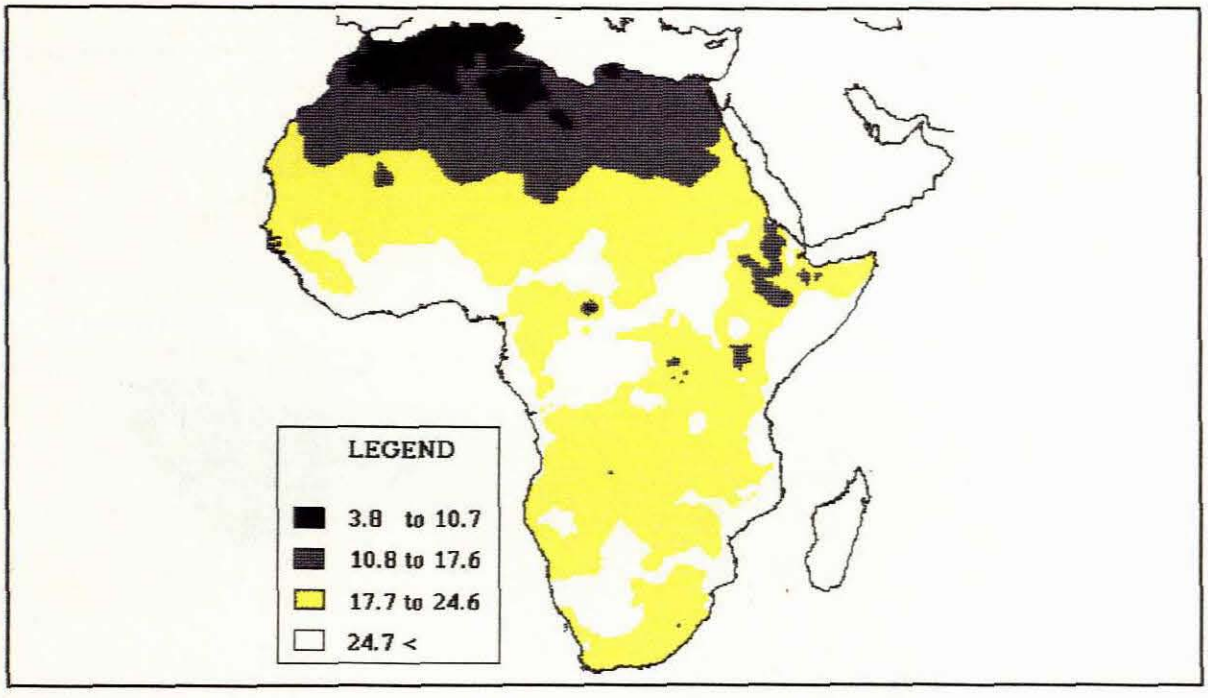

Figure 2.6: January mean daily surface air temperatures (°C) (from Legates and Willmott, 1989)

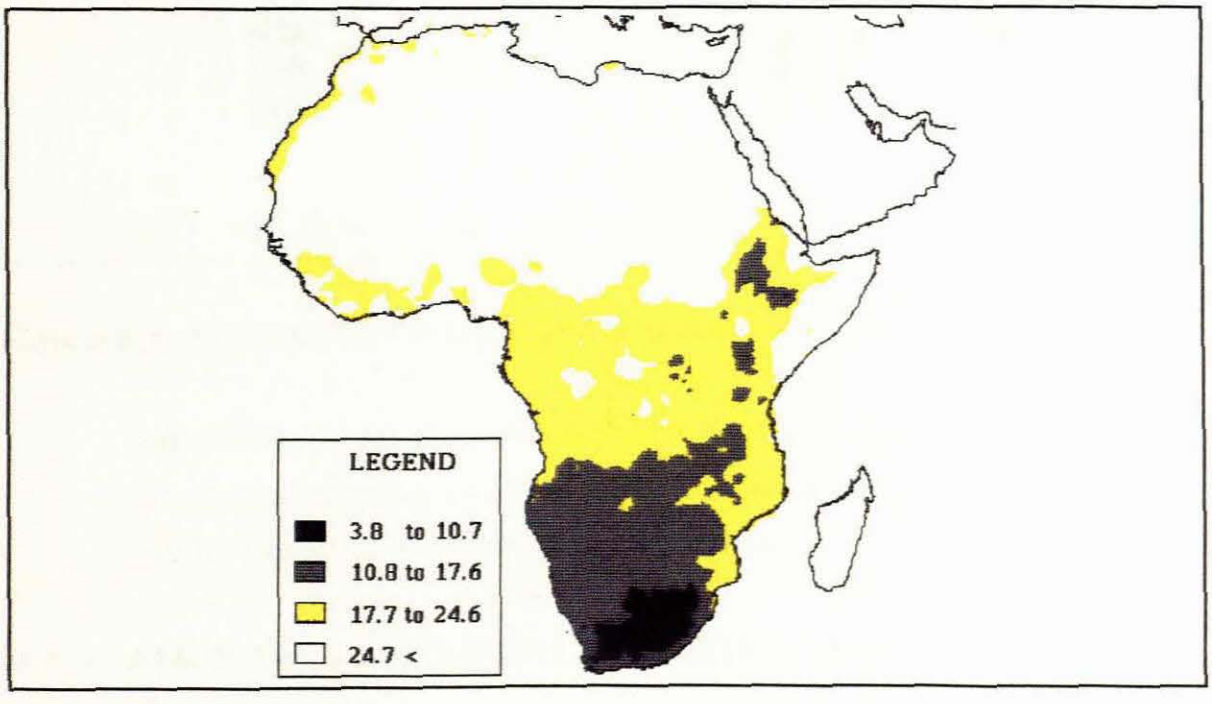

Figure 2.7: July mean daily surface air temperatures (°C) for Africa (from Legates and Willmott, 1989)

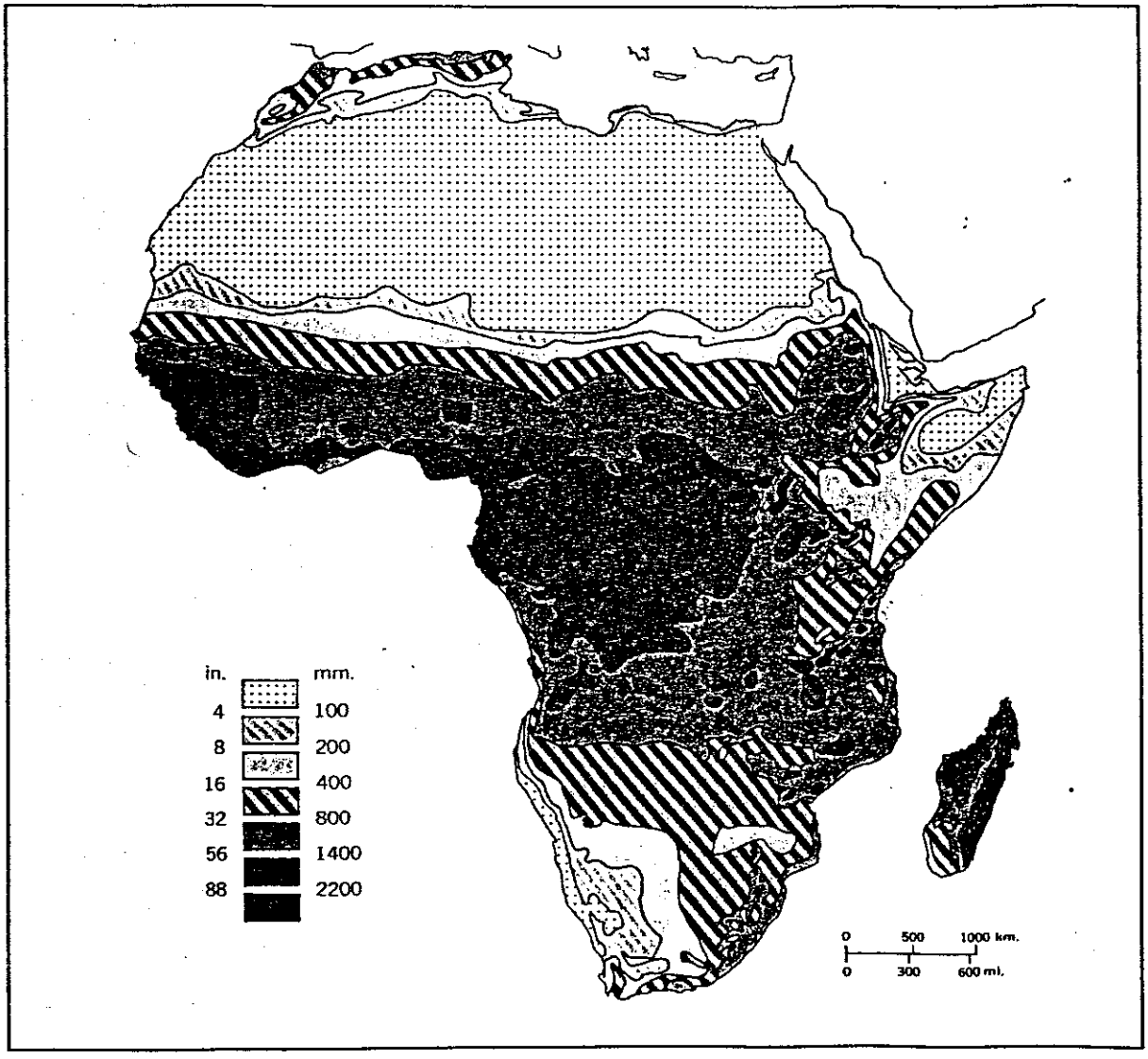

Figure 2.8: Mean annual rainfall over Africa (from Best and de Blij, 1977)

particularly those associated with the Hadley Circulation. Consequently, changes in the global circulation which influence temperature changes may also be expected to influence rainfall trends.

2.4.3. ATMOSPHERIC PRESSURE, AIR MASSES, AND FRONTS

The basic rainfall and temperature patterns of Africa are a result of the solar radiation distribution and the resultant quasi-stationary atmospheric

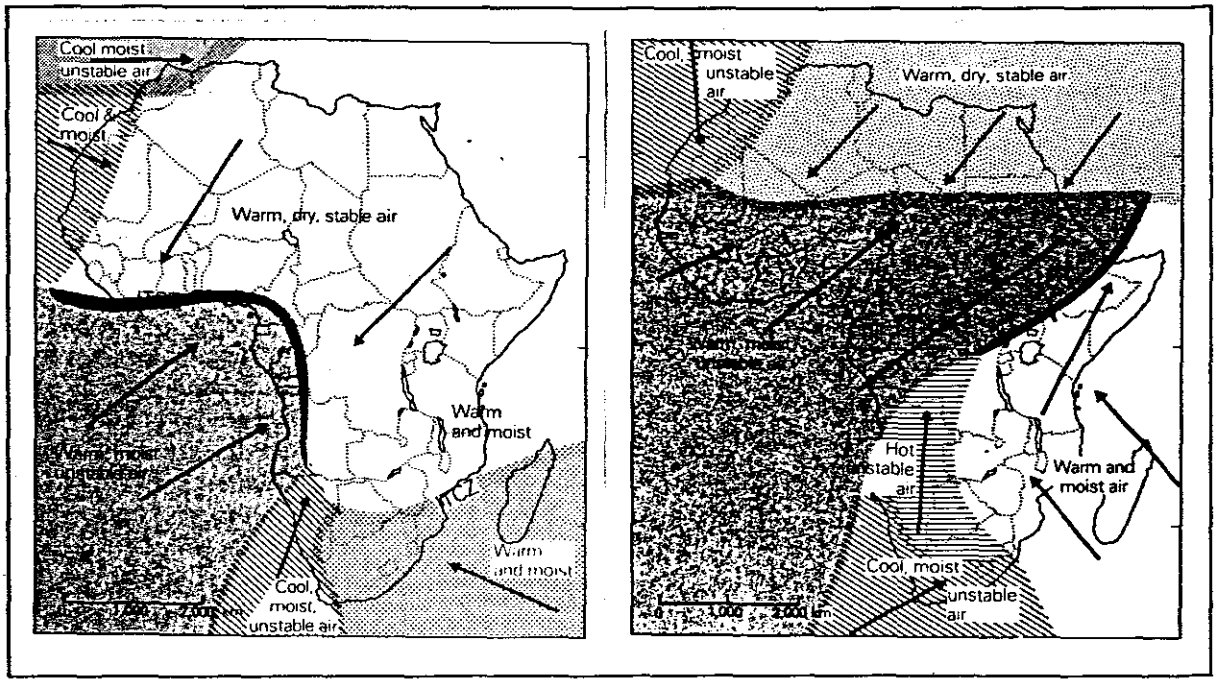

Figure 2.9: Air mass movements and position of air mass fronts during January (left) and July (right) (from Pitchard, 1982).

pressure systems which produce characteristic wind patterns and air masses (Pitchard, 1982) (Figure 2.9). From November to April (southern hemisphere summer), the insolation intensity over southern Africa causes a southward shift of the equatorial low pressure belt and the southern hemisphere sub-tropical anticyclones. During this period North Africa is dominated by high pressure systems except for the Mediterranean region. In July, the circulation pattern shifts north so that the low pressure trough extends along the west coast of Africa into the southern Sahara and across into Arabia. The high pressure generally extends across southern Africa and adjacent oceans during this period.

2.5. CLIMATIC CLASSIFICATIONS

Climatic classification is a geographic technique which simplifies and generalises the spatial distribution and characteristic patterns of climatic variables over the earth's surface. Some classifications are based on the fundamental physical causes

of climate, which involve atmospheric variables that are not easily measured, such as global or continental air mass properties, atmospheric pressure patterns, air masses and frontal zones (World Meteorological Organisation, 1983). Other classifications are based on biophysical criteria such as temperature, precipitation, evapo-transpiration, soil moisture, and vegetation (World Meteorological Organisation, 1983). Examples of these biophysical classifications are Köppen's, Thornthwaite's, Trewartha's and others. A brief description of these classification systems is provided below because they are used in evaluating temperature trends for a possible causes and effect relationship.

2.5.1. KÖPPEN'S CLIMATIC CLASSIFICATION

Köppen's objective classification scheme was to analyse readily measurable meteorological elements (monthly and annual means of temperature and precipitation) which influence the growth of vegetation. This scheme has been used to delineate areas of the globe according to the seasonal variation and numerical values which these elements displayed. In other words, Köppen intended to show that definite climatic values could be assigned to the boundaries between the natural vegetation regions (WMO. No.100, 1987 and Money, 1988). Six major climatic types designated by letters A to E and H, are used to distinguished his temperature classification (Table 2.1) and a second lower case letter is used to describe the rainfall distribution. For example, in the 'A' climatic region, 'f' indicates that no month has a mean rainfall of less than 60mm.

Köppen's classification was criticised because it did not consider the causes of the climate described, nor of the relation between the location of the climatic region and those of air mass source regions or of other likely influences (Money, 1988 and McBoyle, 1973). Some critics of this system, developed alternative classification systems that attempted to improve the empiricism of Köppen's methods. Amongst these were Thornthwaite and Trewartha (Money, 1988).

Major Type	First Order Sub-divisions	Second Order Sub-divisions
A. (Tropical, rainy)	Af (wet at all seasons) Aw (dry winters) As (dry summers—rare) Am (monsoon type)	Axi (isothermal)
B. (Dry)	BS (steppe) BW (desert)	Bxh (hot) Bxk (cool)
C. (Warm, temperate, rainy)	Cf (wet at all seasons) Cs (dry summers) Cw (dry winters) Csf (rather dry summer, very wet winter)	Cxa (summers long and warm) Cxb (summers long and cool) Cxc (summers short and cool)
D. (Cold snow-forest)	Df (wet at all seasons) Ds (dry summers) Dw (dry winters)	Dxa (summers long and warm) Dxb (summers long and cool) Dxc (summers short and cool) Dxd (ditto, but great winter cold)
E. (Snow climate)	ET (tundra) ES (permanent snowfields)	—
H. (Mountain climates)	—	—

Table 2.1: The climates in Koppen's classification (from Boyle, 1973)

2.5.2. THORNTHWAITE'S CLASSIFICATION

According to Money (1988), Thornthwaite objected to Koppen's use of temperature to define major climatic types, and pointed out that changes in temperature regime do not lead to abrupt boundaries of soil or vegetation. In his improvement of the Koppen's classification, Thornthwaite added moisture index and potential evapotranspiration, on top of precipitation and temperature, as measures of climatic classification. The fundamental idea behind Thornthwaite's classification methods was that of climatic efficiency, i.e. the capacity of the climate to support the growth of plant communities. The factors that govern the growth are moisture, precipitation and thermal indexes as well as potential evapotranspiration and these were used to define the climatic types.

Precipitation effectiveness, vegetation characteristics, and thermal efficiency formed the basis of Thornthwaite's classification (Table 2.2).

Table 2.2: Humidity provinces in Trewartha's classification (from Money, 1988)

Humidity Province		Vegetation	P/E Index
A	wet	rainforest	over 128
B	humid	forest	64 - 127
C	sub-humid	grassland	32 - 63
D	semi-arid	steppe	16 - 31
E	arid	desert	under 16

2.5.3. TREWARTHA'S MODIFICATION OF THE KÖPPEN'S SYSTEM

In the modification of Köppen's classification scheme, Trewartha (in Money, 1988) stressed the value of supplementing empirical classifications with some description of the mode of origin of the climatic features used to define the boundaries. Table 2.3. provides an explanation of the climatic types according to Trewartha's modification scheme. Figure 2.10 shows the distribution of the Trewartha's modified classification for most continents.

2.6. CLIMATIC REGIONS FOR AFRICA

In this study, Trewartha's modified Köppen classification system (Money, 1988; Lewis and Berry, 1988) was used to investigate links to observed temperature changes. This classification system stresses the use of the mode of origin of the climatic features to define the climatic boundaries. This is the basis on which the system was chosen for its use in this study to facilitate the linking of observed temperature changes to other climatic features. The Köppen's classification scheme was not used in this study because it regarded vegetation as the sole indicator of climatic boundaries.

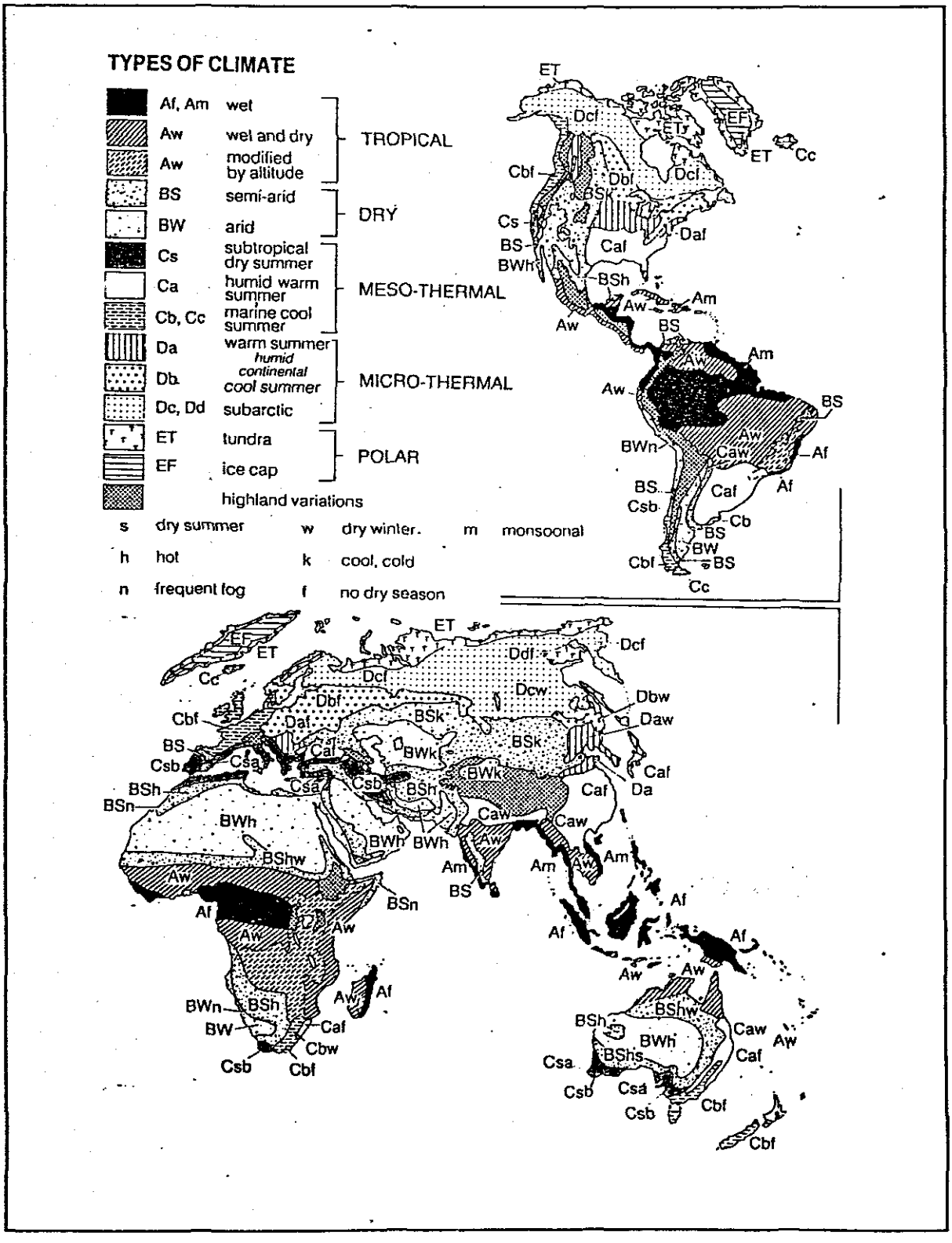

Figure 2.10: The climates of the continents based on Trewartha's modification of Köppen's classification. The system uses H for undifferentiated highland climates (from Money, 1988)

GROUP A
TROPICAL RAINY CLIMATES: temperature of the coolest month over 18°C

Af *no dry season*: driest month over 60 mm; ITCZ with mT or mE air movements
Am *short dry season*: but rainfall sufficient to support rainforests; (wet monsoon type)
Aw *dry during of low sun (winter)* - driest month under 60 mm; dry cT air in winter; wet during period of high sun when ITCZ moves poleward and moist mT air flows in

GROUP B
DRY CLIMATES: evaporation exceeds precipitation (W - arid; S - semi-arid)

boundary between BW/BS is where, for winter precipitation maximum, r/t = 1; for summer maximum, r/t + 14 = 1; for evenly distributed precipitation, r/t + 7 = 1. (r = annual rainfall in cm; t mean temperature in °C)

BWh *hot desert* - mean annual temperature over 18°C; source region of cT air; dry cT winds
BSh *semi-arid*, tropical/sub-tropical: cT air mainly but short rainy season
BWk *middle latitude interior desert*: cT air mass in summer, cP air mass in winter; large annual temperature range
BSk *semi-arid middle latitude*: meagre rainfall, mostly in summer, when main cT air; cP air in winter (n - neble is used to show frequent fog along coastlands with cool water offshore)

GROUP C
HUMID MESOTHERMAL (moist temperate): coldest month between 18° and 0°C (f - no dry season; w - dry winter)

Cs *sub-tropical, dry summer*: at least three times as much rain in wettest winter month as in driest summer month; driest month less than 30 mm; summer dominated by sub-tropical high, cT air; winter with mP air, cyclonic storms and rain
Csa *hot summer*: warmest month averages over 22°C
Csb *warm summer*: warmest month averages under 22°C
Ca *humid sub-tropical, hot summer*: warmest month over 22°C; in summer moist, unstable mT air after ocean passage from sub-tropical high; in winter cP air invading, with cyclonic storms
Caf *no dry season*: driest month over 30 mm
Caw *dry winter*: at least ten times the rain in wettest summer month as in driest winter month
Cb *marine climate, cool/warm summer*: warmest month under 22°C; mainly mid-latitude coast; moist mP air; series of depressions; rain in all seasons
Cbf *no dry season*: the most common Cb type; (Cbw describes parts of south-east Africa
Cc *marine climate, shot cool summer*: warmest month below 22°C; less than four months over 10°C; rain in all seasons

GROUP D
HUMID MICROTHERMAL (rainy/snowy, cold): coldest month under 0°C; warmest month over 10°C

Da *humid continental, warm summer*: warmest month over 22°C; precipitation in all seasons; summer maximum; winter snow cover; frequent slashes between polar/tropical air; variable weather
Db humid continental, cool summer: warmest month below 22°C; as for Da, long winter snow cover

Dc *sub-Arctic*: warmest month below 22°C; less than four months over 10°C; winter cP air masses, cold stable air; summer occasional cyclonic storms with mP air; precipitation light; low winter evaporation rate, so remains moist
Dd *sub-Arctic, very cold winter*: coldest month below -38°C; precipitation very light

GROUP E
POLAR: temperature of warmest month less than 10°C

ET *tundra*: warmest month above 0°C; mP, cP, and air masses interact; cyclonic storms; light precipitation, mainly in summer
EF *ice cap, perpetual frost*: no month over 0°C mean temperature; source regions for Arctic/Antarctic air masses.

Table 2.3: Trewartha's modification of the Köppen's system (from Money, 1988)

To compare the temperature change model for Africa with the Trewartha's modified Köppen classification system for Africa, the map of the climatic zones was digitised as homogeneous polygons and rasterised using the IDRISI GIS system (Figure 2.11) to create a spatial image of the same resolution as the temperature field images provided by the Global Change Database Project: Pilot Project for Africa. Specific aspects of each region are examined for features which could be linked to temperature fields.

2.6.1. TROPICAL RAINY CLIMATES (Af) are experienced on a narrow strip along the West African Coast and throughout most of the Zaïre Basin. These areas have no dry season. The mean annual temperature is above 18°C all the year round and the annual rainfall varies between 1750 and 2500 mm with the driest month having over 60 mm of rainfall. This area is directly linked to the Intertropical Convergence Zone (ITCZ) and any changes in this circulation pattern will have a marked influence on the climate of the region (Figure 2.9).

2.6.2. TROPICAL WET AND DRY CLIMATES (Aw) are the most typical climates of Central Africa. They cover the regions from the Cape Verde Islands on the west coasts (off Senegal), south of Lake Chad to Sennar in Sudan, and to margins of the Ethiopian Highlands. These climates also extends to the south of the equator in Angola and Zaïre, and through the portions of Somalia, Kenya, Tanzania, and Malawi and further South into southern Africa. These areas receive rainfall between 400 and 2000 mm. These climatic regions can also be subdivided into regions modified by altitude (Ash) (Figure 2.11). This area is closely associated with the seasonal movement of the ITCZ across Africa. Low rainfall seasons are often due to a failure of the ITCZ to be fully established in the region or failure to migrate along the recognised paths (Figure 2.9).

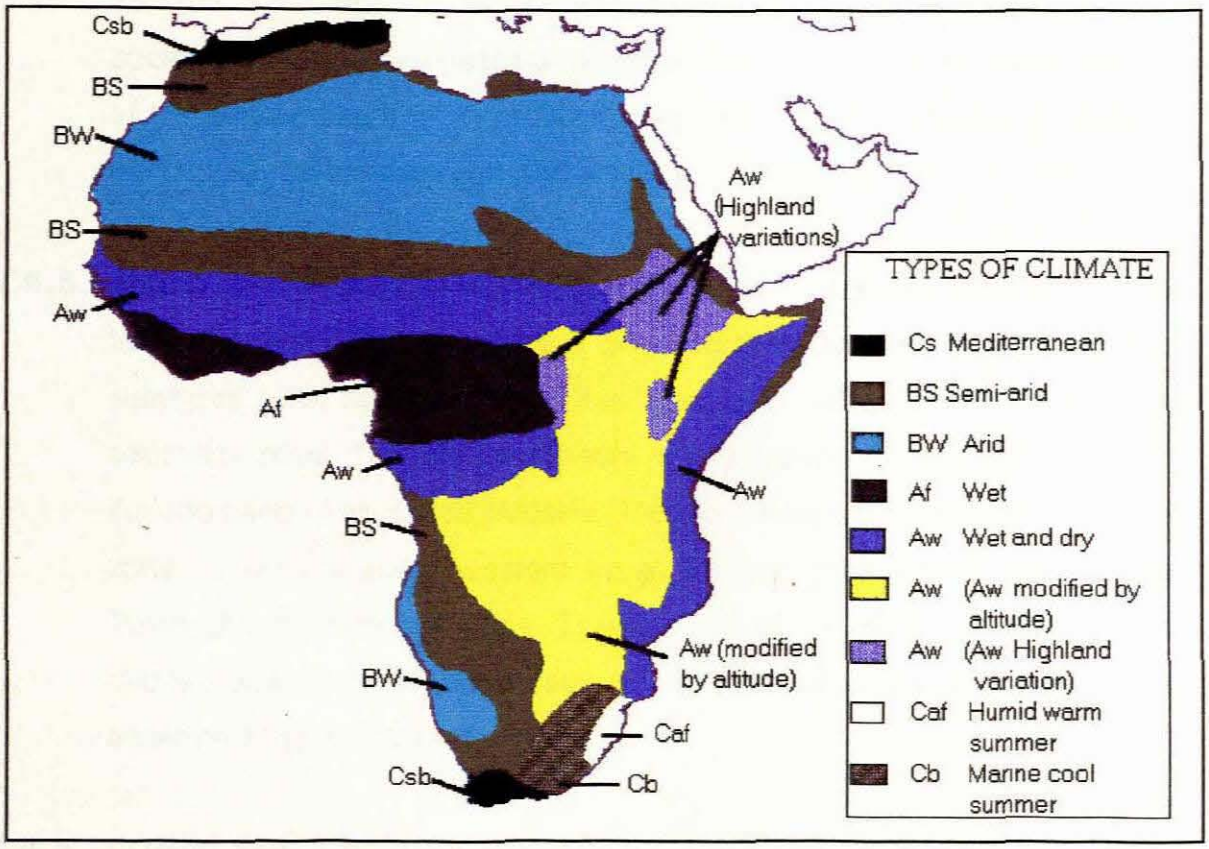

Figure 2.11: Climatic regions of Africa (from Money, 1988)

2.6.3. SEMI-ARID CLIMATES (BS) are experienced in the regions along the northern and southern margins of the Sahara desert and over the low-lying areas of Ethiopia and Somalia. They also occur along the peripheral areas of the Namib-Kalahari desert. These areas form transitional belts surrounding the Kalahari and Sahara deserts, which separate the deserts from the humid climates. Rainfall is generally between 250-500mm and the average temperature is 28°C. The rainfall migration mechanism for the Southern Saharan zone is still linked to the ITCZ, but may be more dependent on the Atlantic circulation particularly in the case of the Namib zone (Figure 2.9).

2.6.4. HOT DESERT CLIMATES (BW) cover the central parts of the Sahara and Namib-Kalahari deserts. These areas are characterised by very hot summers and cool winters, with annual average rainfall of less than

250mm. Temperatures range from 30°-35°C in hot months to 10°-15°C in cooler months. The climates of this zone are influenced by the subsidence of the descending branch of the Hadley and Ferrels circulations. They are controlled by the strength and position of these cells.

2.6.5. MEDITERRANEAN CLIMATES (Cs) occur along the northern and southern tips of Africa. These areas are characterised by wet winters and dry summers. The northern zone has generally hotter summers than the southern zone. The Mediterranean climate areas on the northern zone include parts of Morocco, Algeria, Tunisia, Libya and Egypt. The southern zone covers the south-western tip of the continent which include Cape Town and the Western Cape. These climates are generally controlled by mid-latitude systems which are strongly affected by the presence or absence of land masses.

2.6.6. HUMID SUB-TROPICAL CLIMATES (Caf) cover the Natal coastal belt area up through the southern region of Mozambique. These climates are characterised by mean temperature of 22° - 30°C, and no dry season.

2.6.7. COOL TEMPERATE HUMID CLIMATES (Cbf and Cbw): The Cbf regions are characterised by mild summers with no marked dry season. These climates are characteristic of areas along the southern region of the eastern Cape of southern Africa and represent a transitional zone between the mid-latitude and tropical systems. The Cbw regions are characterised by mild summers and dry winters, and are found along the east-facing slopes of Natal.

CHAPTER 3

A DOCUMENTARY SURVEY OF TEMPERATURE CHANGES FOR DIFFERENT CLIMATIC REGIONS OF AFRICA

3.1. INTRODUCTION

This chapter assesses the climatic temperature changes that have occurred and been reported for the various climatic regions of Africa during the recent historical period. Before attempting to address this objective, a brief review of the historical global palaeotemperature changes is presented. It must be noted that only documentary sources are used, and that the focus has been put on their reflections of temporal temperature variations, particularly those which may be reflected in Africa.

3.2. GLOBAL SURFACE AIR TEMPERATURE CHANGES

Since time immemorial, temperature has been changing (Tyson, 1988). Over the past 100 000 years, the earth has experienced a series of glacial periods (McBoyle, 1973). The period between 120 000 to 80 000 years Before Present (BP) was the time of generally warm conditions with temperatures similar to those being experienced today. This period was interrupted by a few cold spells. The global temperatures in the period between 70 000 to 15 000 years BP were 2° to 5°C lower than the temperatures experienced today (Gates, 1976a & b; and others cited in Bolin, *et al* 1989). The lowest temperatures during this period were experienced around 20 000 to 15 000 years BP.

The last glacial period occurred during the 15 000 to 10 000 BP period. From 10 000 BP to the present, it is claimed that the temperatures are progressively increasing (Webb and Wigley, 1985 cited in Bolin, *et al* 1989).

The causes of these temperature changes are not yet known, but numerous theories have presented clues as to their causes (McBoyle, 1973 and Dickinson in Bolin, *et al* 1990). These theories include:

1. long- and short-term variations in solar radiation (McBoyle, 1973)
2. variations in atmospheric transparency (McBoyle, 1973),
3. changes in Earth's geometry (McBoyle, 1973 and Dickinson in Bolin, *et al* 1990),
4. changes in terrestrial geography (McBoyle, 1973 and Dickinson in Bolin, *et al* 1990).

The analysis of the longest surface air temperature data series from 1854 - 1990 by Jones *et al*, (1986 cited in Roberts, 1994) indicated that the earth's surface has warmed by 0.45°C (0.03°C/decade) since the middle of the 19th Century. This trend is shown in Figure 3.1. From the 1910's to the 1940's and again since the mid 1970's to the present date, there has been a relatively rapid ("global") warming. This latter period of increase in temperature has been ascribed to the tremendous increase of atmospheric concentrations of CO_2 and other GHGs (Leggett, 1990). The period between 1940 to 1970 was characterised by cooling.

The predictions of future global temperature changes have been linked to predicted atmospheric concentrations of CFCs, tropospheric ozone, and other greenhouse gases, particularly carbon dioxide (Leggett, 1990 and Bolin, *et al* 1989). The Intergovernmental Panel on Climatic Change (IPCC), Working Group 3 (Houghton and Jenkins, 1990) developed four scenarios of future human-made emissions by which future global temperature trends will be affected. The first of these scenarios assumes that few or no step are taken to limit GHGs emissions and it was therefore termed Business-as-Usual (BaU). This scenario also assumes that CO_2 will double before the year 2050. The second (B), third (C) and fourth (D) scenarios assume three progressively increasing levels of controls to reduce the growth of emissions.

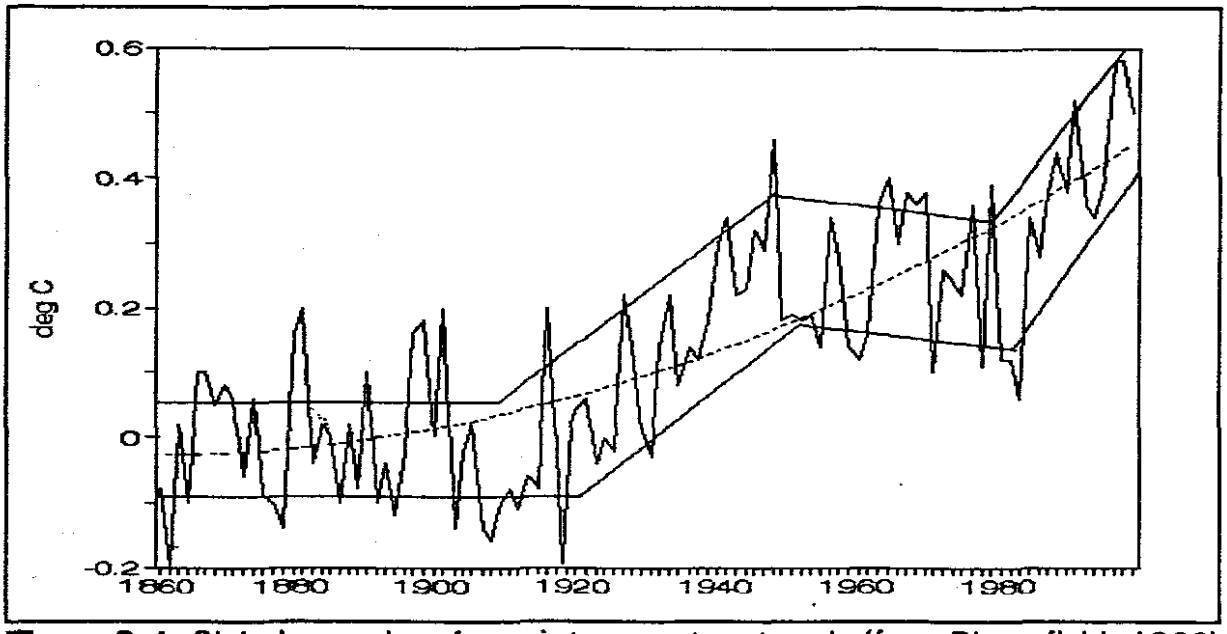

Figure 3.1: Global annual surface air temperature trends (from Bloomfield, 1992)

In terms of the BaU (Scenario A) emissions of the GHGs, the average rate of the global mean temperature (GMT) increase during the next century is estimated to be 0.3°C per decade. This will produce a likely increase in GMT of about 1°C above the present value (about 2°C above that in the pre-industrial period) by the year 2025 and 3°C above today's GMT (about 4°C above pre-industrial) before the end of the next century. Figure 3.2 illustrates the projected temperature rise to the year 2100 with high, low and best-estimates in terms of scenario A (Houghton and Jenkins, 1990). If emissions are subject to controls, average rates of increase in GMT over the next century are estimated to be about 0.2°C per decade (scenario B), just above the 0.13°C per decade predicted for scenario C and about 0.1°C per decade for scenario D (Houghton and Jenkins, 1990). Figure 3.3 illustrates these results with the BaU case shown for comparison. Only the best estimate of the temperature rise is shown in each case.

The question of lower and upper limits of the global mean equilibrium responses to doubling of the carbon dioxide is still debated. Various models obtain differing results (Houghton and Jenkins, 1990). Tables 3.1 to 3.3 show the results of various models predictions. These results have been adjusted to reflect temperature change per decade. It is assumed that the date of publication is the

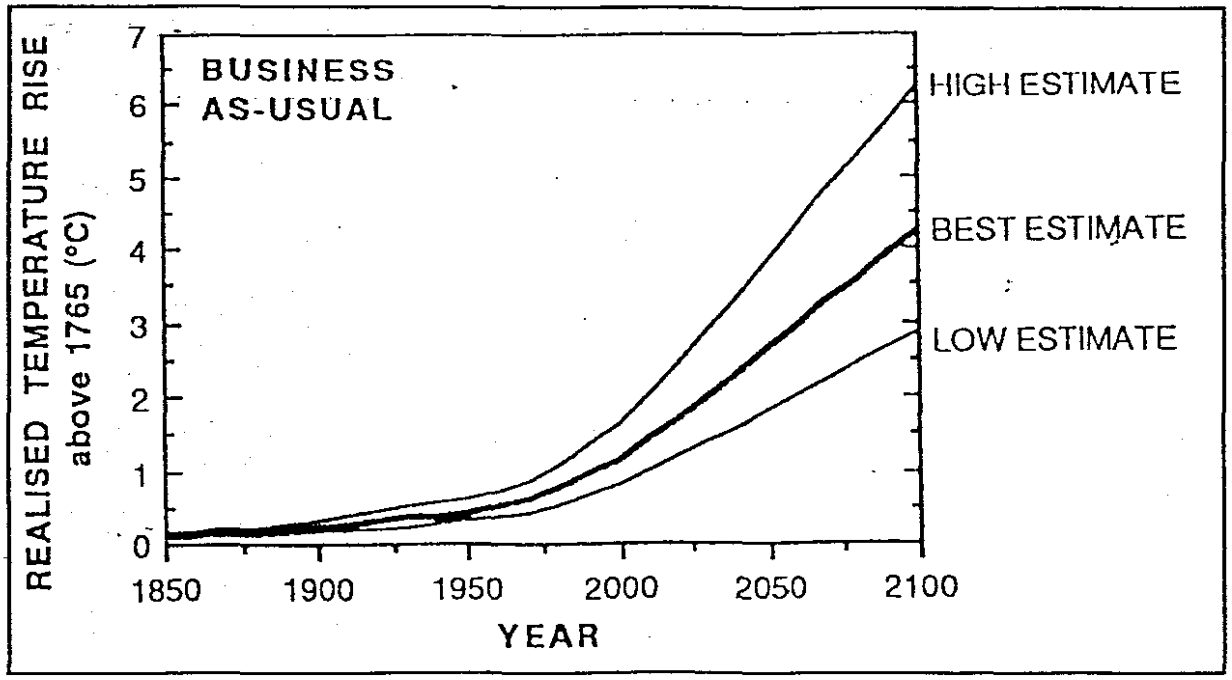

Figure 3.2: Simulation of the increase in GMT from 1850 to 1990 due to increase in GHGs, and predictions of the rise between 1990 and 2100 resulting from the BaU emissions (from Houghton and Jenkins, 1990).

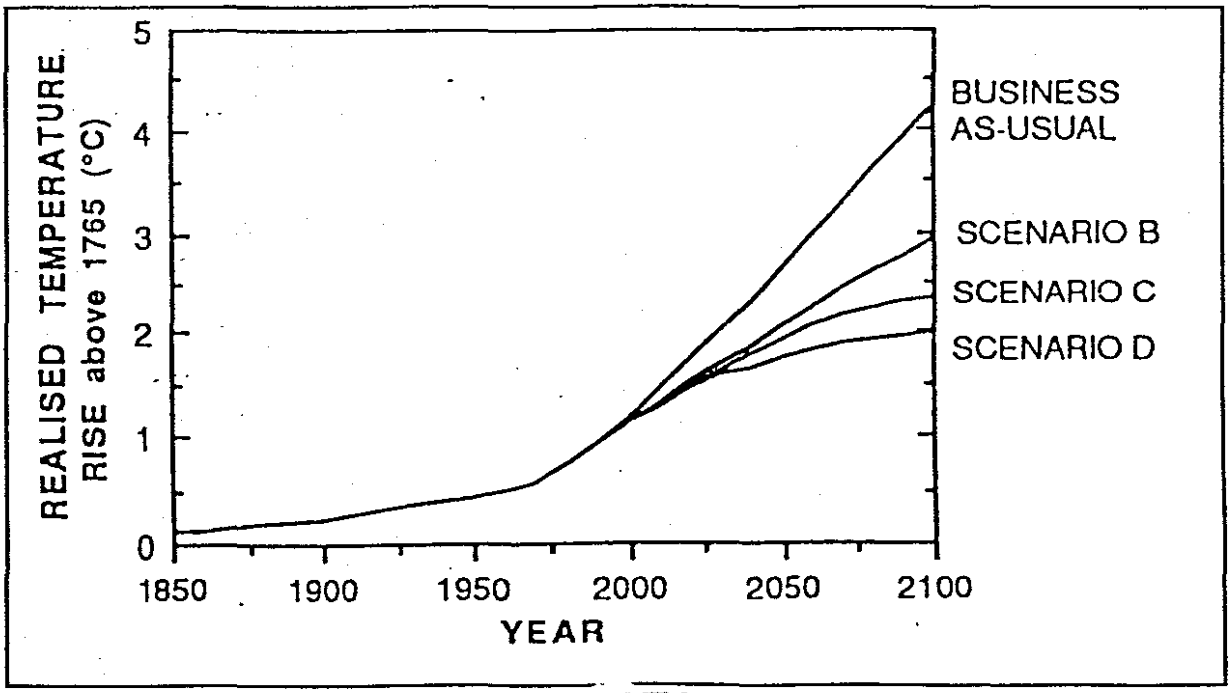

Figure 3.3: Simulation of the increase in GMT from 1850 to 1990 due to increases in GHGs, and predictions of the rise between 1990 and 2100 resulting from the IPCC scenario B, C and D emissions, with the BaU case for comparison (from Houghton and Jenkins, 1990).

start of the prediction period which ends in the year 2050 when the CO_2 concentration in the atmosphere is assumed to have doubled.

Houghton and Jenkins (1990) have maintained that it is very difficult to choose a best model because a particular model may be more reliable than the other for one climatic parameter but not the other, and that a result which is common to most models may merely reflect the fact that many models use similar (possibly erroneous) representation of complex atmospheric processes. Nevertheless, there is a general consensus that the global mean equilibrium warming caused by the doubling of the carbon dioxide atmospheric concentration will lie between 1.5° and 5.5°C (0.25° and 0.92°C/decade) by the year 2050.

Table 3.1: Global average surface temperature changes (δT) predicted by selected Radiative-Convective Models (RCMs) following a doubling of the atmospheric CO_2 concentration (adapted from Tyson, 1990).

Author(s)	δT (°C/decade)
Manabe and Witherald (1967)	0.16 - 0.36
Manabe (1971)	0.24
Augustsson and Ramanathan (1977)	0.27 - 0.46
Rowntree and Walker (1978)	0.11 - 0.39
Hunt and Wells (1979)	0.26 - 0.31
Wang and Stone (1980)	0.28 - 0.6
Charlock (1981)	0.22 - 0.32
Hensen, *et al* (1981)	0.17 - 0.5
Hummel and Kuhn (1981a)	0.11 - 0.27
Hummel and Kuhn (1981b)	0.11 - 0.17
Hummel and Reck (1981)	0.24 - 0.29
Hunt (1981)	0.09 - 0.26
Wang, *et al* (1981)	0.21 - 0.4
Hummel (1982)	0.18 - 0.26
Lidzen, *et al* (1982)	0.21 - 0.27
Lal and Ramanathan (1984)	0.3 - 0.4
Somerville and Remer (1984)	0.08 - 0.29

Table 3.2: Global average of surface temperature changes (δT) predicted by Energy Balance Models (EMBs) as a consequence of the doubling atmospheric concentration of CO_2 (adapted from Tyson, 1990).

Authors	δT (°/Cdecade)
Callender (1938)	1.3
Moller (1963)	9.6
Rasool and Schneider (1971)	0.6
Newell and Dopplick (1979)	0.24
Ramanathan, *et al* (1979)	3.3

Table 3.3: Global average surface temperature changes (δT) predicted by various GCMs for a doubling of the CO_2. In all cases non-interactive oceans have been coupled to atmospheric models (adapted from Tyson, 1990).

Model	Study	δT (°C/decade)
GFDL	Manabe and Wetherald (1975)	0.4
GFDL	Manabe and Wetherald (1980)	0.4
GFDL	Wetherald and Manabe (1986)	0.5
OSU	Schlesinger (1983)	0.3
OSU	Schlesinger and Zhao (1989)	0.5
NCAR	Washington and Meehl (1983)	0.2
NCAR	Washington and Meehl (1984)	0.5
NCAR	Washington and Meehl (1989)	0.3
GISS	Hansen, *et al* (1984)	0.6
GISS	Hansen, *et al* (1988)	0.6
UKMO	Wilson and Mitchell (1987)	0.8

3.3. REGIONAL PAST CLIMATIC TEMPERATURE CHANGES FOR AFRICA

3.3.1. TROPICAL RAIN CLIMATIC REGIONS (Af)

The historical temperature changes for tropical rainfall climatic regions were inferred from Hulme's (Roberts, 1994) results of analysis of long surface air temperature records for the whole world. These results indicated that most of the tropical rainfall regions (Af) of Africa have experienced a temperature

change of -0.08° to 0.0°C/decade over the period between 1931 to 1960 and 1961 to 1990, except for the eastern parts of the Central African sector which was characterised by a temperature change of -0.16° to -0.08°C/decade.

3.3.2. TROPICAL WET AND DRY CLIMATIC REGIONS (Aw)

The palaeotemperature change scenarios for this region were inferred from the results of pollen analyses in Burundi (Bonnefille, *et al* 1990 cited in Vincens, 1991) and at Mpulungu Basin (Zaïre) (Vincens, 1991). These studies indicate a temperature decrease of -0.001° to -0.002°C/decade between 30 000 and 13 000 years BP. On the other hand, the early investigations of Coetzee, (1967); Van Zindern, (1969); and others (cited in Vincens, 1991) and that of Scott and Vogel (1991) have indicate that, during the Late Pleistocene, particularly during the period between 25 000 and 15 000 years, temperatures were 5° to 6°C lower than temperatures experienced today BP. The coldest episode is suggested to have occurred between 22 000 and 15 000 years BP (Vincens, 1991 and Scott, 1990).

The period after 15 000 years BP was characterised by an increase in temperature. This rise in temperatures could have reached its peak between 8 000 and 5 000 years BP (Scott and Vogel, 1983; Scott, 1989; Partridge, *et al* 1990). Following this period, there was further warming which was neither continuous over space nor through time (Vincens, 1991; Scott, 1989 and 1990). On the other hand, Hulme (Roberts, 1994) found that a surface air temperature change of -0.08° to 0.0°C/decade did occur in these climatic regions during the period between 1931 to 1960 and 1961 to 1990. This rate of temperature change (which ranges between 0.2° and 0.7°C per decade for the period between 1950 and 1985) is low when compared with a much faster rate calculated for the regions of Southern Africa by Karoly (Thackery, 1990).

3.3.3. SEMI-ARID CLIMATIC REGIONS (BShs, BSn and BShw)

The recent palaeotemperature changes for the southern African semi-arid regions showed great similarity with the global palaeotemperature scenarios, especially that of the glaciation period before 10 000 years ago and warm periods thereafter (Scott, 1989).

Scott (1987, cited in Lee-Thorp and Beaumont, 1990), through faunal analysis, indicated that temperatures in the western Cape were as low as 5° to 6°C below the present temperatures during the late Pleistocene. On the other hand, Lee-Thorp and Beaumont (1990) have maintained that this region's Pleistocene temperatures were not more than 3° to 4°C lower than temperatures experienced today.

The northern sector of Africa's semi-arid regions have experienced a surface air temperature change of -0.08° to 0.0°C/decade over period between 1931 to 1960 and 1961 to 1990, whereas the southern (Africa's) sector of these climatic regions have experienced a change of 0.0° to 0.08°C/decade over a similar period (Roberts, 1994).

3.3.4. HOT DESERT CLIMATIC REGIONS (BW, BWn and BWh)

The palaeotemperature changes for desert regions were obtainable from the results of Haynes and Haas's investigations (Lezine and Casanova, 1989). These results were based on radiocarbon dating for Holocene recharge of groundwater in the Western desert at Kiseiba-Nakhlai sampling site (Egypt). The indications are that isotopic palaeotemperatures were 4°C colder than they are at present.

Over the recent historical period, the North African hot desert climatic regions have experienced a surface air temperature change of -0.08° to 0.08°C/decade between the periods 1931 to 1960 and 1961 to 1990

(Roberts, 1994). The southern African sector with these desert climates has experienced a surface air temperature increase of 0.0° to 0.08°C/decade over a similar period (Roberts, 1994).

3.3.5. MEDITERRANEAN CLIMATIC REGIONS (Cs and Csb)

The evidence of palaeotemperature changes for the Mediterranean climatic regions were inferred from nine recent reviews. These include: Tyson (1986, 1988, 1990, 1992), Partridge (1990); Partridge, *et al* (1990); Scott and Vogel (1990); Scott (1990); and Wengler and Vernet (1992).

The measurements of the oxygen isotope speleothem of the stalagtites from the Cango Caves (South Africa) by Talma and Vogel (1987, cited in Tyson, 1986, 1988, 1990, 1992) indicated that the interval between 30 000 to 16 000 years ago was characterised by prolonged cold conditions with the coldest conditions at 16 000 years BP (Figure 3.4). These results indicated that a mean temperature of around 5° to 6°C lower than at present occurred between 17 000 and 21 000 years BP. Partridge, *et al* (1990) reduced this estimate one degree to 4° to 5°C and inferred that the temperature over the last 5 000 years BP did not deviate by more than 2°C from the present mean. This interval was followed by a rapid rise of temperatures up to the present.

The abovementioned temperature series at Cango Cave share similarity with recently obtained temperature curves from Vostok ice cores in Antarctica which are shown in Figure 3.5 (Partridge, *et al* 1990; Heusser, 1989).

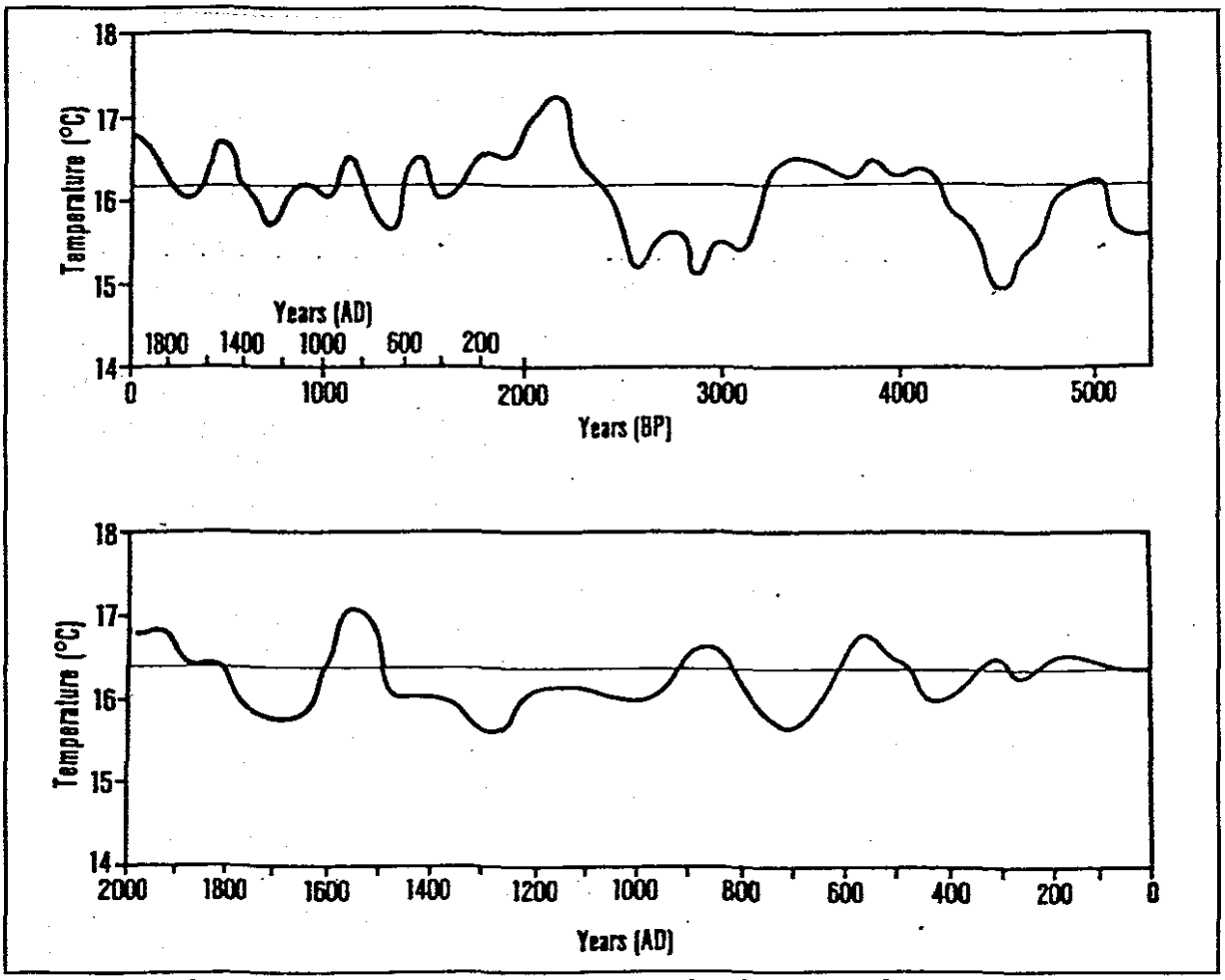

Figure 3.4: Oxygen isotope temperature curve for Southern Cape from Cango Cave (from Talma and Vogel, 1988 cited in Tyson, 1990).

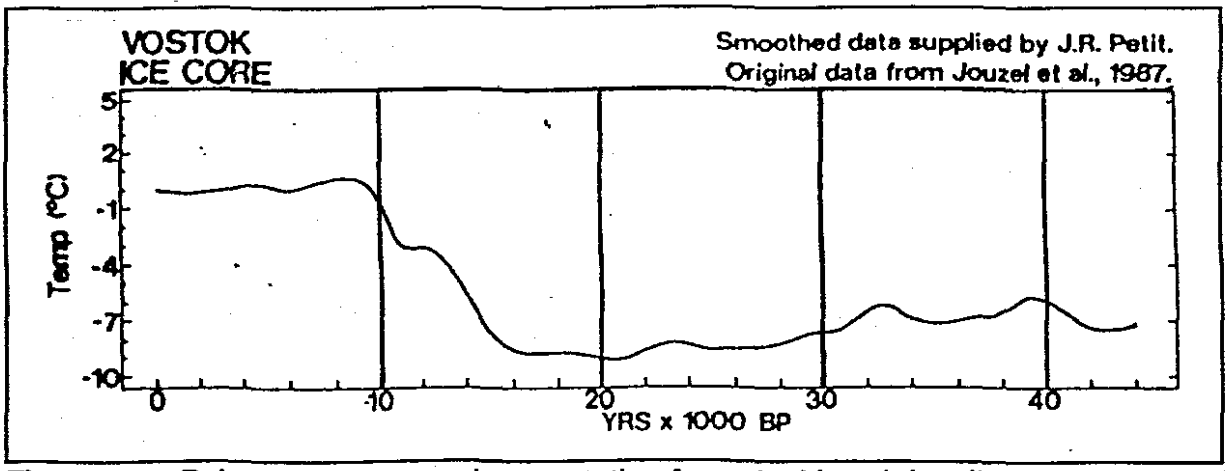

Figure 3.5: Palaeo-temperature interpretation from the Vostok Ice (from Jouzel, *et al* 1987 cited in Partridge, *et al* 1990).

The palaeotemperature trends for the North African Mediterranean region were obtainable from the results of Wenigler and Vernet's (1992) investigations on vegetation, sedimentary deposits and climates during the late Pleistocene and Holocene period in Morocco (Figures 3.6 and 3.7). These results were derived from charcoal analyses from several geological and archaeological sites at the Oujda Plain, the Oujda Mountains, Oued El Hay Plain and the Grotte Des Pigeons.

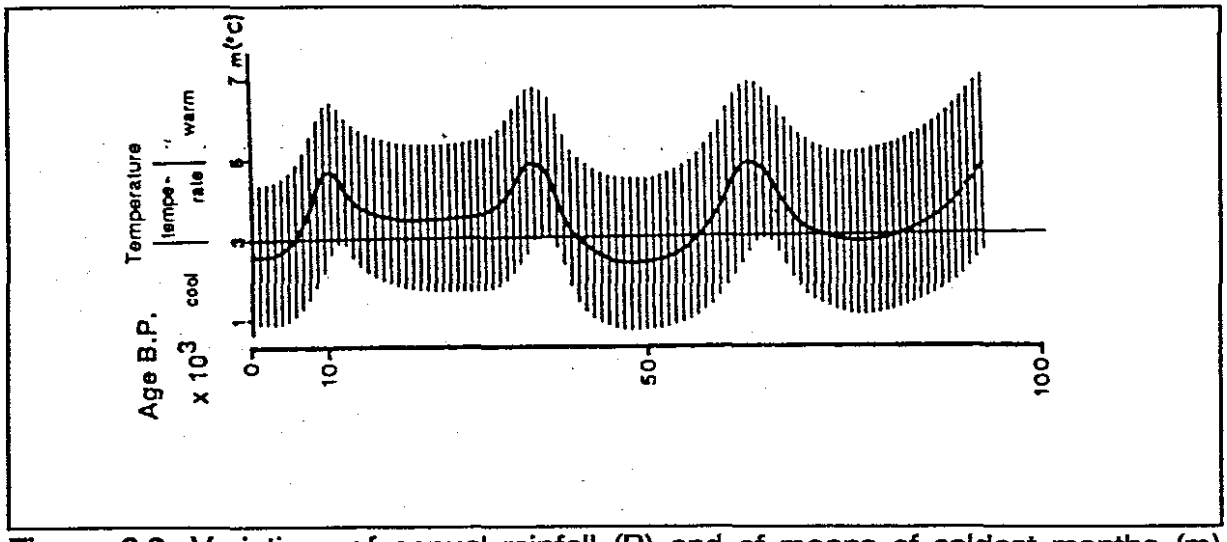

Figure 3.6: Variations of annual rainfall (P) and of means of coldest months (m) during the late Pleistocene in western Morocco (from Wengler and Vernet, 1992)

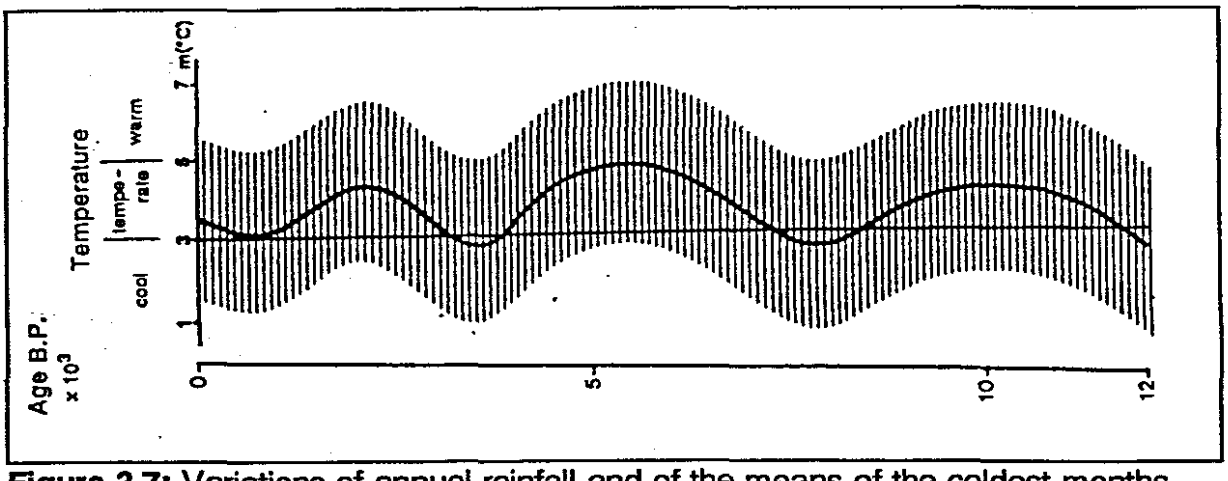

Figure 3.7: Variations of annual rainfall and of the means of the coldest months minima (m) during the Rharbian in the western Morocco (from Wengler and Vernet, 1992)

Temporal thermal trends for the Mediterranean region are depicted in Figures 3.4 to 3.7 and indicated that:-

1. the period between 40 000 and 20 000 years BP was characterised by temperature decreases,
2. the period between 20 000 to 16 000 years BP was characterised by fluctuating temperatures,
3. the period between 16 000 to 4 000 years BP was characterised by general warming with some temperature fluctuations,
4. from 4 000 years BP to the present, temperatures are warming.

More recent historical temperature changes for Mediterranean regions were evaluated from the results of Hulme's analysis of long-term surface air temperature records (Roberts, 1994). The results indicated that these regions have experienced a temperature increase of 0° to 0.08°C/decade between 1931 to 1960 and 1961 to 1990.

3.3.6. HUMID SUB-TROPICAL CLIMATIC REGIONS (Caf)

According to Roberts (1994), the Caf climatic regions have experienced a surface air temperature change of 0.0° to 0.08°C/decade over the period between 1931 to 1960 and 1961 to 1990.

3.3.7. COOL TEMPERATE HUMID CLIMATIC REGIONS (CB and Cbw)

The prolonged worldwide pre-Holocene cold conditions and a rapid rise of temperatures after 16 000 years BP, also manifested themselves in the cool humid regions. These palaeotemperature changes for this region were inferred from the results of pollen analysis in some areas in South Africa, namely, Wonderkrater (Scott, 1989 and Partridge, *et al* 1990), Tote Vado (Scott, 1989), Scott (Scott, 1990), and Rietvlei (Scott and Vogel, 1983 and

Scott, 1989). Micromammalian remains at Wonderwerk in South Africa (Scott, 1990 and Scott and Thackery, 1987 cited in Scott, 1989); and the artesian groundwater temperature measurements of the Uitenhage aquifers of South Africa (Partridge, *et al* 1990) as well as pollen grains, charcoal, macro- and micro-mammal, oxygen isotopes and microfauna curves of speleothems at the archaeological site at Boomplaas Caves in South Africa (Scott, 1990; Partridge, *et al* 1990). also indicate these changes. Figure 3.8 and 3.9 exemplify palaeotemperature trends for this region.

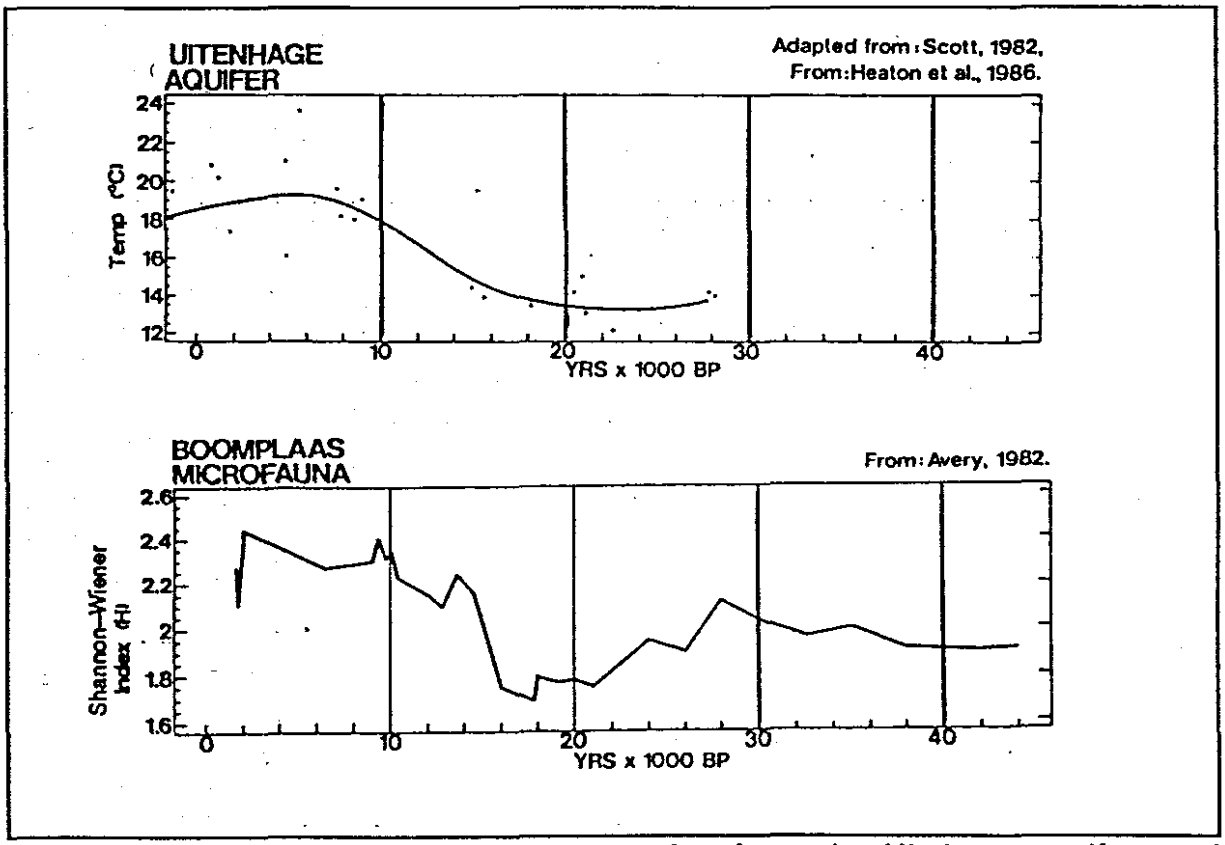

Figure 3.8: Palaeo-temperature interpretation from the Uitehage aquifer, and Shannon-Wiener index for microfauna preserved at Boomplaas Cave (from Partridge, *et al* 1990.

The Uitenhage-Boomplaas Holocene scenarios, shown in Figure 3.9, depict a continuous warming trend during the early Holocene phases. The period between 8 000 and 5 000 years BP was characterised by maximum warming (the Holocene maximum) when the temperature was 3°C higher than the present (Dupisani and Partridge, 1989). After 5 000 years BP, (the

late Holocene) several fluctuations of relatively low amplitude were observed in temperatures of this region. The highest peak was experienced around

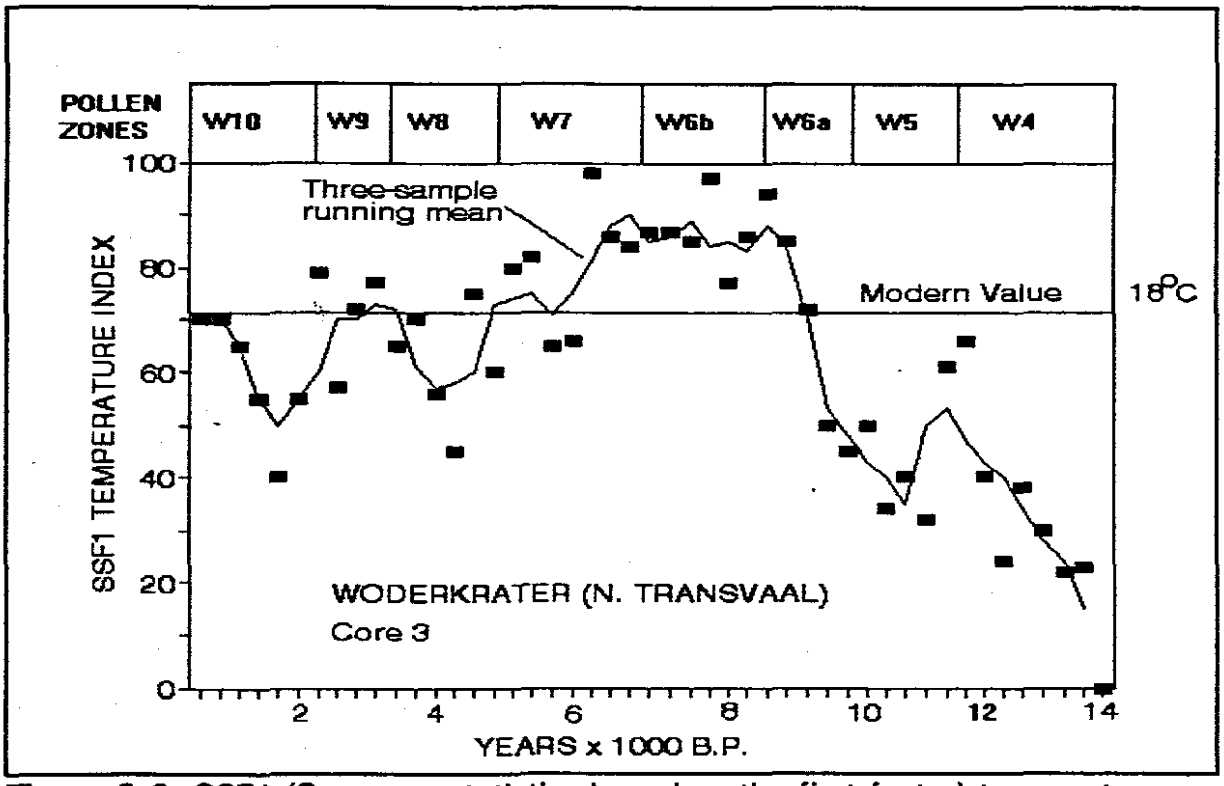

Figure 3.9: SSF1 (Summary statistics based on the first factor) temperature indexes for pollen assemblages (squares) calculated from multivariate analysis of pollen spectra from Wakerkrater, South Africa (from Scott and Thackeray, 1987 in Thackeray, 1990).

3 600 years BP and the minor peak at 1 000 years BP. Lower temperatures occurred around 4 500 and 2 000 years BP. The gradual warming of the period between 4 200 and 2 000 years BP was followed by a world-wide decrease of temperature between 2 000 and 3 000 years BP (Dickinson, in Bolin, *et al* 1990). Over the period between 1931 to 1960 and 1961 to 1990, these regions (Cbf and Cbw) have experienced a surface air temperature change of 0.0° to 0.08°C/decade (Roberts, 1994).

3.4. ESTIMATIONS OF POSSIBLE REGIONAL FUTURE CLIMATIC TEMPERATURE CHANGES FROM GLOBAL MODELS

In the absence of studies estimating possible future climatic temperature changes for any specific climatic region in Africa, we rely on the results of high resolution General Circulation Models (GCMs) for estimation of possible regional future climatic temperature changes. Only temperature changes for arid, semi-arid, Mediterranean, and tropical wet and dry climates could be traced in the literature.

3.4.1. MEDITERRANEAN CLIMATIC REGIONS

Future climatic temperature change estimates for Mediterranean climatic regions were inferred from the results of the IPCC, Working Group 3 (Houghton and Jenkins, 1990) for Southern Europe. These results indicated a warming of about 2°C (0.5°C/decade) in summer and about 2°-3°C (0.75/decade) in winter by the year 2030.

3.4.2. TROPICAL WET AND DRY CLIMATIC REGIONS

The estimates for these regions were derived from the results of the IPCC, Working Group 3 (Houghton and Jenkins, 1990) for South East Asia which also has a tropical wet and dry climate. This region was predicted to experience warming of 1° to 2°C (0.25° to 0.5°C/decade) by the year 2030. These estimates were expected to vary from 2°C (0.5°C/decade) during cold seasons to 1°C (0.25°C/decade) during warm seasons.

3.4.3. SEMI-ARID CLIMATIC REGIONS

The results from the Villach Statement (Abrahamson, 1989; Ardil and Boyle, 1988; Leggett, 1990) have indicated that by the year 2030, the annual mean temperatures for semi-arid and arid regions will have increased by 1° to 3°C (0.25° to 0.75°C/decade). Mabbutt (1989) also predicts these results.

On the other hand, the IPCC, Working Group 3 (Houghton and Jenkins, 1990) estimated a temperature increase of 1° to 2°C (0.25° to 0.5°C/decade) by the year 2030.

3.4.4. HOT DESERT CLIMATIC REGIONS

The hot desert climatic regions are also expected to experience temperature increase of 1° to 3°C (0.25° to 0.75°C/decade) by the year 2030 which is similar to the semi-arid regions (Villach Statement in Abrahamson, 1989; Ardil and Boyle, 1988; Leggett, 1990).

3.5 CONCLUSION

The palaeotemperature change events that occurred in many other parts of the world, were also experienced in Africa. The recent historical temperature changes for Africa are summarised in Table 3.4 and their spatial patterns are shown in Figure 3.10. There is a clear indication that the continent has experienced temperature decrease over the period between 1931 to 1960 and 1961 to 1990. The global warming trends are predicted to be occurring in most parts of the African continent. The summary of these predicted temperature trends are given in Table 3.5 and 3.6. Figure 3.11 shows the spatial patterns of these results in terms of the identified climatic regions.

Table 3.4: Surface air temperature changes for Africa for different climatic regions during the period between 1931 to 1960 and 1961 to 1990 according to Roberts (1994).

CLIMATIC REGION	TEMPERATURE CHANGE/decade
Tropical rain (Af)	-0.08° to 0.0°C
Tropical rain (Af) (in Central Africa)	-0.25° to -0.08°C
Tropical wet and dry (Aw)	-0.08° to 0.0°C
Semi-Arid (BShs, BSn and BShw) (Northern sector)	-0.08° to 0.0°C
Semi-Arid (BShs, BSn and BShw)(Southern Sector)	0.0° to 0.08°C
Hot desert (BW, BWn and BWh) (Northern sector)	-0.08° to 0.08°C
Hot desert (BW, BWn and BWh) (Southern Sector)	0.0° to 0.08°C
Mediterranean (Cs and Csb)	0° to 0.08°C
Humid Sub-tropical (Caf)	0° to 0.08°C
Cool Temperate Humid (Cb and Cbw)	0° to 0.08°C

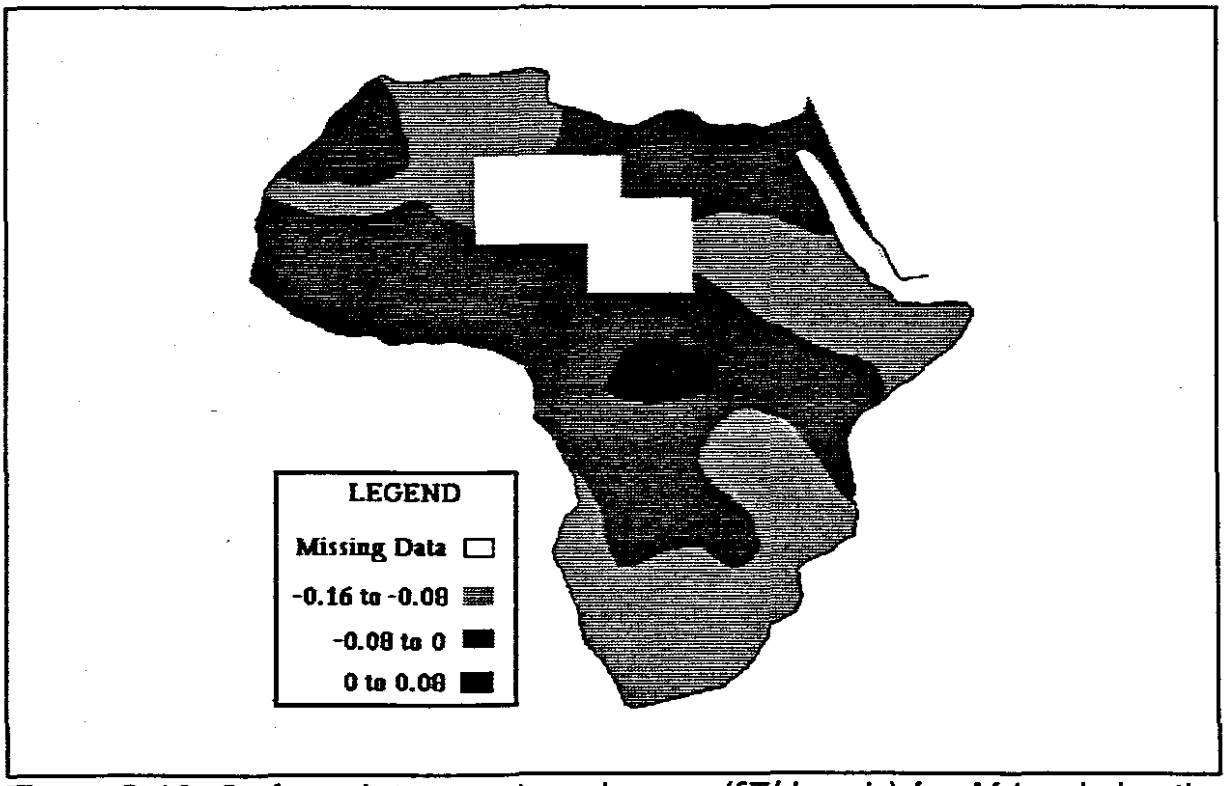

Figure 3.10: Surface air temperature changes (δT/decade) for Africa during the period between 1931 to 1960 and 1961 to 1990 (from Roberts, 1994).

Table 3.5: Predicted temperature changes from GCMs.

SOURCE	REGION	δT/decade	MODEL
Houghton and Jenkins (1990)	Sahel	0.5°C	GCM
	Mediterranean	0.5°C	GCM
Houghton and Jenkins (1990)	Semi-arid	0.25° - 0.75°C	GCM
Mabbutt (1989)			

Table 3.6: Extrapolated results

SOURCE	REGION	δT/decade	MODEL
Houghton and Jenkins (1990)	Tropical Wet and Dry	0.25° - 0.5°C	GCM
Houghton and Jenkins (1990)	Mediterranean	0.5° - 0.75°C	GCM

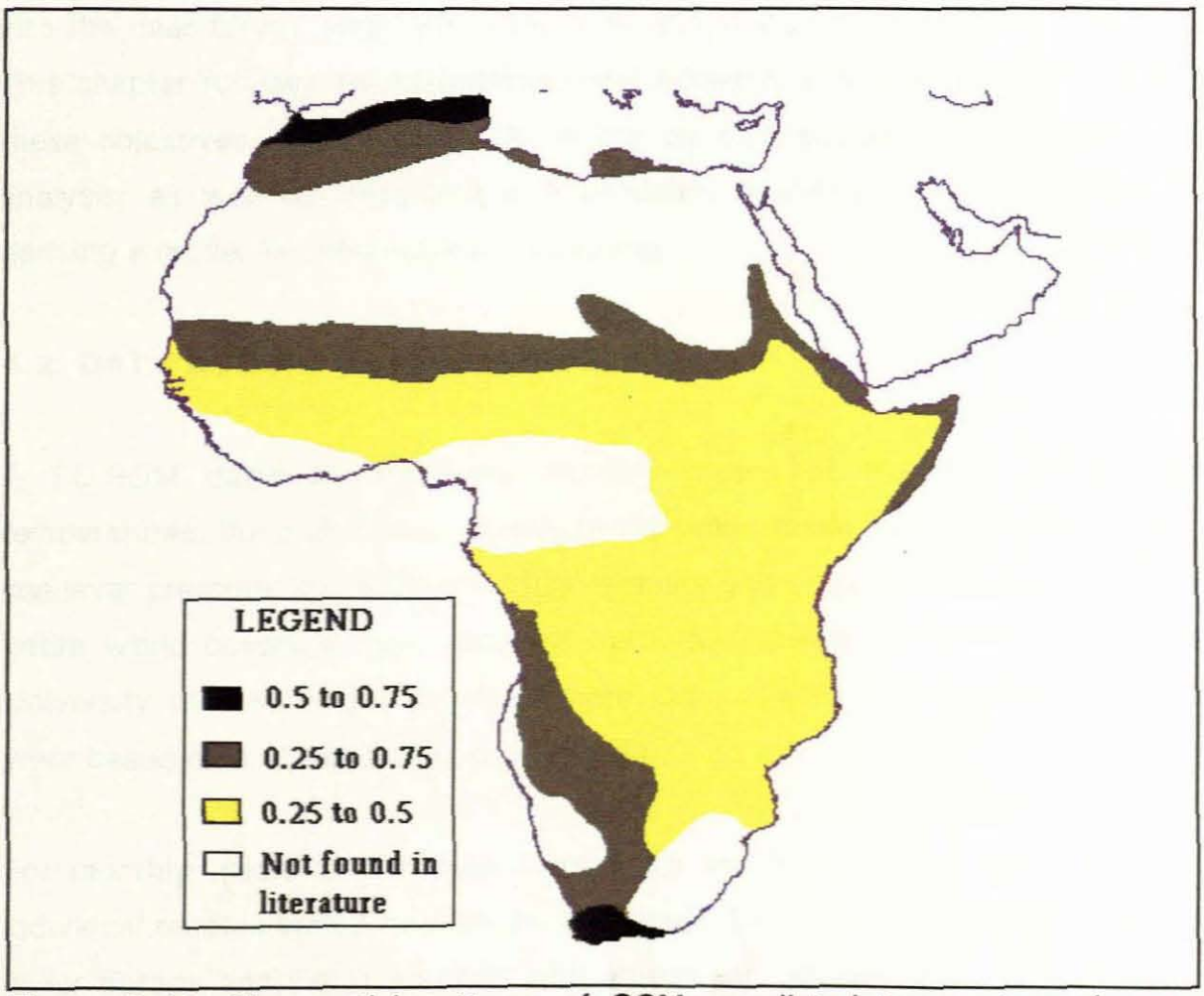

Figure 3.11: The spatial patterns of GCMs predicted temperature changes (δT/decade) for Africa for 2030.

CHAPTER 4

ANALYSIS OF TEMPERATURE SERIES

4.1. INTRODUCTION

The evidence of large fluctuations in temperatures over geological time scales have been presented in Chapter 3. GCM simulations have suggested natural and anthropogenic effects are causing a rise in the present temperature trends for most regions of Africa (Figure 3.11), while observations indicate extensive areas of decreasing temperatures (Figure 3.10). In order to evaluate these models and to verify their predicted trends in temperatures and their projections into the near future, long-term surface air temperature records were analysed. This chapter focuses on methodology and research strategies used to achieve these objectives. Specific attention is put on data acquisition, selection, and analysis, as well as Geographical Information Systems (GIS) applications in deriving a model for temperature forecasting.

4.2. DATA ACQUISITION AND SELECTION

A CD-ROM database containing monthly means of the daily surface air temperatures, the cumulative monthly precipitation totals and the monthly mean sea-level pressure (for both individual stations and regional averages), for the entire world coverage, was obtained from the Climatic Research Unit at the University of East Anglia (World Climate Disc, 1990). The regional averages were based on a 5° latitude by 5° longitude.

For monthly mean of the daily surface air temperature data, the length of individual records varied from 20 to 250 years. The best geographical coverage is for Europe and North America with a relatively sparse network over Africa and elsewhere. These datasets were derived from various sources which include the World Weather Records and the Monthly Climatic Data for the World,

published by US Weather Bureau, at the Smithsonian Institute, and the World Meteorological Organisation (WMO). These sources have been augmented by data which was made available by national meteorological services (World Climate Disc, 1990).

All available weather stations within the African mainland were initially considered for selections. However some of stations in the World Climate Disc Data sets were rejected for not having temperature datasets, while others were rejected for having temperature data series of less than 40 years (a selected minimum record length). As a result, only 130 stations were used in this analysis. Unfortunately, these 130 stations were unevenly distributed, with 35 stations situated in the Southern Hemisphere and 95 in the Northern Hemisphere on the African continent.

For each station, the monthly mean of the daily temperatures and the annual mean of the monthly surface air temperatures were extracted. The length of time series data and other station descriptive data (each station names and its respective country, its WMO Number, elevation, and specific location (latitude and longitude)) were also extracted. Station descriptive data are summarised in Table 4.1.

4.3. DATA ANALYSIS

Each station's annual mean of the daily surface air temperature (referred to hereafter as the annual surface air temperature) data series were imported into Statsgraphics (Version 6) programme for trend analysis with the aim of deriving models for temperature forecasting into the near future. Both linear and quadratic trends were derived for all station time series data. The quadratic trends had the lowest mean square error for all the models fitted to the time series data and consequently, it was chosen for further analysis. The Statsgraphics (1991) trend analysis determines the quadratic model as

$$Z(t) = a + bt + ct^2$$

where t represents the time index, Z(t) is the predicted value of temperature at time t, 'a' is the y intercept or the temperature at the start of the series, and 'b'

STATION NAME	COUNTRY	WMO No.	LATITUDE	LONGITUDE	HEIGHT (m)	YEARS OF RECORD
Accra	Ghana	654720	05° 09'N	03° 33'W	68	1911 to 1975
Agadez	Niger	610240	16° 34'N	07° 35'W	501	1926 to 1990
Agadir	Moroco	602500	30° 13'N	09° 20'W	27	1923 to 1990
Alexander Bay	South Africa	684060	28° 20'S	16° 19'E	21	1951 to 1990
Aliwal North	South Africa	685460	30° 25'S	26° 25'E	348	1881 to 1990
Aktapame	Togo	653760	07° 21'N	01° 04'E	400	1951 to 1990
Bamako	Mali	612910	12° 19'N	07° 35'W	380	1923 to 1990
Bambari	C. Rep. of Africa	646600	05° 30'N	20° 23'E	474	1953 to 1990
Bangassou	C. Rep. of Africa	646560	04° 26'N	22° 30'E	499	1946 to 1990
Bangui	C. Rep. of Africa	646500	04° 14'N	18° 18'E	365	1941 to 1990
Banjul/Yundum	Gambia	617010	13° 12'N	16° 28'E	36	1910 to 1990
Bechar	Algeria	605710	31° 22'N	02° 08'W	806	1951 to 1990
Beira	Mozambique	672970	19° 28'S	34° 32'E	10	1931 to 1990
Benina	Libya	620530	32° 03'N	20° 09'E	132	1945 to 1990
Berberati	C. Rep. of Africa	646000	04° 09'N	15° 28'E	582	1951 to 1990
Bilma	Niger	610170	18° 24'N	12° 33'E	355	1950 to 1990
Birao	C. Rep. of Africa	646580	10° 10'N	22° 28'E	463	1951 to 1990
Bimi-N'koni	Niger	610750	13° 28'N	05° 09'E	272	1951 to 1990
Biskra	Algeria	605250	34° 28'N	05° 26'E	81	1932 to 1990
Bissau (A	Guinea	617660	11° 31'N	15° 23'W	39	1941 to 1990
Bitam	Gabon	645100	02° 03'N	11° 17'E	600	1945 to 1990
Bloemfontein	South Africa	684420	29° 03'S	26° 10'E	351	1951 to 1990
Bobo-Diou	Upper Volta	655100	11° 06'N	04° 11'W	460	1941 to 1990
Bonthe	Sierra Loerne	618660	07° 19'N	12° 18'W	7	1955 to 1990
Bouake	Coute de Viore	655550	07° 26'N	05° 02'W	376	1951 to 1990
Bouar	C. Rep. of Africa	646010	05° 34'N	15° 22'E	19	1951 to 1990
Bougouni	Mali	612960	11° 15'N	07° 18'W	350	1951 to 1990
Brazzaville	Zaire	644500	04° 09'S	15° 09'E	319	1941 to 1990
Bulawayo	Zimbabwe	679640	20° 05'S	28° 22'E	343	1888 to 1990
Cairo	Egypt	623660	30° 04'N	31° 14'E	64	1951 to 1990
Casablanca	Moroco	601550	33° 20'N	07° 24'W	62	1924 to 1990
Chileka	Malawi	676930	15° 24'S	34° 34'E	766	1939 to 1990
Chipinge	Zimbabwe	679830	20° 07'S	32° 22'E	131	1933 to 1990
Cocobeach	Gabon	645040	01° 00'N	09° 21'E	12	1951 to 1990
Conakry	Guinea	618320	09° 20'N	13° 22'W	26	1905 to 1980
Constentine	Algeria	604190	36° 10'N	06° 22'E	660	1882 to 1980
Dakar/Yof	Senegal	616410	14° 26'N	17° 18'W	27	1898 to 1990
Dar-Es-Salaam	Tanzania	638940	06° 31'S	39° 07'E	55	1951 to 1990
Daru	Siera Loerne	618910	07° 35'N	10° 30'W	185	1951 to 1990
Der-el-Beida	Algeria	603900	36° 25'N	03° 09'E	25	1856 to 1990
Dimbokro	Coute de Viore	655620	06° 23'N	04° 25'W	92	1951 to 1990
Diourbel	Senegal	616660	14° 23'N	16° 08'W	7	1951 to 1990
Djuboti	Somalia	631250	11° 19'N	43° 05'E	13	1951 to 1990
Durban	South Africa	685880	29° 34'S	30° 34'E	80	1885 to 1990
El Fasher	Sudan	627600	13° 22'N	25° 12'E	733	1941 to 1990
El Golea	Algeria	605900	30° 20'N	02° 31'E	398	1892 to 1990
Fada N'gourma	Upper Volta	655070	12° 01'N	00° 13'E	308	1951 to 1990
Gagnoa	Coute de Viore	655570	06° 04'N	05° 34'W	205	1951 to 1990
Gaoua	Upper Volta	655220	10° 12'N	03° 06'W	333	1951 to 1990
Harare	Zimbabwe	677750	17° 33'S	31° 04'E	479	1898 to 1990
Helwane	Egypt	623780	29° 31'N	31° 12'E	149	1904 to 1990
Hombori	Mali	612400	15° 12'N	01° 24'W	287	1951 to 1990
Inhambane	Mozambique	673230	23° 31'S	35° 13'E	14	1931 to 1990
Jan Smuts	South Africa	683680	26° 04'S	28° 08'E	694	1951 to 1990
Johannesberg	South Africa	683697	26° 12'S	28° 06'E	753	1905 to 1960
Juba	Sudan	629410	04° 31'N	31° 21'E	460	1941 to 1990
Kaolack	Senegal	616790	14° 04'N	16° 92'W	6	1931 to 1990
Kasama	Zambia	674750	10° 07'N	31° 04'E	382	1934 to 1990
Kayes	Mali	612570	14° 15'N	11° 15'W	47	1896 to 1990
Keetmanshoop	Namibia	683120	26° 19'S	18° 04'E	67	1931 to 1990
Khartoum	Sudan	627210	15° 21'N	32° 19'E	382	1901 to 1990
Kimberly	South Africa	684380	28° 28'S	24° 27'E	198	1897 to 1990

Table 4.1: Station descriptive data.

STATION NAME	COUNTRY	WMO No.	LATITUDE	LONGITUDE	HEIGHT (m)	YEARS OF RECORD
Kindal	Mali	612140	18° 15'N	01° 12'E	458	1953 to 1990
Kolda	Senegal	616980	12°31'N	13°34'W	10	1951 to 1990
Kufra	Libya	622710	24°07'N	23°10'E	435	1951 to 1990
Lamberene	Gabon	645510	00°25'S	10°08'E	27	1951 to 1990
Libraville	Gabon	645000	00°16'N	09°15'E	12	1896 to 1990
Lichinga	Mozambique	672170	13°10'S	35°09'E	364	1954 to 1990
Linguere	Senegal	616270	15°13'N	15°04'W	20	1951 to 1990
Livingstone	Zambia	677430	17°29'S	25°29'E	985	1918 to 1990
Logos/Ikeja	Nigeria	652010	06°21'N	03°12'E	40	1892 to 1977
Lome	Togo	653870	06°06'N	01°09'E	20	1951 to 1990
Luanda	Angola	661600	08°30'S	13°08'E	74	1879 to 1990
Lungi	Sierra Loeme	618560	08°22'N	13°07'W	25	1891 to 1990
Maine-Sor	Niger	610960	13°08'N	11°35'E	338	1951 to 1990
Meknes	Morocco	601500	33°31'N	05°19'W	576	1923 to 1990
Makokou	Gabon	645560	00°20'N	12°31'E	509	1953 to 1990
Malakal	Sudan	628400	09°19'N	31°23'E	387	1941 to 1990
Mamou	Guinea	618200	10°13'N	12°03'W	783	1923 to 1990
Man	Coute de Viore	655480	07°13'N	07°18'W	339	1951 to 1990
Mang	Togo	653520	10°13'N	00°16'E	145	1951 to 1990
Maputo/	Mozambique	673410	25°33'S	32°20'E	39	1892 to 1990
Maradi	Niger	610800	13°16'N	07°03'E	372	1951 to 1990
Marrakech	Moroco	602300	31°22'N	08°01'W	468	1901 to 1990
Matam	Senegal	616300	19°35'S	23°15'E	15	1951 to 1990
Mayumba	Gabon	645030	03°15'S	10°23'E	31	1951 to 1990
Mersa Matruh	Egypt	623060	31°12'N	27°07'E	25	1951 to 1990
Mitzic	Gabon	645520	00°28'N	11°19'E	583	1951 to 1990
Mogadiscio	Somalia	632600	02°01'N	45°12'E	10	1911 to 1990
Mongu	Zambia	676330	15°09'S	23°05'E	52	1939 to 1990
Mopti	Mali	612650	14°18'N	04°03'W	276	1924 to 1990
Mouila	Gabon	645500	01°31'S	10°00'E	88	1951 to 1990
Nairobi/Kenyat	Kenya	637400	01°11'S	36°33'E	624	1951 to 1990
N'dele	C. Rep. of Africa	646540	08°14'N	20°23'E	510	1951 to 1990
Niamey-Ae	Niger	610520	13°17'N	02°06'E	323	1905 to 1990
Nioro du Sahel	Mali	612300	15°08'N	09°12'W	235	1951 to 1990
Nouadhibo	Sengal	614150	20°33'N	17°01'W	5	1923 to 1990
Nouakchot	Sengal	614420	18°03'N	15°34'W	2	1941 to 1990
Odienne	Coute de Viore	655282	09°18'N	07°20'W	434	1951 to 1990
Oran Es S	Algeria	604900	35°22'N	00°21'W	90	1852 to 1990
Ouagadougou	Upper Volta	655030	12°12'N	01°18'W	316	1924 to 1990
Pemba	Mozambique	672150	12°34'S	40°18'E	49	1947 to 1990
Pietersberg	South Africa	681740	23°31'S	29°16'E	230	1932 to 1990
Podor	Sengal	616120	16°23'N	14°34'W	6	1951 to 1990
Port Elizabeth	South Africa	688420	33°35'S	25°21'E	60	1885 to 1990
Port Gentile	Gabon	645010	00°25'S	08°27'E	3	1941 to 1990
Port Sudan	Sudan	626410	19°21'N	37°07'E	3	1943 to 1990
Pretoria	South Africa	682620	25°26'S	28°06'E	330	1951 to 1990
Quelimane	Mozambique	672830	17°31'S	36°31'E	11	1926 to 1990
Saint Louis	Sengal	616000	16°01'N	16°16'W	4	1862 to 1990
Sassandra	Coute de Viore	655990	04°34'N	06°03'W	62	1951 to 1990
Segou	Mali	612720	13°14'N	06°05'W	288	1951 to 1990
Sikasso	Mali	612970	11°12'N	05°24'W	374	1951 to 1990
Sokode	Togo	653610	08°35'N	01°05'E	386	1951 to 1990
Tabou	Coute de Viore	655920	04°15'N	07°13'W	21	1941 to 1990
Tahoua	Niger	610430	14°32'N	05°09'E	386	1951 to 1990
Tamanrasset	Algeria	606800	22°28'N	05°18'E	1378	1951 to 1990
Tambacoun	Sengal	616870	13°27'N	13°24'W	49	1923 to 1990
Tessalit	Mali	612020	20°07'N	00°35'E	494	1951 to 1990
Tete	Mozambique	672610	16°06'S	33°21'E	123	1952 to 1990
Tillabery	Niger	610360	14°07'N	01°16'E	209	1951 to 1990
Tomboucto	Mali	612230	16°25'N	03°00'W	263	1897 to 1990

Table 4.1: Continued from above

STATION NAME	COUNTRY	WMO No.	LATITUDE	LONGITUDE	HEIGHT (m)	YEARS OF RECORD
Tripoli	Libya	620100	32°24'N	13°05'E	81	1892 to 1990
Tunis-Carthage	Tunisia	607150	36°30'N	10°08'E	3	1887 to 1990
Upington	South Africa	684240	28°14'S	21°09'E	836	1951 to 1990
Wau	Sudan	628800	07°25'N	28°00'E	438	1942 to 1990
Windhoek	Namibia	681100	22°20'S	17°03'E	728	1917 to 1990
Yalinga	C. Rep. of Africa	646610	06°18'N	23°09'E	601	1953 to 1990
Ziguincho	Sengal	616950	12°19'N	16°09'W	26	1923 to 1990
Zinder	Niger	610900	13°28'N	08°35'E	452	1923 to 1990

Table 4.1: Continued from above

and 'c' are the magnitude of first and second quadratic terms.

The data series was analysed in Statsgraphics to determine these functions (a, b, c) describing the model. The model was then used to forecast ten years into the future because most stations have temperature records of about 40 years and therefore extrapolation beyond 10 years would result in an unacceptible error and reduced reliability of the derived model.

The standard error and the coefficient of variation were also derived for each station. The system (Statigraphics programme) derives the standard error (Se) as a function of

$$Se = s/\sqrt{n}$$

where 's', is the standard deviation, and 'n', is the number of years analysed. The coefficient of variation (Cv) is determined as a function of

$$Cv = (s/\bar{u})100$$

where '$\bar{u}$' is the mean temperature.

4.4. GIS APPLICATIONS TO SPATIAL ANALYSIS

Calculated mean annual surface air temperature trends for all the stations were captured into the IDRISI GIS (distributed by Clarke University in USA through the World Data Center-A (WDC-A), National Oceanic and Atmospheric Administration (NOAA), USA). GIS is a suite of computer programmes for the

capture, storage, retrieval, analysis and display of spatial data. GIS is an important decision-making support system which uses spatial data in vector or rasterised form for spatial analysis. The vector form of data uses the x and y coordinates of station location while the rasterised images are formed from regular grids of picture elements (pixels).

In preparation for data capturing, geographical coordinates of each meteorological station were converted into row and column coordinates which denoted their pixel location in terms of the African geographic window which was provided by the International Geosphere-Biosphere Program (IGBP): Pilot project for Africa with the IDRISI Programme. This unprojected window of Africa contained the entire African mainland with the coordinates shown in Figure 4.1. The image pixel resolution of the data provided by IGBP (Pilot project for Africa) was 10 minutes longitude by 10 minutes latitude. The pixel size of 10' in latitude and 10' in longitude produces 438 rows and 480 columns for this image. Figure 4.1 shows the cell sequencing and registration. Both column and row numbering start on the left upper corner.

The preparation of data for capturing was done through the Lotus spreadsheet programme. Coordinates for each station were all referenced to the Greenwich meridian (with positive values indicating East and negative values indicating West) and to the equator (with positive values indicating North and negative values indicating South). These coordinates were converted into their respective pixel coordinates. Each Lotus spreadsheet file was exported as an ASCII file for direct input as vector file into IDRISI. The structure of an IDRISI vector file is shown in Figure 4.2.

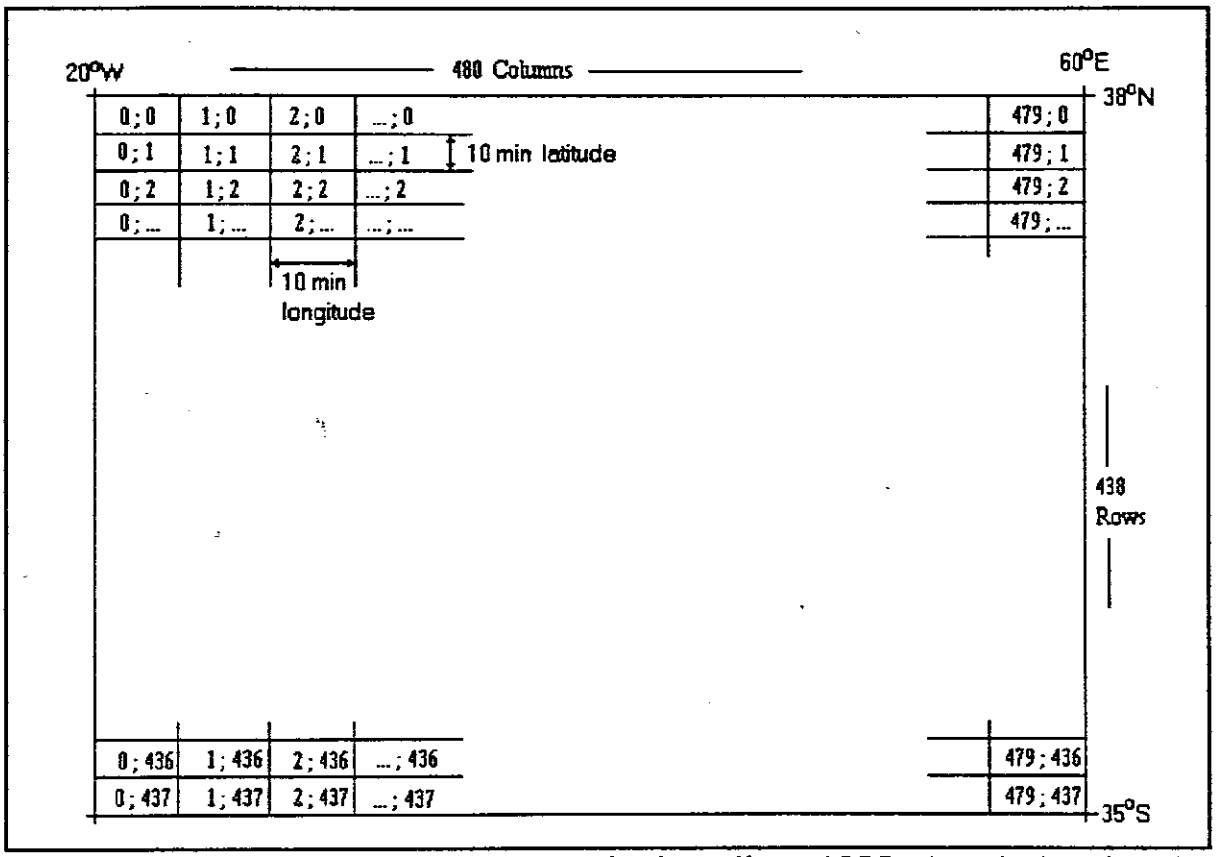

Figure 4.1: The unprojected window of Africa (from IGBP, 1990) showing the boundary co-ordinates and the rasterised resolution and co-ordinates.

To check whether all images were spatially synchronized and whether all stations were located accurately within the African mainland and surrounding islands, the image with stations locations was compared to the vector outline of the African continent provided by the IGBP (Pilot Project for Africa) (Figure 4.3).

The distribution of stations is not homogeneous and there are large areas of Africa with very poor representation. Nevertheless, each station is assumed to be representative of the surrounding region.

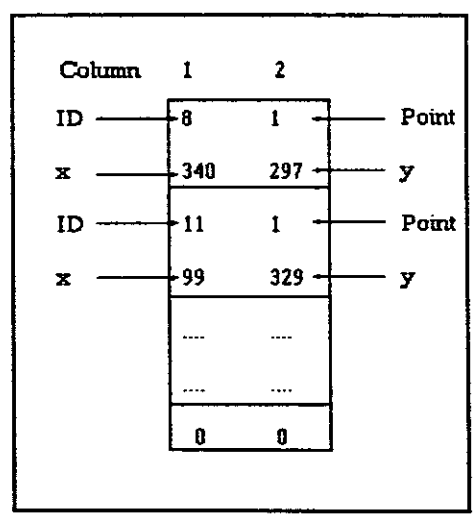

Figure 4.2: The structure of an IDRISI vector file. ID = feature identifier, point = feature, y = latitude, and x = longitude.

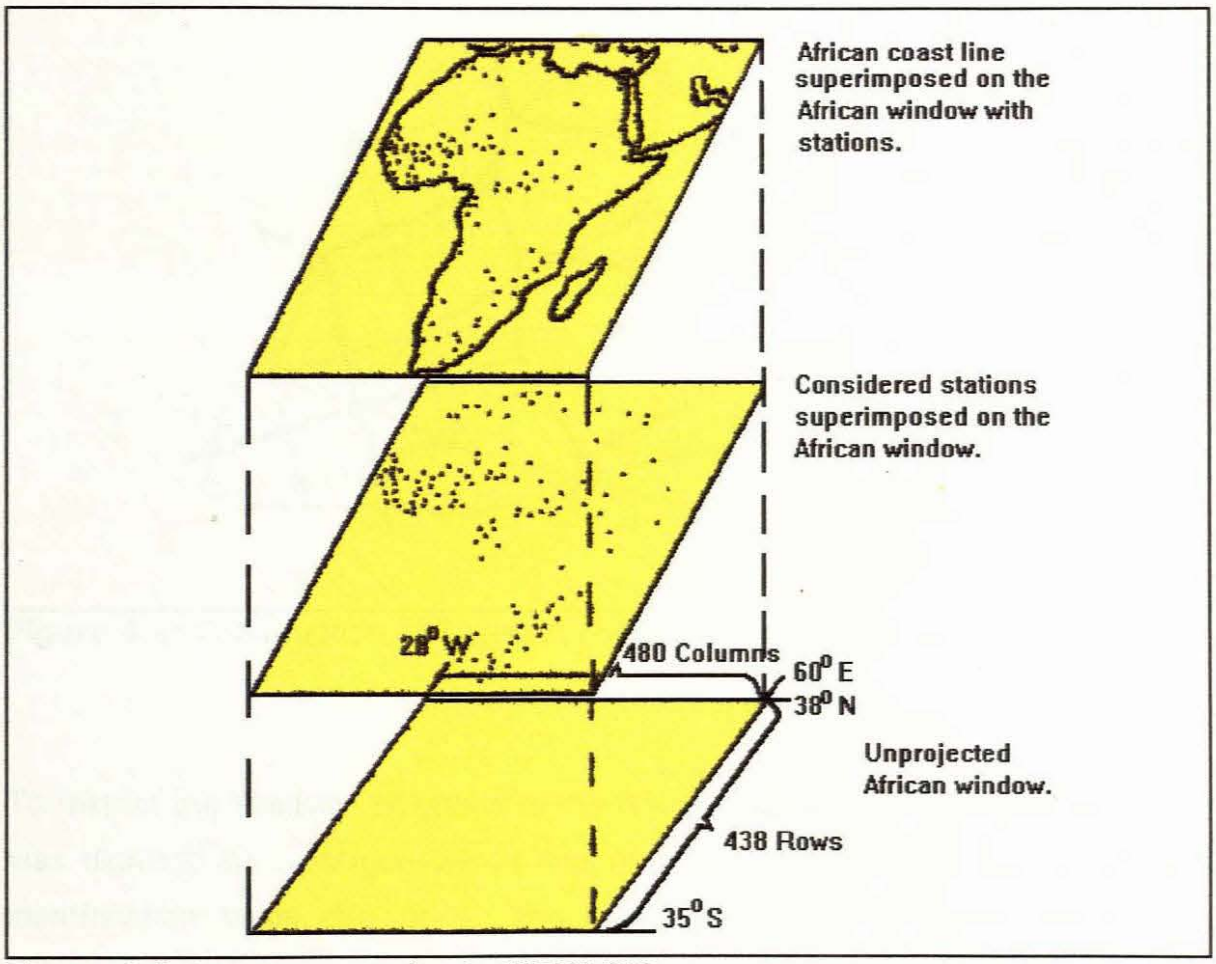

Figure 4.3: Image processing in IDRISI GIS.

To define the regions represented by each station, Theissen polygons were constructed around each station pixel. The use of Theissen polygons made some allowance for the uneven distribution of stations throughout the continent. Figure 4.4 illustrates the construction of Theissen polygons. In deriving Theissen polygons (Ward, 1990), perpendicular bisectors are drawn through the straight lines joining all adjacent stations. This leaves each station in the centre of a polygon, formed by the perpendicular bisection, which varies in size according to the spacing between stations. These polygons were derived for each station and used to create images of spatial patterns of the annual temperature trends as well as images of the mean square errors, the standard errors, and the coefficients of variation of the annual temperatures series.

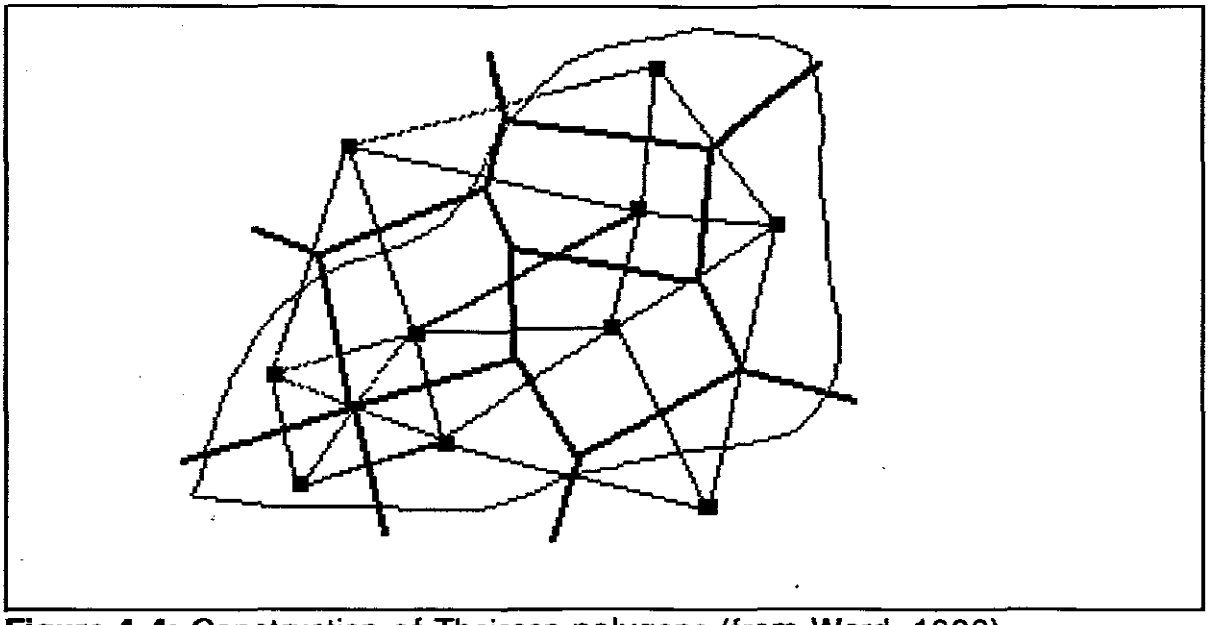

Figure 4.4: Construction of Theissen polygons (from Ward, 1990).

To restrict the Theissen polygons to the African mainland, the African coast line was digitised as a polygon which was rasterised as an image with a constant identification value (ID) of 1. The background or surrounding ocean was designated an ID value of 0 so that when this image was multiplied with other images it removed all spatial patterns over the oceans (ID = 0). Figure 4.5 summarise the step-wise process of producing these images which were used in subsequent analysis.

4.5 CONCLUSION

This chapter has clearly outlined research strategies used to achieve the results discussed in the next chapter. The use of Theissen polygons on point data produced presentable images of spatial generalisation.

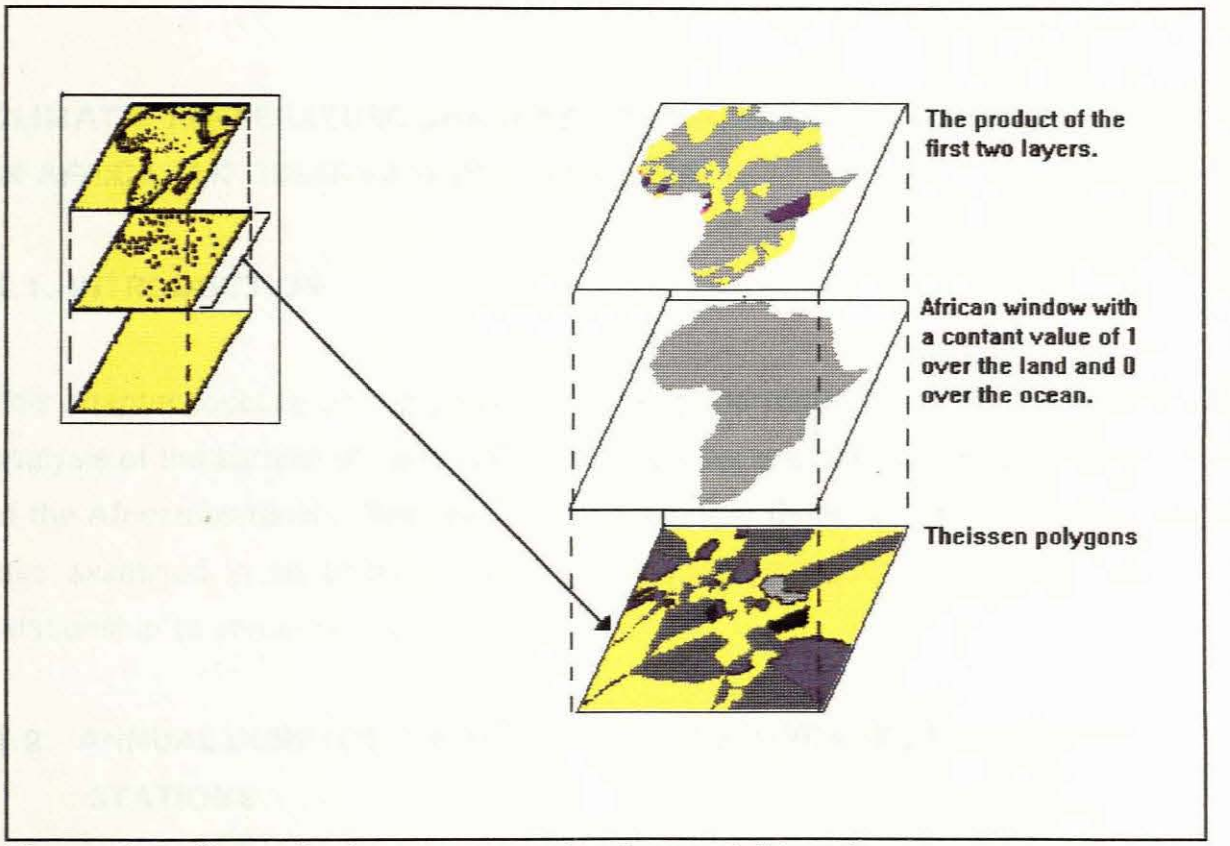

Figure 4.5: Step-wise image processing for spatial trends.

CHAPTER 5

CLIMATIC TEMPERATURE CHANGES FOR DIFFERENT CLIMATIC STATIONS IN AFRICA: AN OBSERVATIONAL ANALYSIS

5.1. INTRODUCTION

This chapter focuses on the presentation and interpretation of results from the analysis of the surface air temperature changes for the different weather stations of the African continent. The spatial arrangement of these temperature trends are also examined in an effort to identify significant patterns which may have a relationship to some forcing functions.

5.2. ANNUAL SURFACE AIR TEMPERATURE FORECASTS FOR INDIVIDUAL STATIONS

The derived annual surface air temperature trends for all the available stations in Africa are shown in Table 5.1.

- Column A gives the quadratic equations describing the temperature change with time (T) in years from the start of each station temperature records.

- Column B represents actual or predicted temperatures for 1990 in terms of the model. An asterisks show those stations with predicted temperatures because they were without data in 1990,

- Column C presents the predicted temperatures for the year 2000.

- Column D represents the predicted temperature change for the decade from 1990 to 2000. The range of temperature changes lies between -3.02° and 1.75°C. These extreme lower and upper limits are predicted for Conakry in Guinea and El Fasher in Sudan, respectively.

STATION	A (quadratic model)	B T (1990)	C T (2000)	D δT	E Se_1	F Se_2	G Cv
Accra	26.34+2.008E-03*T+9.087E-05*T^2	27.07 *	27.24	0.17	0.16	0.05	1.61
Agadez	29.47-9.614E-02*T+1.374E-03*T^2	28.95	29.88	0.94	0.44	0.11	2.86
Agadir	19.25-4.265E-02*T+4.396E-04*T^2	18.25	18.37	0.21	0.25	0.07	3.01
Alexander Bay	16.2 -7.087E-03*T+6.489E-04*T^2	16.91	17.14	0.50	0.17	0.08	2.85
Aliwal North	14.79+2.104E-02*T-1.680E-04*T^2	15.09	14.91	0.17	0.19	0.05	3.11
Aktapame	25.9 -3.895E-02*T+8.704E-04*T^2	25.71	26.09	0.38	0.13	0.07	1.47
Bamako	28.08+7.063E-03*T-2.092E-04*T^2	27.61	27.38	-0.23	0.84	0.12	3.35
Bambari	26.39-7.939E-02*T+1.384E-03*T^2	25.35	25.72	0.37	0.16	0.10	2.03
Bangassou	26.64-1.110E-01*T+1.979E-03*T^2	25.59	26.42	0.83	0.08	0.08	1.86
Bangui	26.29-1.956E-02*T-7.094E-05*T^2	25.16	27.18	-0.27	0.09	0.07	1.76
Banjul/Yundum	25.36-2.269E-02*T+4.772E-04*T^2	26.60	27.18	0.58	0.31	0.09	2.82
Bechar	21.48-7.110E-02*T+2.351E-03*T^2	19.06	18.56	-0.50	1.49	0.23	6.18
Beira	25.08-5.138E-02*T+7.895E-04*T^2	24.80	25.29	1.36	0.15	0.06	1.79
Benina	19.72+9.156E-03*T+1.814E-04*T^2	20.50	20.77	0.27	0.29	0.09	2.98
Berberati	24.95-5.612E-02*T+7.826E-04*T^2	23.95	24.08	0.13	0.15	0.09	2.04
Bilma	25.99+5.653E-02*T-1.280E-03*T^2	26.21	25.62	-0.59	0.87	0.16	3.62
Birao	26.78-5.546E-02*T+1.706E-03*T^2	27.21	28.16	0.95	0.21	0.09	1.92
Birni-N'koni	28.33+1.977E-02*T-1.609E-04*T^2	28.85	28.91	0.06	0.20	0.08	1.67
Biskra	22.51-8.271E-02*T+1.498E-03*T^2	22.75	23.81	1.06	0.90	0.16	4.84
Bissau	26.40-2.005E-02*T+8.148E-04*T^2	27.37	28.05	0.68	0.05	0.07	1.49
Bitam	24.48-2.642E-02*T-2.664E-04*T^2	22.75	22.22	-0.53	0.14	0.10	2.23
Bloemfontein	*15.78-6.180E-02*T+1.790E-03*T^2*	*16.10*	*17.05*	*0.96*	*0.36*	*0.10*	*4.23*
Bobo-Diou.	27.27-3.318E-02*T+6.369E-04*T^2	27.17	27.53	0.36	0.12	0.05	1.36
Bouthe	26.90-3.143E-02*T+1.583E-03*T^2	27.74	28.69	0.95	0.08	0.07	1.27
Bouake	26.46-8.102E-02*T+1.656E-03*T^2	25.82	26.47	0.65	0.10	0.07	1.57
Bouar	24.77-1.249E-01*T+2.088E-03*T^2	23.07	23.66	0.59	0.23	0.13	3.13
Bougouni	26.99-4.859E-04*T+1.554E-04*T^2	27.21	27.34	0.13	0.15	0.07	1.45
Brazzaville	25.10-2.453E-02*T+7.216E-04*T^2	25.63	26.16	0.53	0.09	0.06	1.44
Bulawayo	26.30-1.349E-01*T+1.176E-04*T^2	26.77	25.67	-1.10	0.26	0.05	2.74
Cairo	21.78-4.543E-02*T+1.844E-03*T^2	22.82	23.98	1.17	0.20	0.13	2.84
Casablanca	17.16+2.334E-02*T-3.166E-04*T^2	17.32	17.11	-0.22	0.24	0.07	2.90
Chileka	22.23+8.815E-03*T-2.312E-04*T^2	22.08	21.91	-0.17	0.15	0.06	1.79
Chipinge	17.96+1.124E-02*T-1.485E-04*T^2	18.12	18.04	-0.07	0.15	0.05	2.20
Cocobeach	26.05-3.589E-02*T+9.334E-04*T^2	13.47	10.71	-2.77	0.04	0.04	0.86
Conakry	26.38+1.636E-01*T-2.588E-03*T^2	21.59 *	18.57	-3.02	1.40	0.25	6.21
Constentein	14.53+4.676E-02*T-4.847E-04*T^2	13.92 *	13.30	-0.63	0.49	0.12	5.26
Daker/Yof	25.26-1.373E-02*T-2.996E-05*T^2	23.74	23.55	-0.20	0.31	0.07	2.90
Dar-Es-Salaam	26.16-5.155E-02*T+1.267E-03*T^2	26.08	26.68	0.60	0.08	0.06	1.25
Daru	25.64+3.747E-02*T-3.327E-04*T^2	26.60	26.68	0.08	0.09	0.08	1.61
Der-el-Beida	18.28-5.749E-02*T+4.202E-04*T^2	18.12	18.72	0.59	0.73	0.10	6.08
Dimbokro	27.41-2.708E-02*T+3.476E-04*T^2	26.88	26.91	0.04	0.23	0.09	1.87
Diourbel	27.31+1.671E-02*T-2.162E-04*T^2	27.63	27.61	-0.02	0.26	0.09	1.90
Djuboti	29.33-5.823E-03*T+7.284E-04*T^2	30.21	30.80	0.58	0.09	0.08	1.43
Durban	20.02-8.684E-03*T+1.652E-04*T^2	20.93	21.21	0.28	0.16	0.05	2.51
El Fasher	25.57-7.335E-02*T+2.300E-03*T^2	27.50	29.25	1.75	0.21	0.13	3.42
El Golea	21.04-2.669E-02*T+4.275E-04*T^2	22.53	23.14	0.61	0.96	0.14	5.30
Fada N'gourma	27.80-3.280E-02*T+1.059E-03*T^2	28.13	28.73	0.60	0.20	0.08	1.77
Gagnoa	26.22-6.671E-02*T+1.429E-03*T^2	25.79	26.38	0.59	0.13	0.08	1.61
Gaoua	27.21+5.649E-05*T+1.939E-04*T^2	27.51	27.68	0.17	0.08	0.05	1.13
Harare	17.72+1.677E-02*T-1.717E-04*T^2	17.81	17.64	-0.17	0.17	0.04	2.36
Helwan	21.08+2.549E-02*T-2.684E-04*T^2	21.28	21.05	-0.23	0.23	0.06	2.34
Hombori	29.73+1.206E-02*T+5.256E-04*T^2	30.00	31.58	0.58	0.28	0.11	2.08
Inhambane	23.77-1.758E-02*T+3.275E-04*T^2	23.88	24.12	0.24	0.10	0.05	1.44
Jan Smuts	15.51-4.099E-02*T+1.488E-03*T^2	16.18	17.08	0.90	0.30	0.10	4.04
Johannesburg	15.05+3.144E-02*T-1.628E-04*T^2	16.55	16.57	0.02	0.18	0.07	3.54
Juba	27.65-8.118E-02*T+1.810E-03*T^2	28.02	29.16	1.14	0.13	0.07	1.61
Kaolack	28.58-5.163E-02*T+8.361E-04*T^2	28.45	29.00	0.55	0.24	0.07	1.89
Kasama	19.98-1.869E-02*T+3.632E-04*T^2	20.07	20.32	0.26	0.07	0.04	1.46
Kayes	29.77-4.500E-03*T-2.934E-05*T^2	29.09	28.98	-0.10	0.36	0.08	2.17
Keetmanshoop	20.73-3.270E-03*T-1.262E-05*T^2	20.49	20.44	-0.05	0.32	0.08	2.79
Khartoum	29.67-3.308E-02*T+3.780E-04*T^2	29.72	30.10	0.38	0.40	0.07	2.32
Kimberly	16.29+2.677E-02*T-1.092E-04*T^2	17.84	17.89	0.05	0.34	0.08	4.27

Table 5.1: Derived Statistics. (see text for description of columns)

STATION	A (quadratic model)	B T (1990)	C T (2000)	D δT	E Se_1	F Se_2	G Cv
Kindal	28.43+3.188E-02*T-2.209E-04*T^2	29.31	29.44	0.13	0.32	0.12	2.12
Kolda	28.02-5.460E-02*T+8.884E-04*T^2	27.24	27.47	0.24	0.28	0.11	2.12
Kufra	22.75+4.943E-02*T-1.048E-03*T^2	23.09	22.66	-0.43	0.46	0.13	3.00
Lamberene	25.71+2.818E-02*T-1.018E-03*T^2	25.26	24.65	-0.61	0.12	0.07	1.49
Libraville	26.01-8.983E-03*T+1.209E-04*T^2	26.24	26.39	0.15	0.14	0.06	1.46
Lichinge	17.99+3.413E-03*T+4.992E-04*T^2	18.76	19.20	0.44	0.08	0.06	2.05
Linguere	27.57+6.399E-02*T-7.477E-04*T^2	28.93	28.91	-0.02	0.31	0.11	2.39
Livingstone	21.85-1.706E-02*T+2.730E-04*T^2	21.77	22.02	0.25	0.23	0.06	2.30
Logos/Ikeja	27.36-2.871E-02*T+1.948E-04*T^2	26.52 *	26.68	0.16	0.24	0.06	2.18
Lome	26.34+3.738E-03*T+2.647E-04*T^2	26.89	27.16	0.27	0.10	0.06	1.40
Luanda	2.89+1.416E-02*T+1.304E-05*T^2	24.62	24.79	0.17	0.19	0.07	2.60
Lungi	27.27-2.224E-02*T+1.510E-04*T^2	26.54	26.64	0.09	0.12	0.04	1.54
Maine-Sorie	27.16+4.646E-02*T-5.672E-04*T^2	28.11	28.07	-0.03	0.34	0.11	2.34
Meknes	16.90+7.012E-03*T-1.338E-04*T^2	16.77	16.64	-0.12	0.52	0.10	4.33
Makokou	24.14-3.277E-02*T+3.585E-04*T^2	23.42	23.40	-0.03	0.06	0.06	1.28
Malakal	27.19-8.373E-02*T+2.218E-03*T^2	28.42	29.98	1.56	0.10	0.07	1.67
Mamou	23.00+5.140E-02*T-9.169E-04*T^2	22.33	21.52	-0.81	0.15	0.08	1.86
Man	24.55+6.058E-02*T-2.562E-03*T^2	22.88	21.15	-1.73	0.10	0.08	1.67
Mango	27.79-2.929E-02*T+1.011E-03*T^2	28.18	28.78	0.60	0.15	0.08	1.61
Maputo	22.67-2.797E-02*T+3.531E-04*T^2	23.32	23.77	0.45	0.21	0.06	2.58
Maradi	26.78+4.704E-02*T-7.660E-04*T^2	27.45	27.24	-0.20	0.40	0.12	2.46
Marrakech	19.41+1.299E-02*T-1.890E-04*T^2	19.07	18.84	-0.23	0.55	0.1	3.94
Matam	27.93+6.074E-02*T+9.139E-05*T^2	30.44	31.13	0.69	0.39	0.17	3.36
Mayumba	25.08+5.731E-03*T-3.642E-04*T^2	24.74	24.48	-0.26	0.10	0.06	1.32
Mersa Matruh	19.35-4.880E-03*T+1.754E-04*T^2	19.42	19.53	0.11	0.07	0.05	1.43
Mitzic	23.26+1.685E-02*T-5.984E-04*T^2	23.01	22.65	-0.36	0.04	0.05	0.98
Mogadiscio	26.55+3.317E-02*T-4.519E-04*T^2	26.35	25.92	-0.43	0.31	0.08	2.17
Mongu	23.15-1.054E-01*T+1.790E-03*T^2	22.43	23.38	0.95	0.15	0.08	2.48
Mopti	28.28-2.125E-02*T+4.260E-04*T^2	28.73	29.12	0.39	0.78	0.12	3.24
Mouila	26.35-2.442E-02*T-1.704E-04*T^2	25.14	24.75	-0.39	0.12	0.09	1.78
Nairobi	19.88-9.905E-02*T+2.208E-03*T^2	12.66	9.72	-2.93	0.09	0.06	2.10
N'dele	26.93-5.341E-02*T+8.067E-04*T^2	26.08	26.25	0.18	0.12	0.09	1.62
Niamey	29.28-5.060E-03*T+2.884E-05*T^2	28.64	28.54	0.00	0.34	0.07	2.03
Nioro du Sahel	27.51+3.119E-02*T+2.065E-04*T^2	29.04	29.54	0.49	0.29	0.12	2.54
Nouadhibou	23.52-5.848E-03*T-6.963E-04*T^2	20.00	18.94	-1.06	5.22	0.34	11.27
Nouakchot	25.55+4.993E-02*T-1.487E-03*T^2	24.43	23.32	-1.11	0.47	0.12	3.13
Odienne	27.18-1.292E-01*T+2.327E-03*T^2	25.68	26.44	0.76	0.14	0.12	2.40
Oran Es S	17.51+4.219E-03*T-4.306E-05*T^2	17.27	17.19	-0.08	0.35	0.06	3.41
Ouagadougou	28.92-2.578E-02*T+2.356E-04*T^2	28.24	28.32	0.08	0.23	0.07	1.83
Pemba	26.12-3.666E-02*T+4.837E-04*T^2	23.65	22.82	-0.83	0.11	0.06	1.50
Pietersburg	17.81+1.894E-02*T-4.044E-04*T^2	17.55	17.23	-0.32	0.23	0.07	2.81
Podor	27.63+1.037E-02*T-5.861E-06*T^2	28.02	28.12	0.10	1.56	0.22	4.58
Port Elizabeth	16.42-8.861E-04*T+1.430E-04*T^2	17.90	18.21	0.31	0.10	0.05	3.28
Port Gentile	26.39-3.626E-02*T+5.410E-04*T^2	25.91	26.13	0.22	0.14	0.06	1.58
Port Sudan	28.22-1.822E-02*T+4.837E-04*T^2	28.43	28.75	0.32	0.23	0.07	1.78
Pretoria	17.85-5.274E-03*T+6.256E-04*T^2	18.60	19.10	0.50	0.19	0.08	2.79
Quelimane	24.25+7.345E-02*T-1.529E-03*T^2	22.69	21.31	-1.38	0.80	0.14	4.70
Saint Louis	23.59+1.613E-02*T-2.551E-05*T^2	25.24	25.33	0.09	0.36	0.07	2.96
Sassandra	26.15-4.289E-02*T+7.542E-04*T^2	25.62	25.86	0.23	0.07	0.06	1.25
Segou	27.47-6.315E-03*T+9.412E-04*T^2	28.66	29.42	0.77	0.38	0.12	2.65
Sikass	27.09-9.829E-03*T-1.246E-04*T^2	26.52	26.31	-0.21	0.11	0.07	1.39
Sokode	26.08-4.235E-02*T+1.083E-03*T^2	26.07	26.60	0.53	0.12	0.06	1.44
Tabou	25.81+1.775E-02*T-6.576E-04*T^2	25.10	24.56	-0.53	0.04	0.04	1.00
Tahoua	28.18+9.536E-02*T-2.235E-03*T^2	28.50	27.49	-1.01	0.44	0.13	2.52
Tamanrasset	21.16+5.084E-02*T-2.966E-04*T^2	22.69	22.94	0.25	0.36	0.15	3.53
Tambacoun	28.31-1.327E-02*T+2.718E-04*T^2	28.64	28.90	0.26	0.25	0.07	1.87
Tessallit	28.86-3.777E-02*T+9.887E-04*T^2	28.89	29.39	0.49	0.34	0.12	2.12
Tete	26.63-5.426E-02*T+1.533E-03*T^2	26.51	27.29	0.78	0.19	0.08	1.82
Tillabery	29.37+1.849E-02*T-4.364E-05*T^2	30.02	30.17	0.15	0.29	0.10	1.95
Tombouctou	27.87-3.278E-02*T+4.585E-04*T^2	28.79	29.36	0.57	0.35	0.11	2.64
Tripoli	19.80-6.194E-03*T+1.342E-04*T^2	20.48	20.70	0.21	0.30	0.08	2.98
Tunis-Carthage	16.74+2.234E-02*T-6.069E-05*T^2	18.40	18.49	0.09	0.29	0.07	3.95

Table 5.1: Continued from above.

STATION	A (quadratic model)	B T (1990)	C T (2000)	D δT	E Se_1	F Se_2	G Cv
Upington	19.87-7.093E-03*T+8.821E-04*T^2	20.93	21.64	0.71	0.38	0.12	3.56
Wau	26.47-4.996E-02*T+1.796E-03*T^2	28.21	29.61	1.40	0.07	0.07	1.67
Windhoek	19.08-9.710E-03*T+2.704E-04*T^2	19.81	20.14	0.32	0.40	0.09	3.50
Yalinga	24.88-2.063E-02*T-4.651E-04*T^2	23.48	22.88	-0.60	0.11	0.10	2.05
Ziguincho	26.27+2.891E-02*T-5.277E-04*T^2	25.84	25.37	-0.47	0.23	0.07	2.03
Zinder	28.84-2.445E-02*T+1.712E-04*T^2	27.97	27.97	0.00	0.49	0.09	2.64

Table 5.1: Continued from above.

- Column E shows the mean standard error (Se_1) in δT for all these models. Most of these are within a small range close to zero (< 0.5°C). The stations with high errors are Bechar (Algeria), Conarkry (Guinea), Nouadhibou (Sahel), and Podor (Sahel) with standard errors of 1.49°, 1.40°, 5.22°, and 1.56°C, respectively.

- The penultimate (F) and the last (G) columns represent the standard error (Se_2) and the coefficient of variation for the analysed annual temperature series for each station, respectively.

Out of the 130 stations examined, 86 (66%) show increasing temperature trends and only 44 (34%) stations show decreasing temperature trends. Figure 5.1 shows the absolute frequency distribution of stations with increasing temperature trends. The temperature trends within a range of 0° to 0.45°C have the highest frequency (36%). The temperature trends lying between 1.46° and 2.45°C have the lowest frequency (2%).

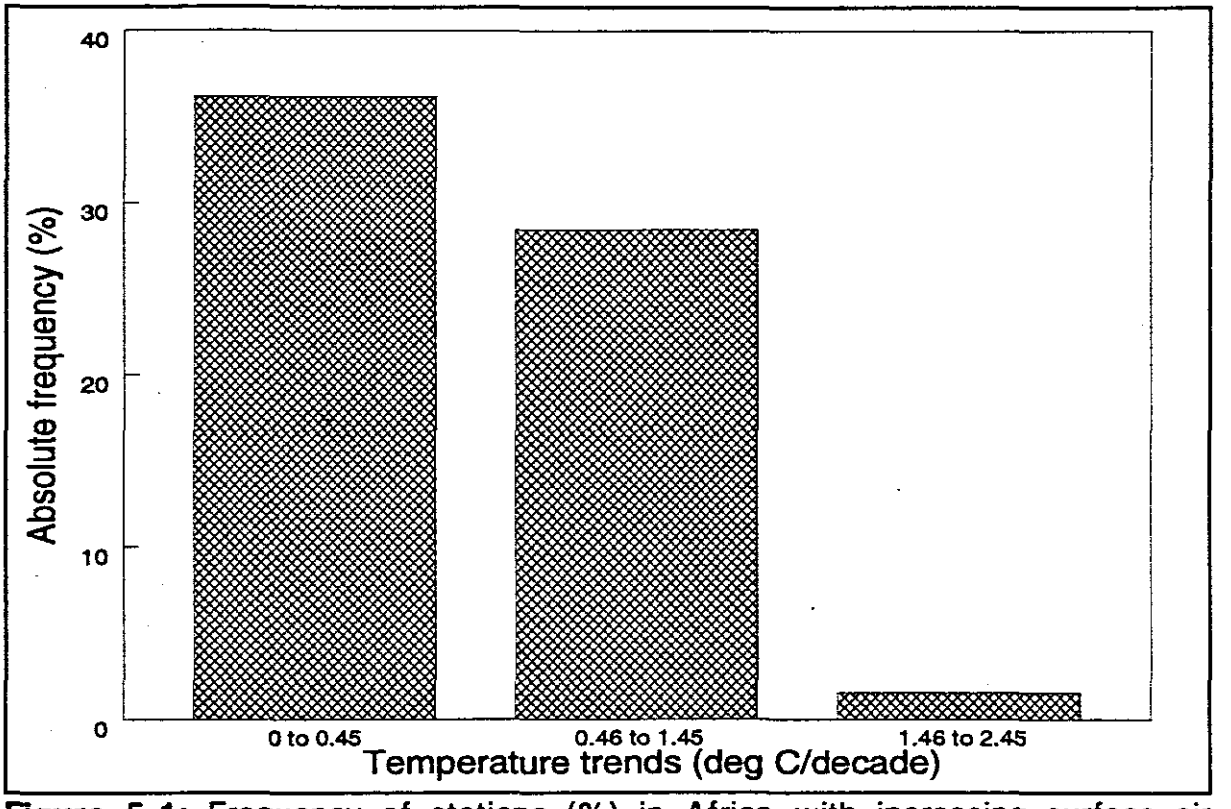

Figure 5.1: Frequency of stations (%) in Africa with increasing surface air temperature trends (Note, unequal class interval).

The absolute frequency distribution of stations with decreasing temperature trends are shown in Figure 5.2. There is a much greater spread in temperature trends than there is in the case of increasing trends shown in Figure 5.1. The temperature trends lying between -0.01° to -0.45°C have the highest frequency (22%).

The absolute frequency distribution of all these temperature trends may approach normality with most of the stations (58%) having temperature trends lying between -0.45° to 0.45°C (median at 0.16°C) (Figure 5.3). The standard deviation, the skewness, and the kurtosis for normal distribution for all the stations examined are 0.72°, -1.69° and 5.88°C, respectively.

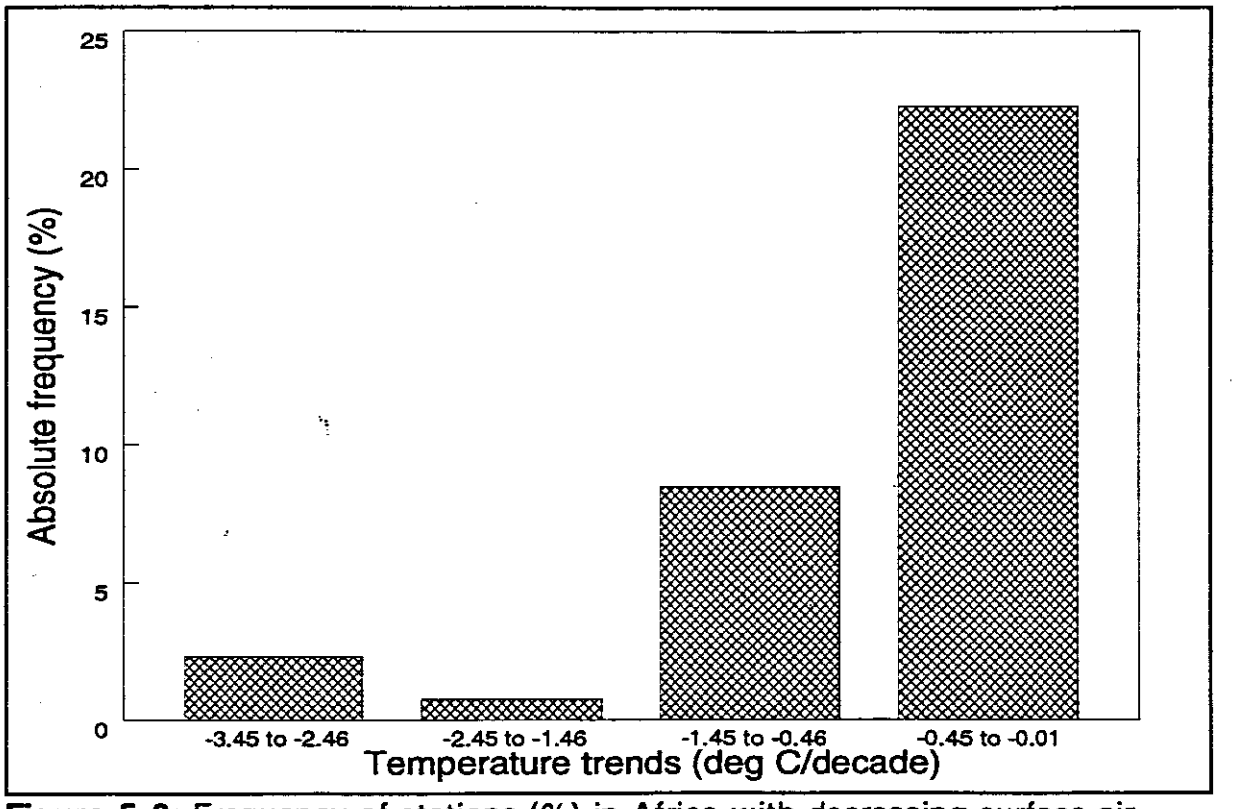

Figure 5.2: Frequency of stations (%) in Africa with decreasing surface air temperature trends.

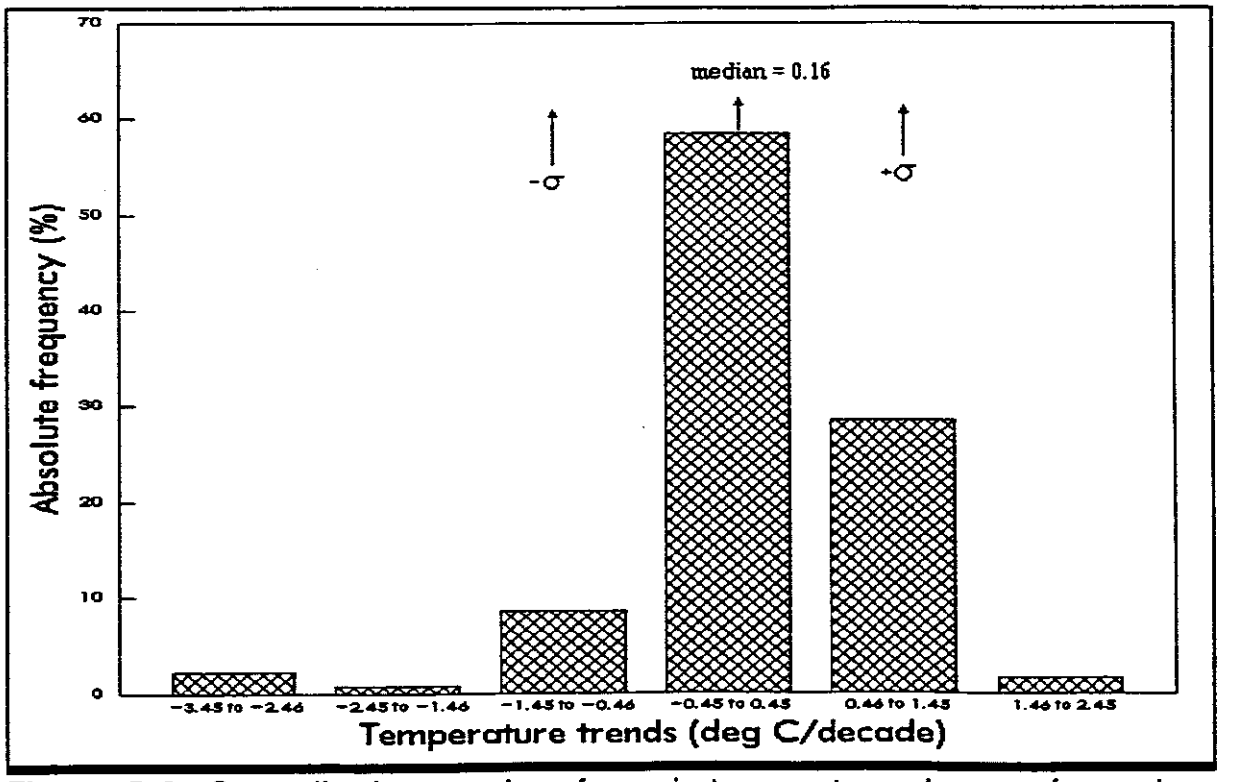

Figure 5.3: Generalised annual surface air temperature changes for various stations in Africa.

5.3. PROBLEMS ON TEMPERATURE CHANGE MODEL RELIABILITY

Many stations analysed in this project have a relatively short time-series data. Some of these series may form part of cyclic trends. Figure 5.4 illustrates the problems in deriving temperature change models from short time-series data using the temperature series from Port Elizabeth where the data series is over 100 years. The fitting of a quadratic trend to the data for 1886 to 1924 period (38 years) produces a temperature trends represented by AB (vertical rectangles). An extended ten year forecast to 1934 (BC) for this model would result in a predicted temperature change of 0.14°C/decade.

The 1914 to 1954 data series (40 years) also incorporates a large range of temperatures which produce a quadratic model shown as DE in Figure 5.4 (horizontal rectangles). The ten year forecast, 1954 to 1964 (EF), for this model is greatly influenced by the recession of the annual temperatures for the last few years and which show a decreasing temperature trend (-0.15°C). When compared with temperature trends derived from the entire long-term time-series data (1886 to 1990), the two scenarios (presented by ABC and DEF) illustrate how unreliable and misleading models may be when derived from short time-series data. In view of the limited time-series data that most stations had, forecasting beyond 10 years following the model DE would result in an unrealistic prediction like that of FG. FG is the direct opposite to the observed annual temperature trends for the entire series.

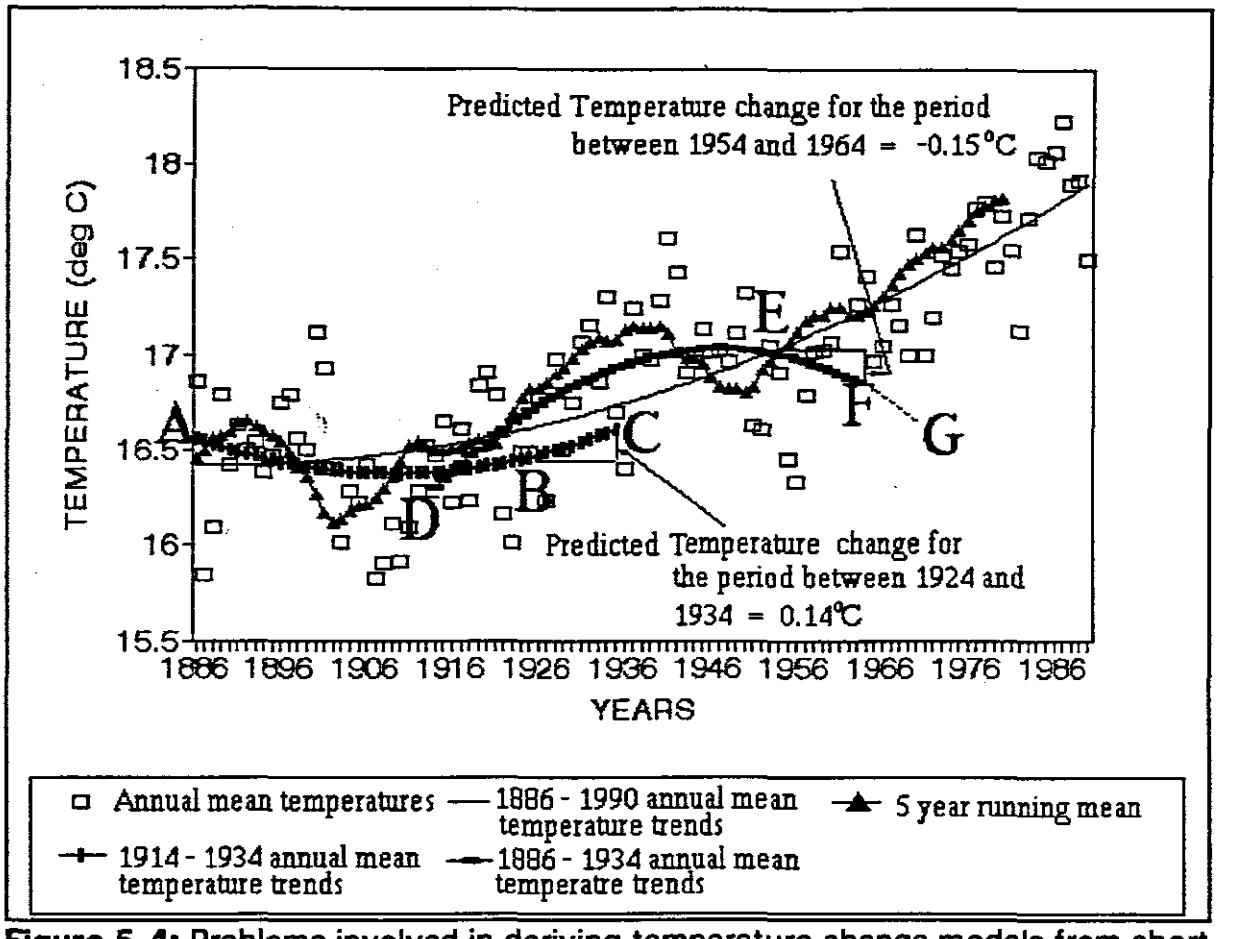

Figure 5.4: Problems involved in deriving temperature change models from short time-series data.

5.4. SPATIAL PATTERNS OF PREDICTED ANNUAL SURFACE AIR TEMPERATURE CHANGES FOR AFRICA

The spatial patterns of increasing and decreasing temperature trends are shown in Figure 5.5. This image is derived using Theissen polygons to produce areas represented by the enclosed station. The section in dark shading indicates those polygons with increasing temperature trends. There is some orientation in the pattern of these changing temperatures. There are three broad bands of decreasing temperature trends which are located :-

1. around the north western coast of Africa (DD_1),
2. from Zaire and the southern Chad Basin through Libya, to Egypt (EE_1),
3. from Namibia through the Zimbabwe Highlands to northern Mozambique and possibly into East Africa (FF_1).

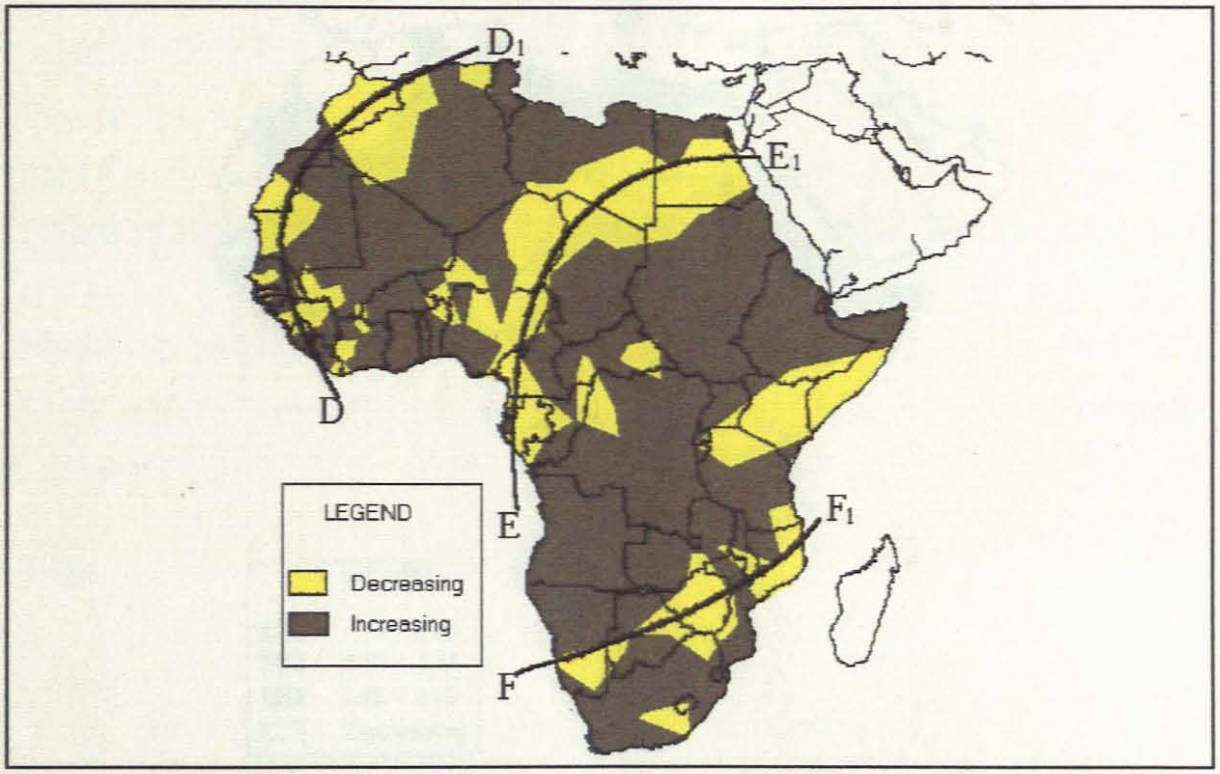

Figure 5.5: Spatial patterns of annual surface air temperature trends for Africa.

5.4.1. SPATIAL PATTERNS OF PREDICTED INCREASING ANNUAL SURFACE AIR TEMPERATURE TRENDS

The predicted increases for annual surface air temperature trends for Africa, shown in Figure 5.6, ranges from 0° (Zinder and Niamey both in Niger) to 1.75°C (El Fasher in Sudan). The regions with increasing temperature trends were classified into three unequal categories:-

1. 0° to 0.45°C, (half of range -0.45° to +0.45°C)
2. 0.46° to 1.45°C, and
3. 1.46° to 2.45°C.

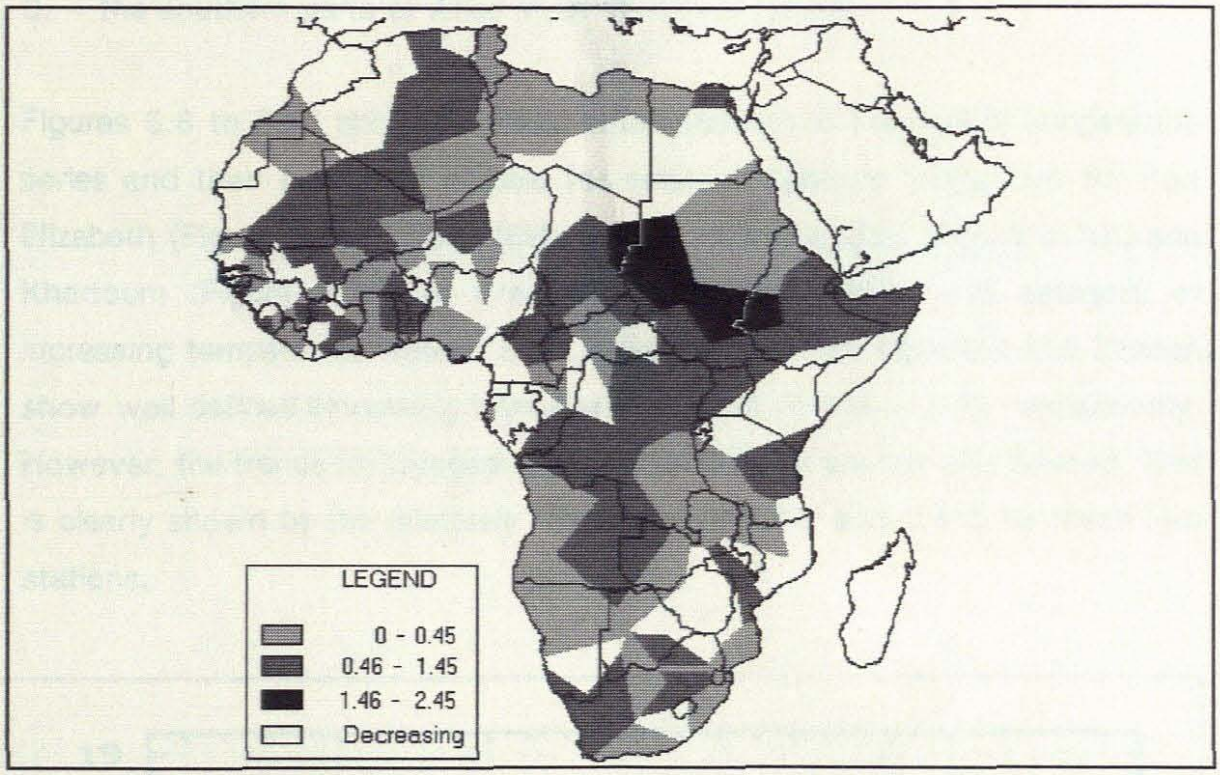

Figure 5.6: Spatial patterns of increasing annual surface air temperature trends (°C/decade) for Africa.

Figure 5.7 shows the spatial pattern of the predicted increasing annual surface air temperature trends which range from 0° to 0.45°C. Generally, these trends are observed in:-

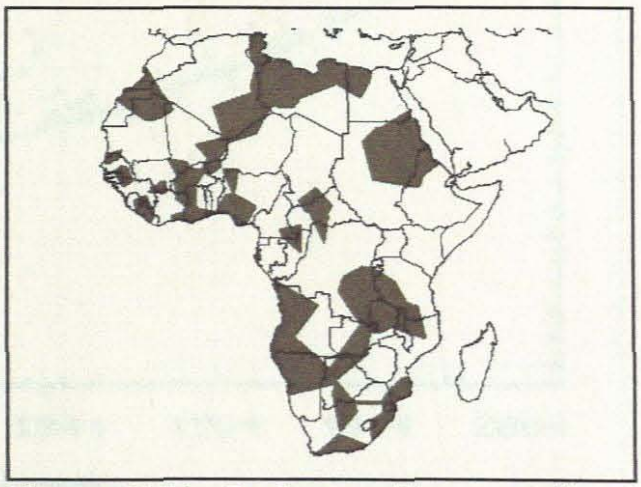

Figure 5.7: Regions with a predicted temperature change of 0° - 0.45°C/decade.

1. the low lying areas of the Gabes and the Libyan Basins to the south through the Ahaggar plateau and the Aïr Highlands (Figure 2.4),

2. the low lying coastal areas of Ghana, Togo, Benin, Coute de Viore, Liberia, and Nigeria, and

3. the southern parts of Atlas Mountains (Anti-Atlas).

Figures 5.8 to 5.11 show graphical representation of the actual temperature series and their prediction models for selected stations. These are for Port Elizabeth (Figure 5.8), Durban (Figure 5.9), Ouagadougou (Figure 5.10), and Khartoum (Figure 5.11) as examples of stations within this category of increasing temperature trends. Both the series for Port Elizabeth and Durban show well defined increasing trends with Se of 0.1° and 0.16°C, respectively. However, the trends for Ouagadougou and Khartoum are not well defined. This is clearly shown by the relatively higher Se_1 of 0.23° and 0.4°C for these two stations.

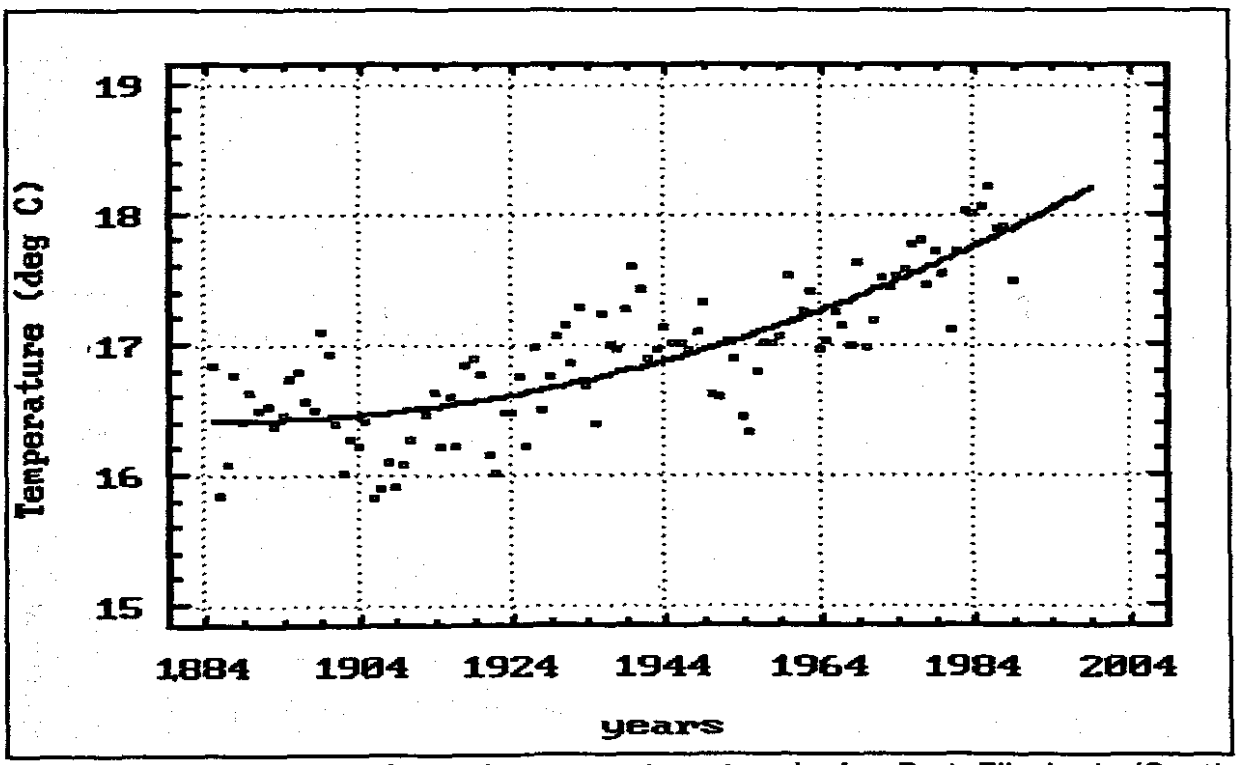

Figure 5.8: Annual surface air temperature trends for Port Elizabeth (South Africa). See Table 5.1 for the fitted model.

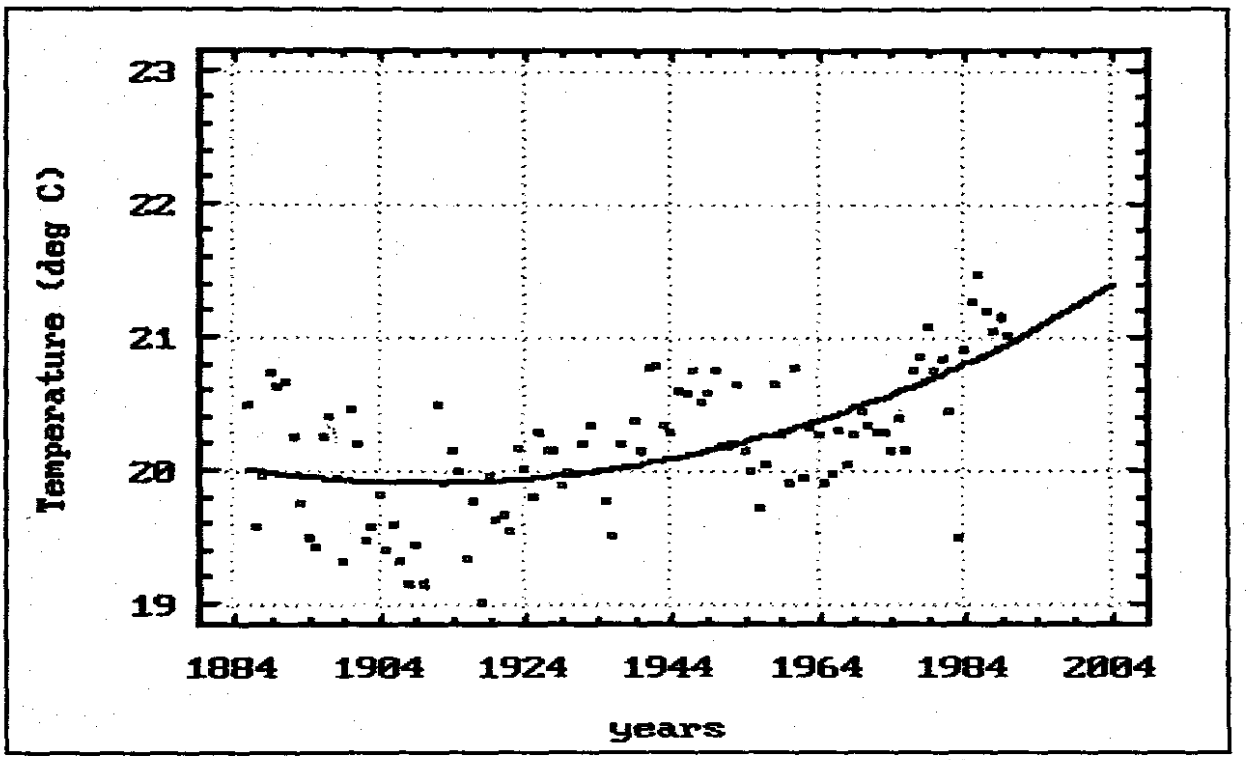

Figure 5.9: Annual surface air temperature trends for Durban (South Africa). See Table 5.1 for the fitted model.

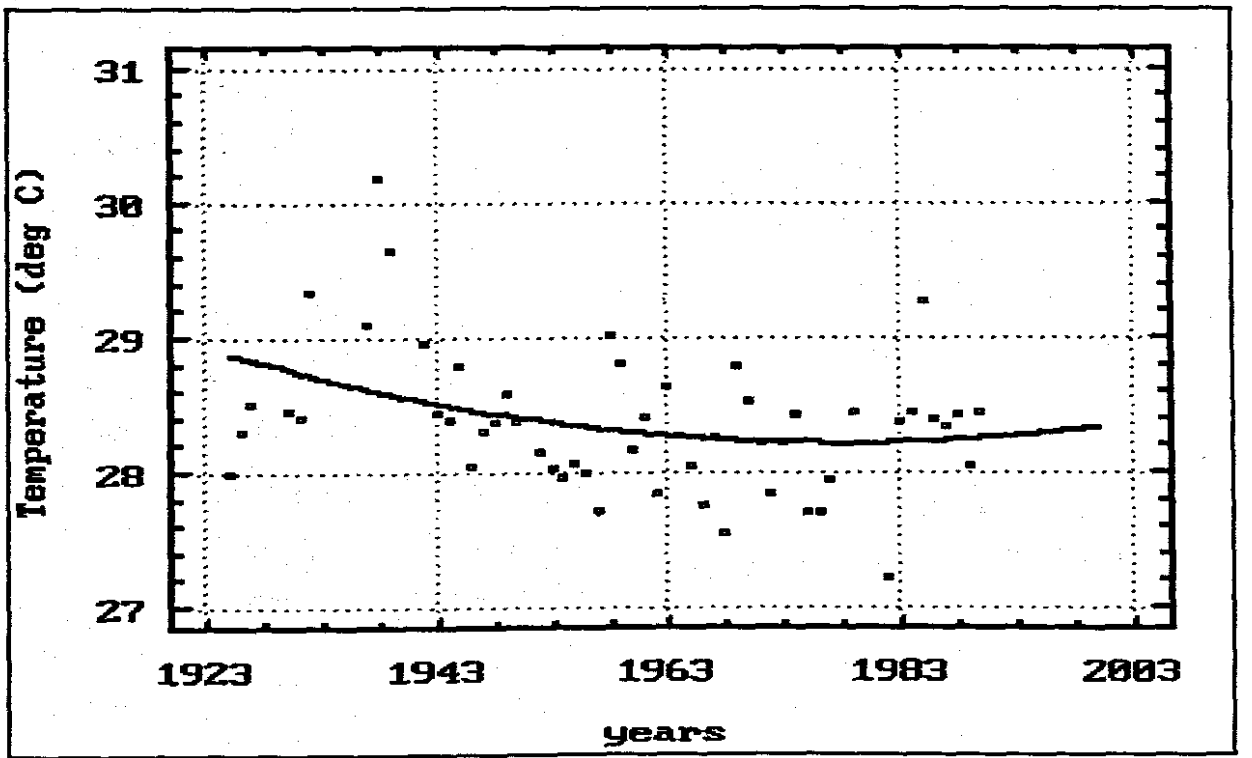

Figure 5.10: Annual surface air temperature trends for Ouagadougou (Upper Volta). See Table 5.1 for the fitted model.

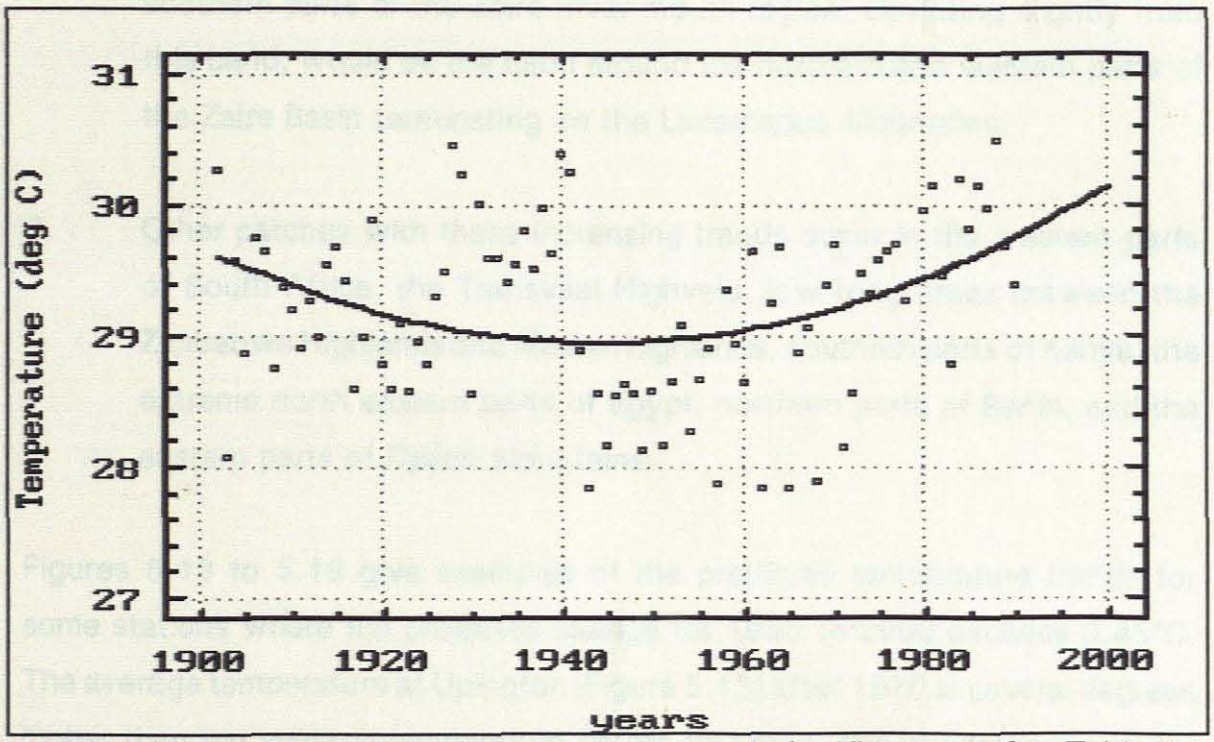

Figure 5.11: Annual surface air temperature trends for Khartoum. See Table 5.1 for the fitted model.

The predicted annual mean surface air temperature changes of between 0.46° to 1.45°C can be identified with (Figure 5.12):-

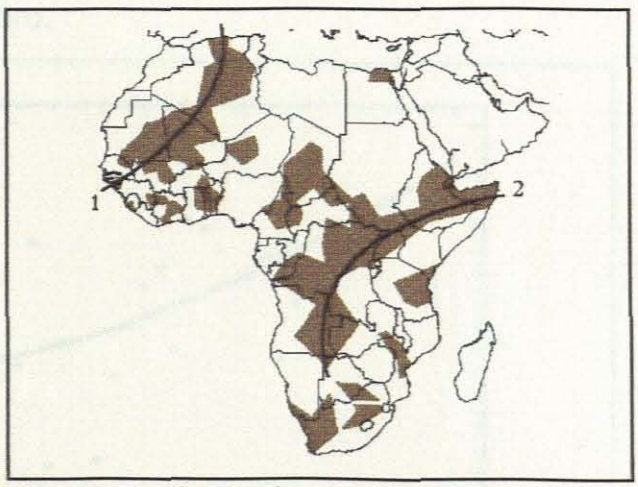

Figure 5.12: Regions with a temperature change of 0.46° to 1.45°C/decade.

1. the low lying areas between the Ahaggar Plateau and the Atlas Mountains through the Tademait Plateau and greater part of Mali to the northern parts of the Senegal Basin,

2. the high lying areas of Somalia and the greater part of Ethiopia and southerly along the western parts of the South Equatorial divide to the

southern parts of the Zaïre River mouth region. Deviating slightly from this band, would be the band around the northern and western parts of the Zaïre Basin terminating on the Ladamaqua Mountains.

3. Other patches with these increasing trends occur in the western parts of South Africa, the Transvaal Highveld, low lying areas between the Zimbabwe Highlands and Malawi highlands, southern parts of Kenya, the extreme north eastern parts of Egypt, northern parts of Benin, and the eastern parts of Djalon Mountains.

Figures 5.13 to 5.16 give examples of the predicted temperature trends for some stations where the projected change for 1990 to 2000 exceeds 0.45°C. The average temperature at Upington (Figure 5.13) after 1970 is several degrees higher than the average temperature before this date. The quadratic model for this station and for Man (Figure 5.14) show well defined increases during the indicated record. However, the increase for Beira (Figure 5.15) and El Golea (Figure 5.16) could easily be a result of one or two extreme values and these trends should probably be closer to zero.

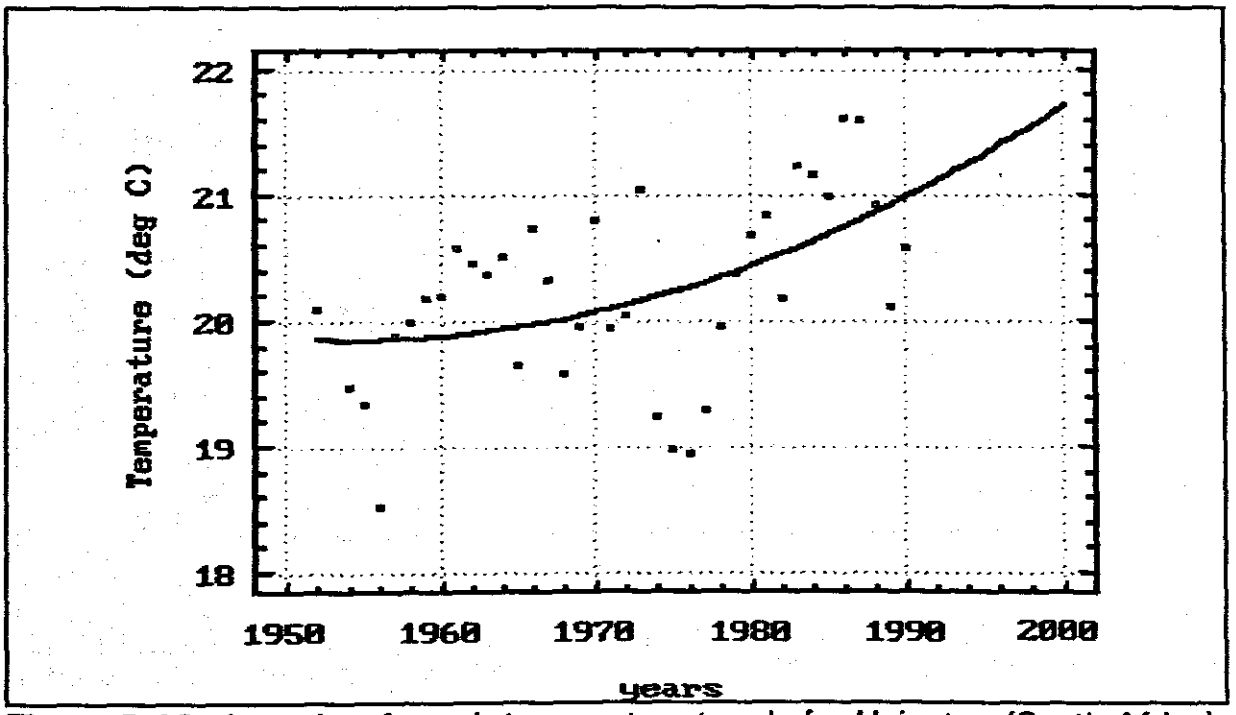

Figure 5.13: Annual surface air temperature trends for Upington (South Africa). See Table 5.1 for the fitted model.

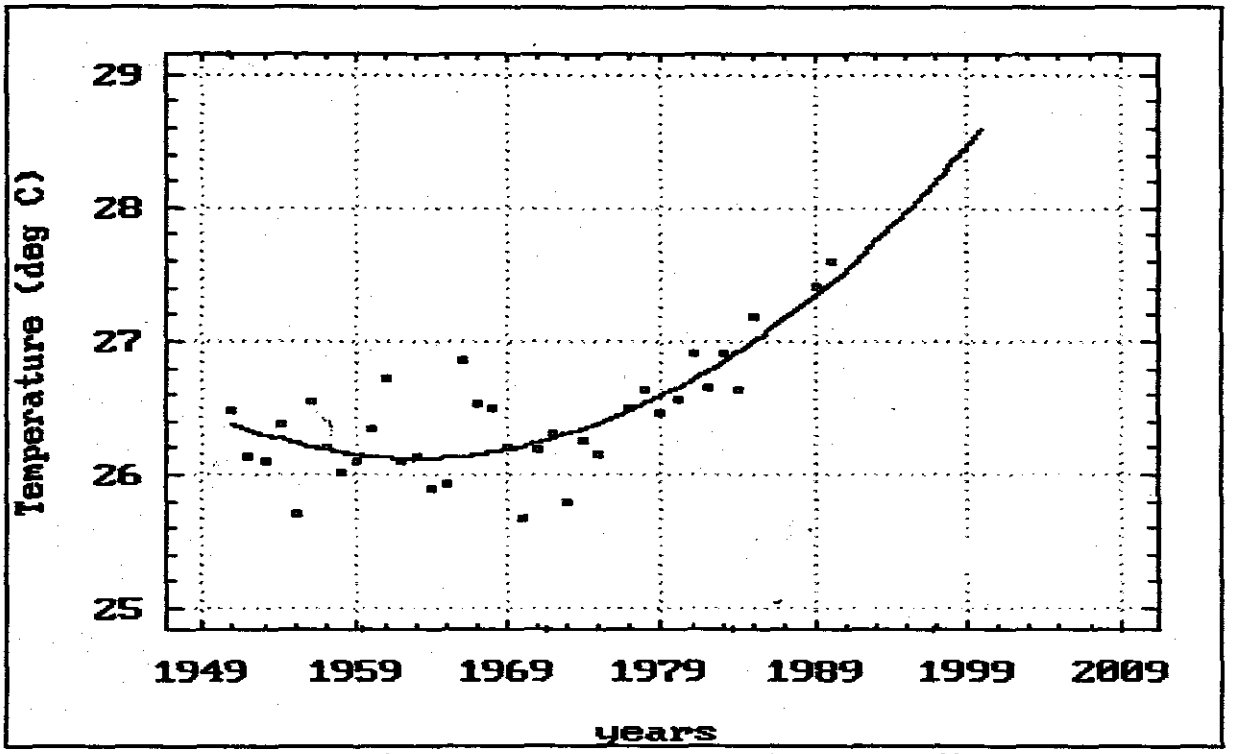

Figure 5.14: Annual surface air temperature trends for Wau (Sudan). See Table 5.1 for the fitted model.

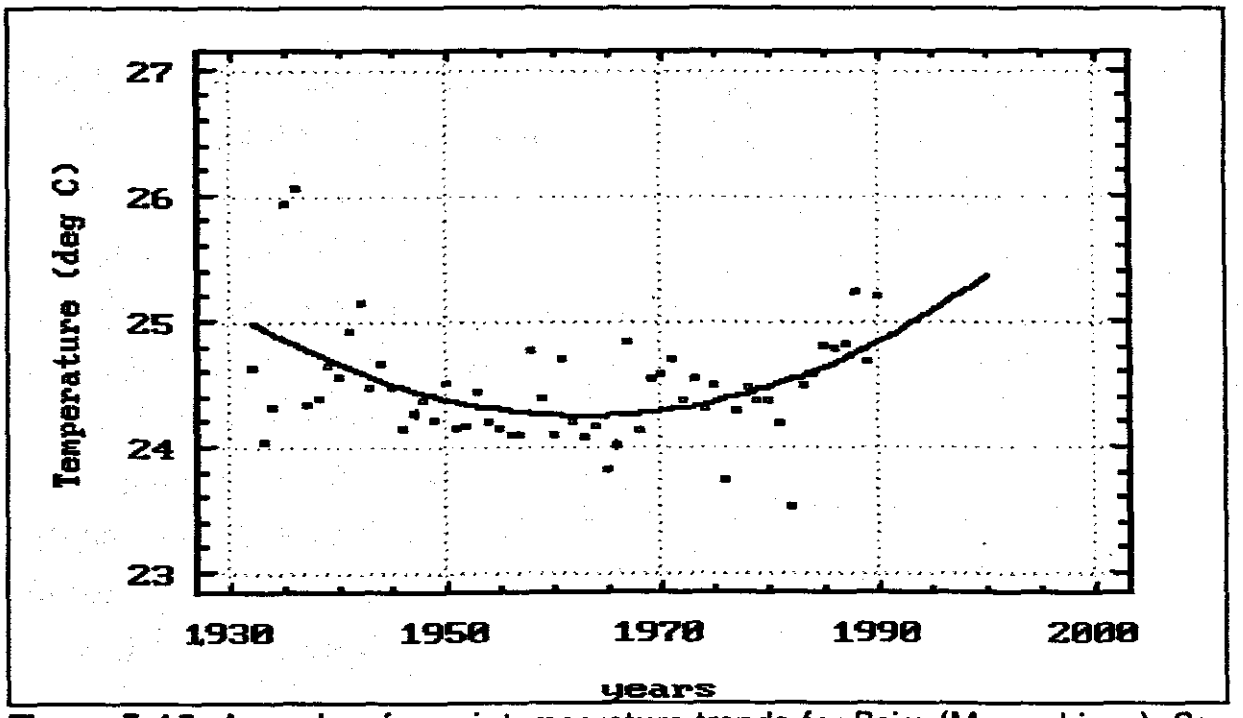

Figure 5.15: Annual surface air temperature trends for Beira (Mozambique). See Table 5.1 for the fitted model.

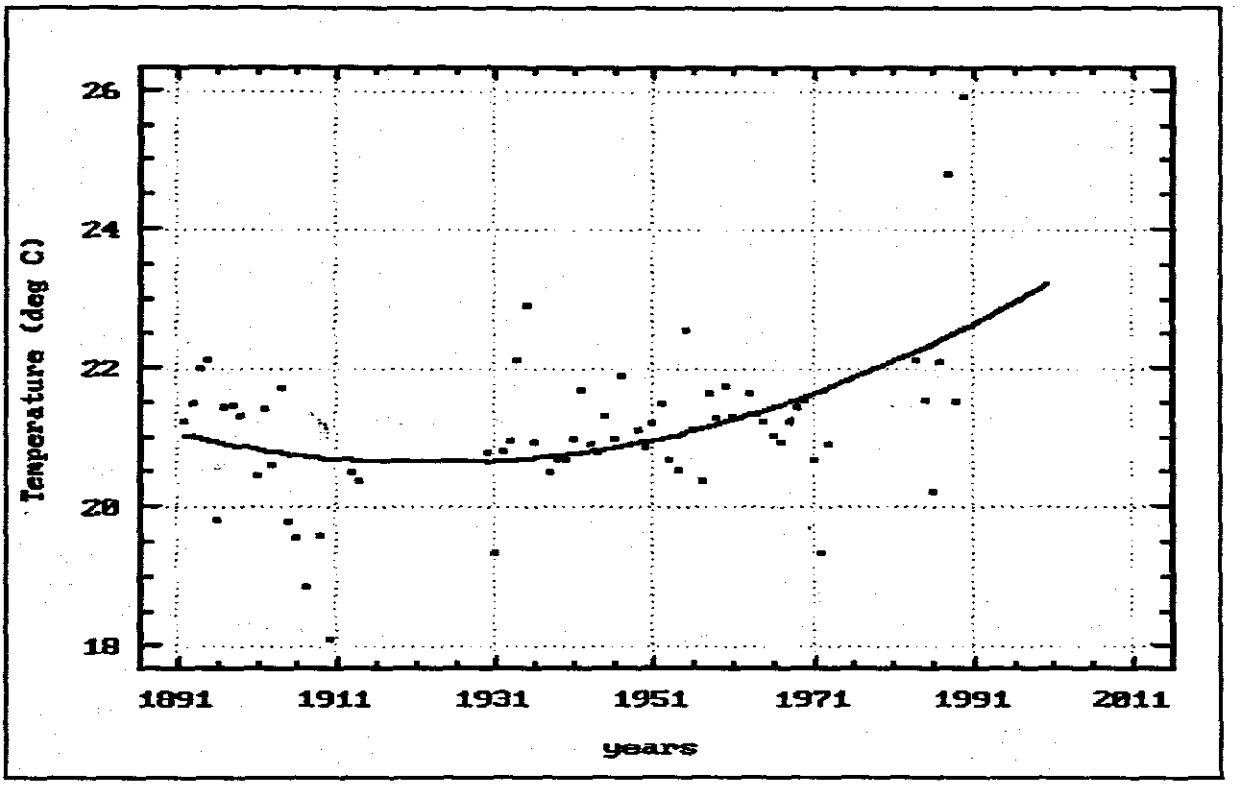

Figure 5.16: Annual surface air temperature trends for El Golea (Algeria). See Table 5.1 for the fitted model.

The predicted annual surface air temperature changes exceeding 1.46° occur in the high lying areas of Sudan, around El Fasher and Malakal (Figure 5.17). The graphical representations of predicted temperature trends for some selected stations are shown in Figures 5.18 and 5.19. The model fit for Malakal (Figure 5.18) is based on a short series of data which are experiencing considerable change where the series may be part of a cyclic trend. However, there is more confidence in the prediction for Elfasher (Figure 5.19).

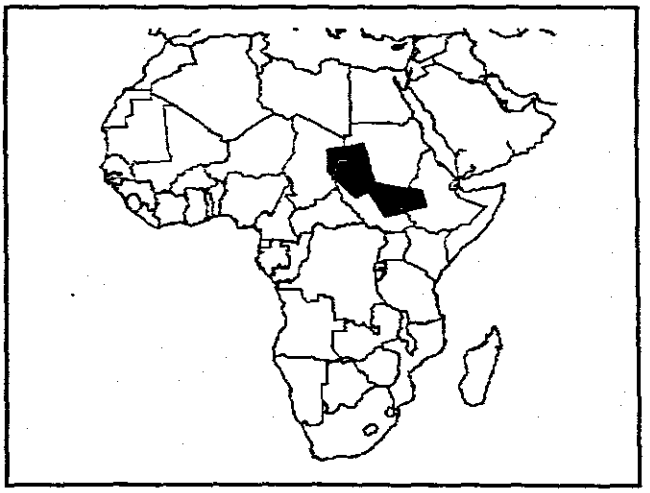

Figure 5.17: Regions with a predicted temperature change exceeding 1.45°C/decade.

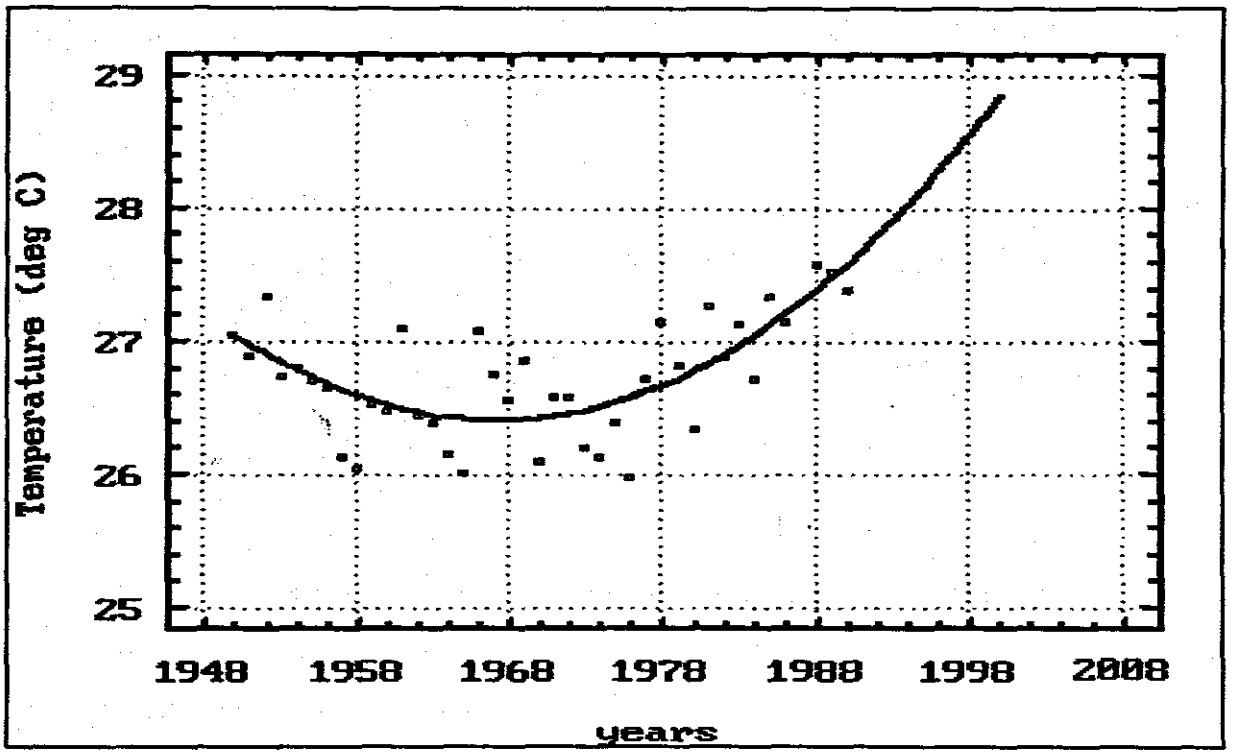

Figure 5.18: Annual surface air temperature trends fro Malakal (Sudan). See Table 5.1 for the fitted model.

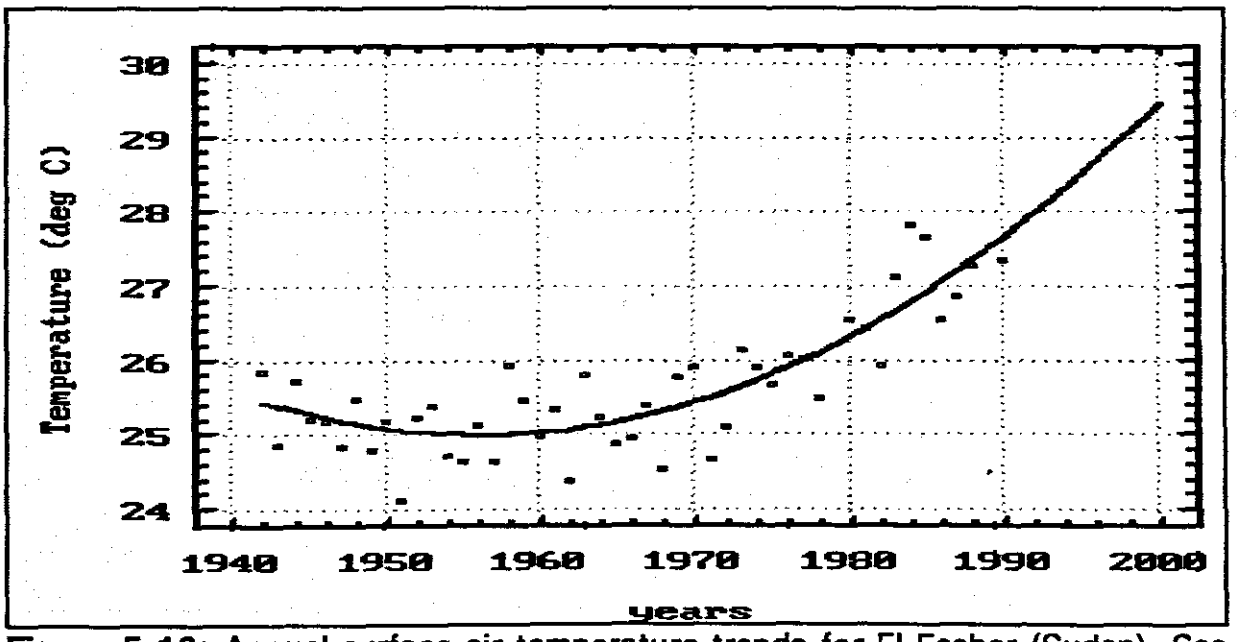

Figure 5.19: Annual surface air temperature trends for El Fasher (Sudan). See Table 5.1 for the fitted model.

5.4.2. SPATIAL PATTERNS OF PREDICTED DECREASING ANNUAL SURFACE AIR TEMPERATURE TRENDS

Of the 130 stations analysed in this study, 44 (34%) stations showed decreasing annual surface air temperature trends. These were classified into four categories:

1. -0.01° to -0.45°C, (half the interval of -0.45° to +0.45°C)
2. -0.46° to -1.45°C,
3. -1.46° to -2.45°C, and
4. -2.46° to -3.45°C.

The spatial pattern of these temperature trends is shown in Figure 5.20. The first category has the highest distribution on the continent because of its much greater frequency of 22% (Figure 5.2).

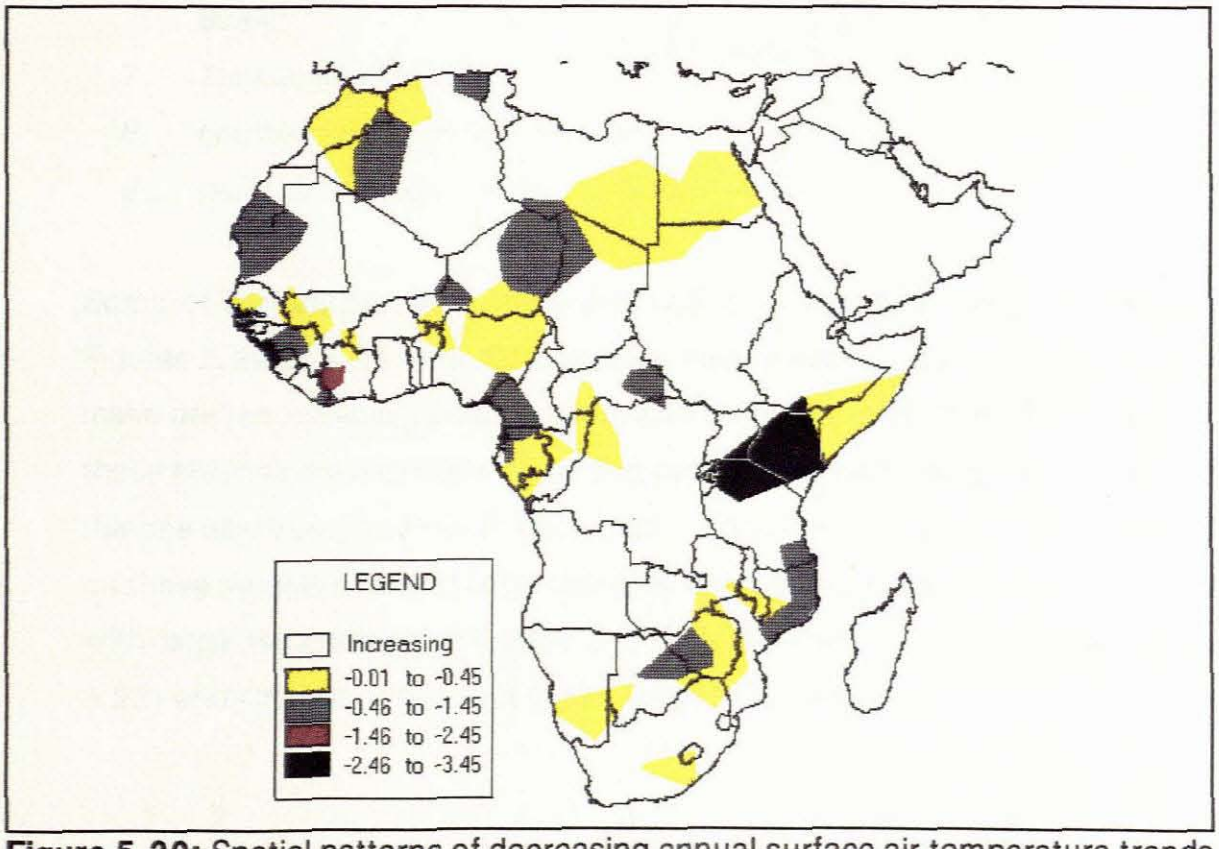

Figure 5.20: Spatial patterns of decreasing annual surface air temperature trends (°C/decade) for Africa.

The temperature trends between 0° and -0.45°C, shown in Figure 5.21, occupy the following areas:-

1. Egypt and the Libyan Desert;
2. sections of Atlas Mountains;
3. northern parts of Djalon Plateau;
4. Chad Basin;
5. Somalia and north-east Kenya;
6. lower lying parts of Zaïre Basin;
7. Zimbabwe Highlands;
8. southern parts of Namibia; and
9. parts of the Karoo region in South Africa.

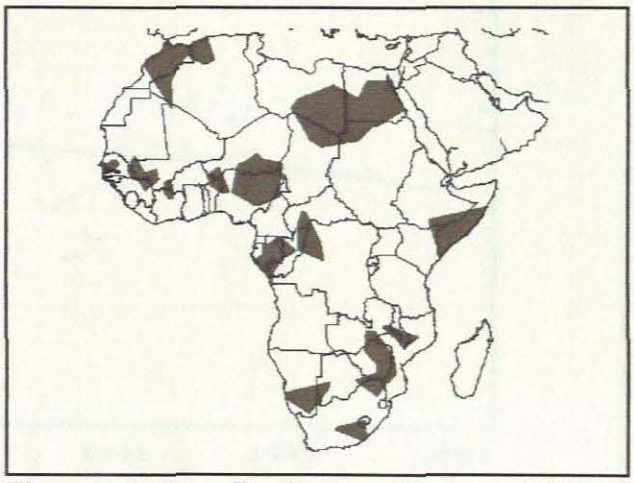

Figure 5.21: Regions with a predicted temperature change of 0° to -0.45°C/decade.

Some of the stations with these decreasing temperature trends are shown Figures 5.22 to 5.24. The data series in many cases is probably too short to make any acceptable extrapolations, and there is a probability that some of these stations are experiencing strong cyclic changes in temperature such as the one apparent for Oran (Figure 5.22). Consequently, extrapolation based on those models showing large changes is not appropriate. All those stations with large temperature decrease and high standard error, Chipinge (Figure 5.23) and Chileka (Figure 5.24) are suspect models.

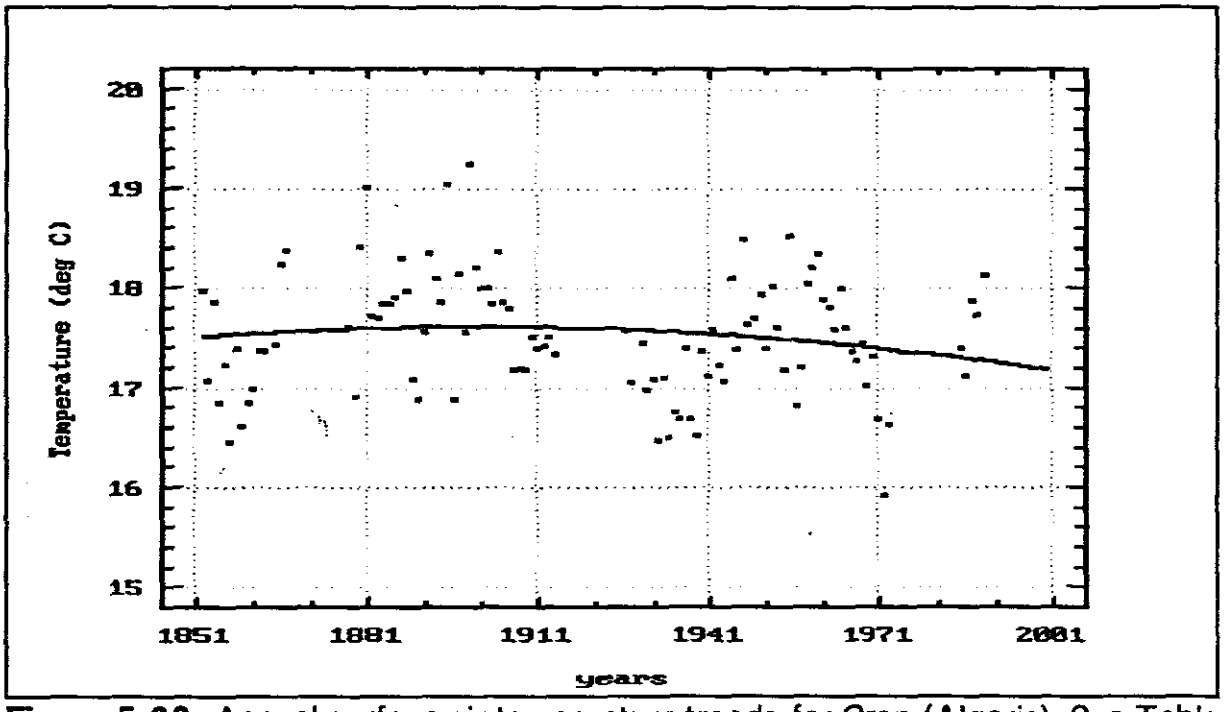

Figure 5.22: Annual surface air temperature trends for Oran (Algeria). See Table 5.1 for the fitted model.

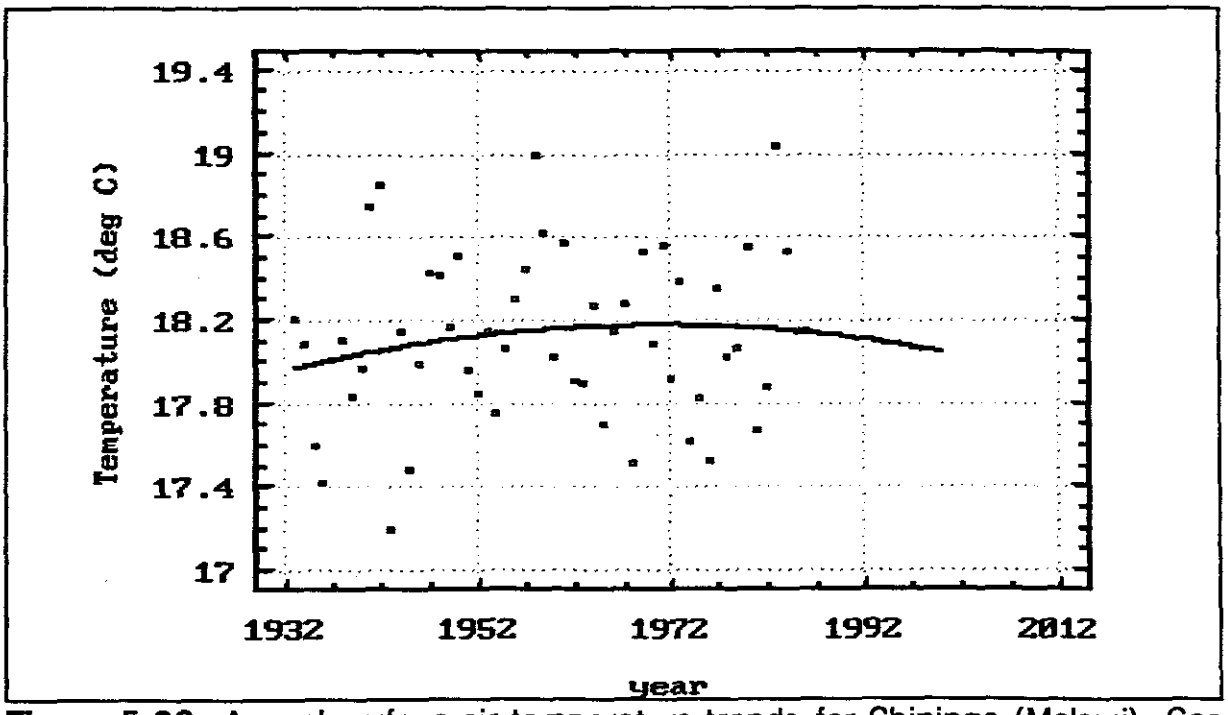

Figure 5.23: Annual surface air temperature trends for Chipinge (Malawi). See Table 5.1 for the fitted model.

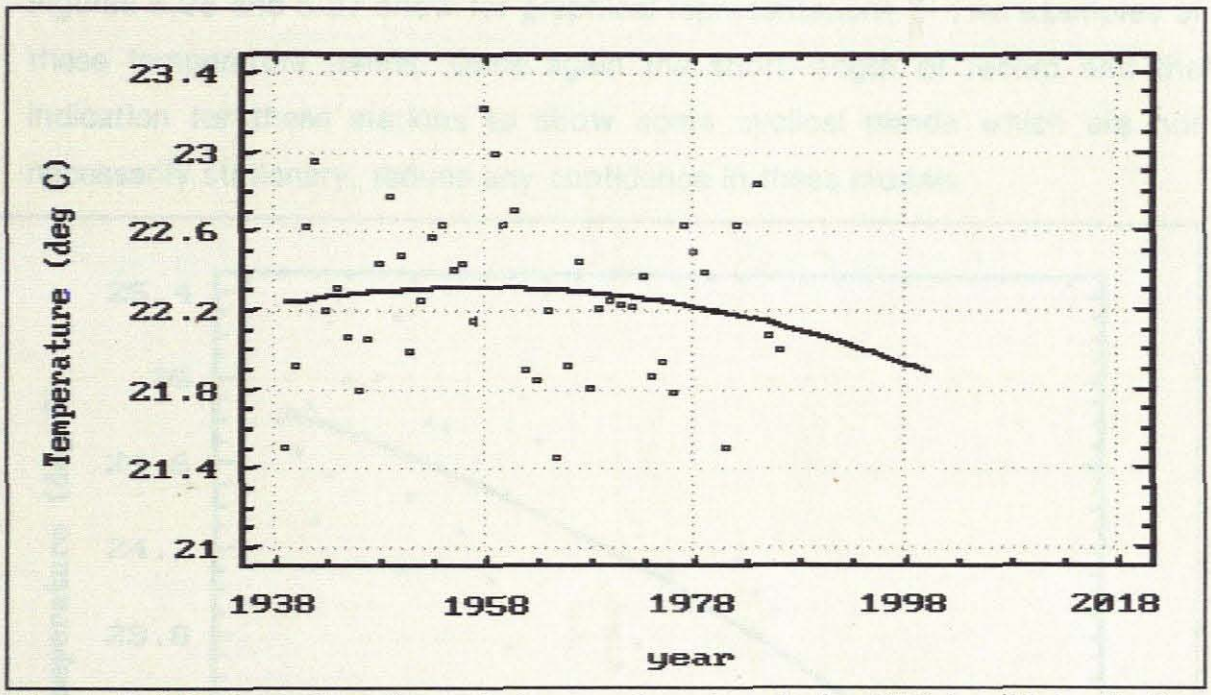

Figure 5.24: Annual surface air temperature trends for Chileka (Malawi). See Table 5.1 for the fitted model.

The predicted annual surface air temperature changes between -0.46° and -1.45°C (Figure 5.25) are found mainly in the following areas:-

1. Sections of Atlas Mountains,
2. east facing slopes of the Atlas Mountains,
3. western parts of Djalon Mountains;
4. Ladamaqua Mountains;
5. the Zimbabwe Highlands, and
6. the northern Mozambique coastal region.

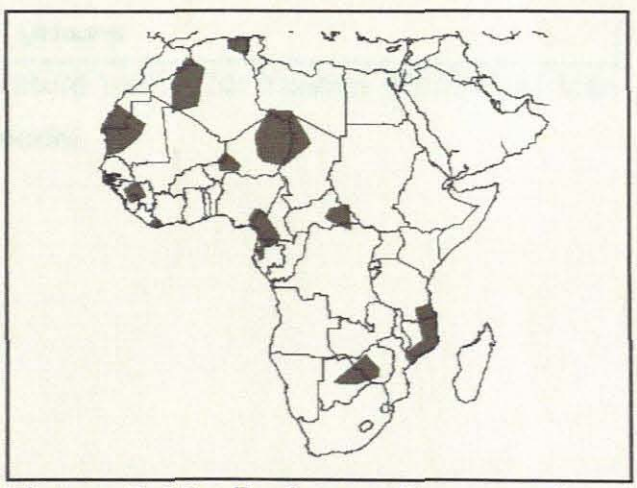

Figure 5.25: Regions with a predicted temperature change of -0.46° to -1.45°C/decade.

Figures 5.26 and 5.27 show for graphical representations of two examples of these temperature trends. Once again the short length of record and the indication for these stations to show some cyclical trends which are not necessarily stationary, reduce any confidence in these models.

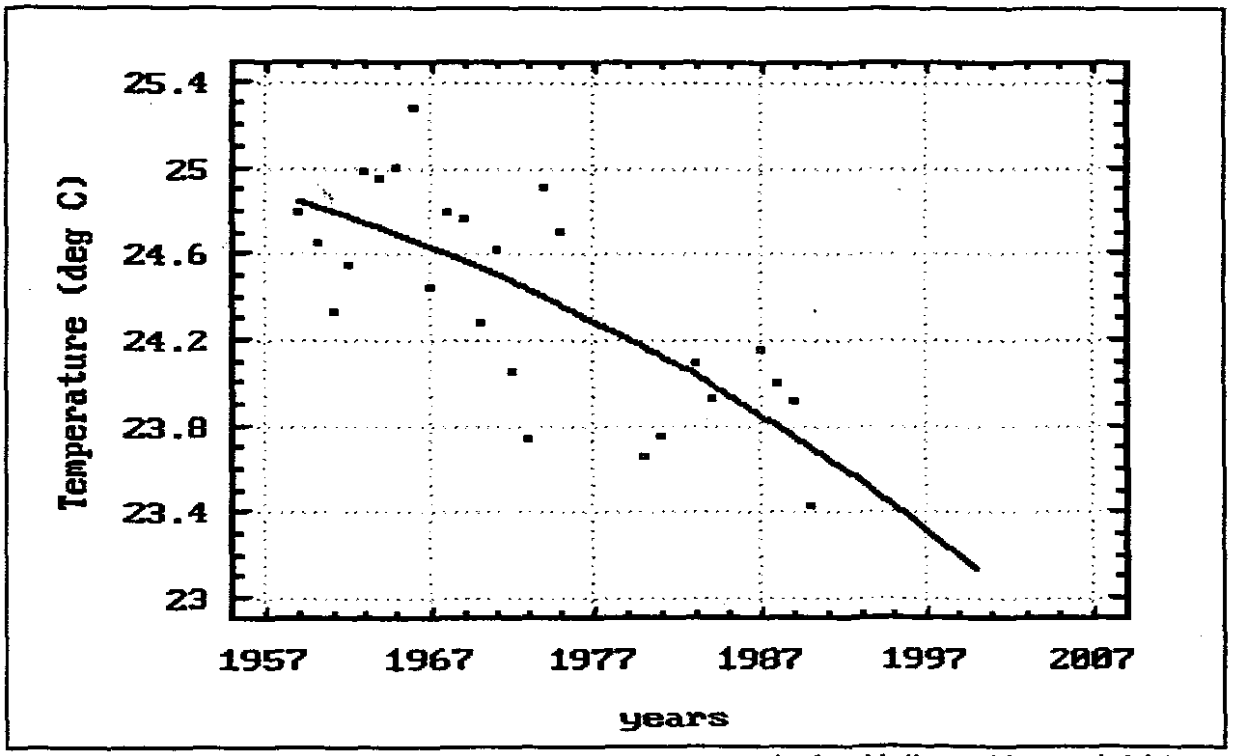

Figure 5.26: Annual surface air temperature trends for Yalinga (Central African Republic). See Table 5.1 for the fitted model.

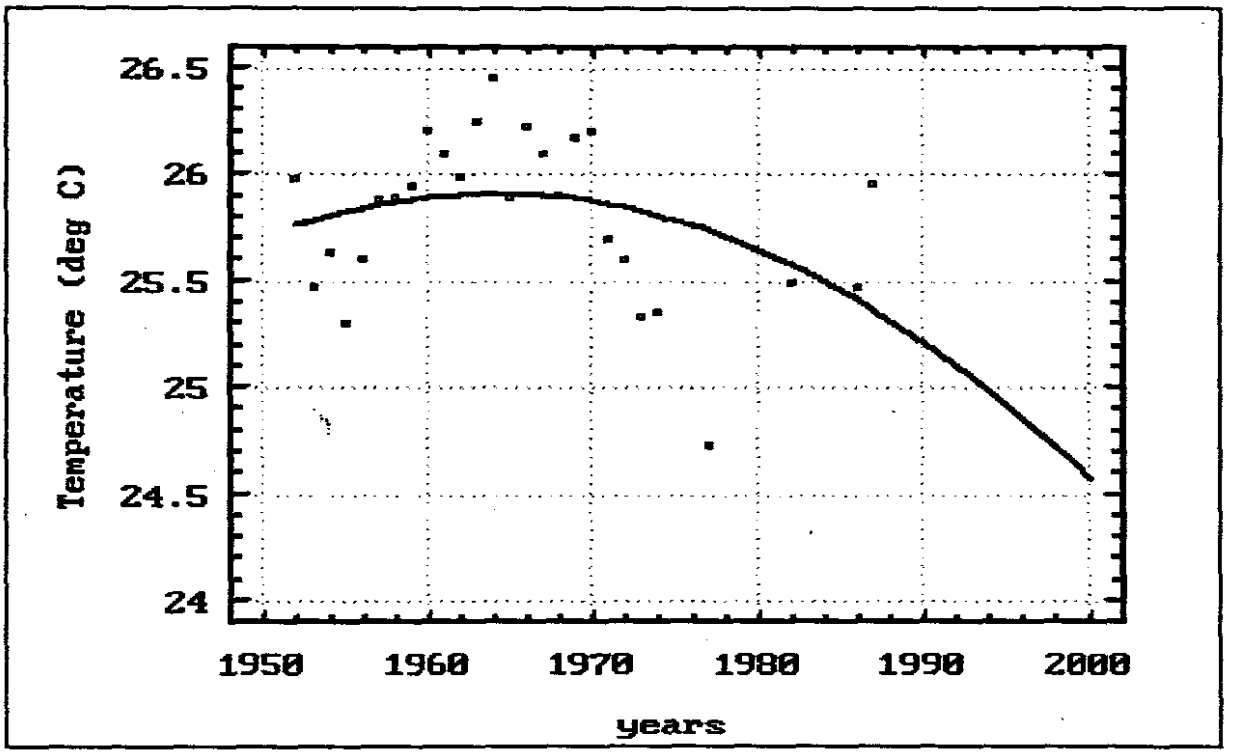

Figure 5.27: Annual surface air temperature trends for Lamberene (Gabon). See Table 5.1 for the fitted model.

The decreasing temperature trends between -1.46° and -2.45°C (Figure 5.28) manifest themselves on the south-east facing slopes of the coastal belt of Coute de Voire. Figure 5.29 shows the graphical representation of these temperature trends for Man. In this case, the quadratic extrapolation model used may be completely inadequate.

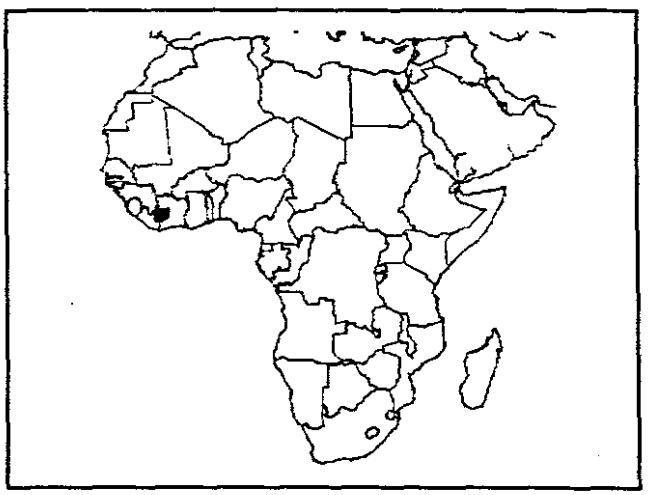

Figure 5.28: Regions with a predicted temperature change of -1.46° to -2.45°C/decade.

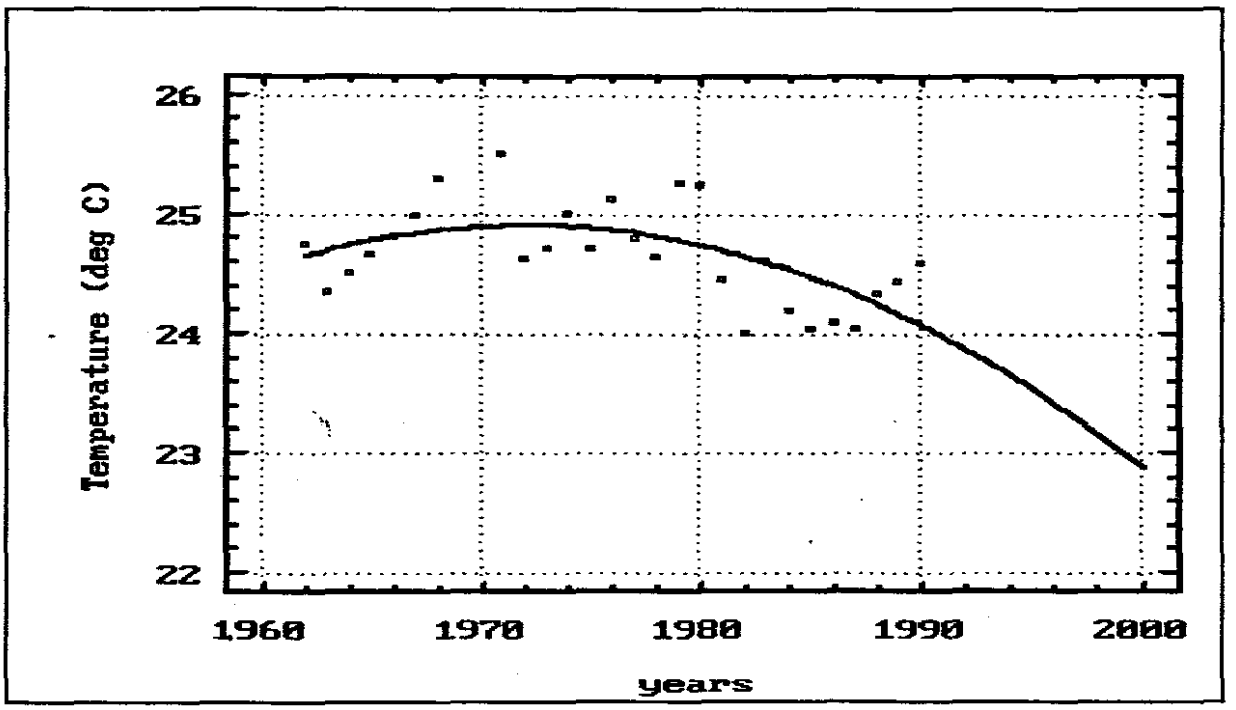

Figure 5.29: Annual surface air temperature trends for Man (Coute de Voire). See Table 5.1 for the fitted model.

5.5. CONCLUSION

The cyclic nature of long-term temperature patterns greatly influence linear prediction models of temperature which are derived from time-series data that are shorter in length than the period of the temperature cycle. Some models derived from short data records indicate models of extreme increasing (< 1.46°C) and decreasing (> -1.46°C) future temperature trends. It is reasonable to maintain that most regions of the African continent will not experience considerable temperature changes in the near future and that any significant change will conform to the range predicted by GCMs.

The relatively better geographical coverage of meteorological station networks in the northern sector of the continent increase the reliability in the spatial resolution of patterns in temperature change in this part of the continent. The sparsity of meteorological station network over the southern sector of the continent may cause doubts on the spatial generalisation from this sparse network.

CHAPTER 6

METEOROLOGICAL IMPLICATIONS OF RESULTS

6.1. INTRODUCTION

The analysis of the annual temperature changes indicate that most parts (58%) of the African main land will not experience considerable change (-0.45° to 0.45°C) in temperatures over the next decade. 52% and 48% of stations with this temperature range of changes show small decreasing and increasing temperature trends, respectively. However, 32% of the continent shows distinct temperature increases greater than 0.45°C/decade while 12% show a corresponding decreasing trend greater than -0.45°C/decade. If these trends are reliable models of climatic change, they should be associated with some meteorological forcing mechanisms. This section examines general features of the predicted temperature change with some meteorological features in an attempt to determine forcing mechanisms.

6.2. ASSOCIATION OF PREDICTED TEMPERATURE CHANGES WITH SOME OF THE PREDOMINANT METEOROLOGICAL FEATURES

The image of predicted temperature changes was compared with air mass movements and the characteristic position of fronts and convergence zones. The generalised air mass positions (Figure 6.1) for July was captured in IDRISI and rasterised as an image for direct correlation with the predicted temperature changes. IDRISI provides a linear correlation between corresponding pixels of two images. For the July air masses and temperature change model, the linear cross-correlation coefficient (r^2) was 0.52. This indicates that 52% of the variance of predicted temperature changes can be explained by the different air masses.

What is more apparent is the correspondence between the thermal convergence boundaries (forming zones of temperature and moisture discontinuity) and the

associated bands of surface air temperature change in Figure 6.2. Figure 6.1 and 6.2 illustrate the concurrence of the predicted temperature changes which occur along the zones of temperature and moisture discontinuity.

The relationship that exist between the July air mass movements boudaries and the spatial patterns of near future temperature changes is indicative of the influence of large scale atmospheric global circulation (AGC) on the long-term temperature changes over the African continent. Any changes on the AGC may import temperature changes over the region of influence through changes in the air masses themselves or by altering the extent or location of convergence zones. The AGC changes do not affect temperature only, but other meteorological variables. The question of which meteorological variable reacts or responds first to the AGC changes is a matter of great concern. These meteorological variables may also have a direct effect on temperature and *vice versa* through ocean-atmospheric feedback processes. Newell and Kidson (1984) found that warm temperatures with strong gradients on both sides of the Equator are maintained by large-scale subsidence in dry periods to the North of the Equator and to the South of the Equator in wet periods.

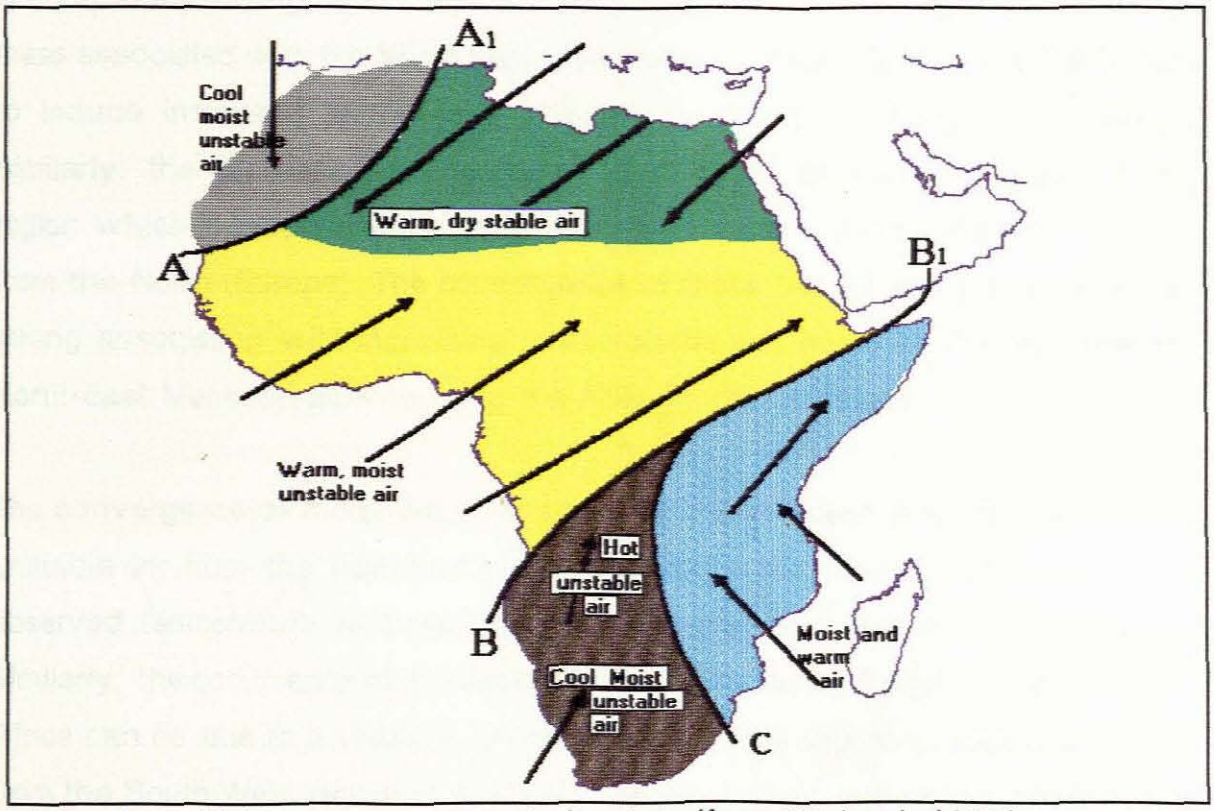

Figure 6.1: Air mass movements during July (from Pitchard, 1982)

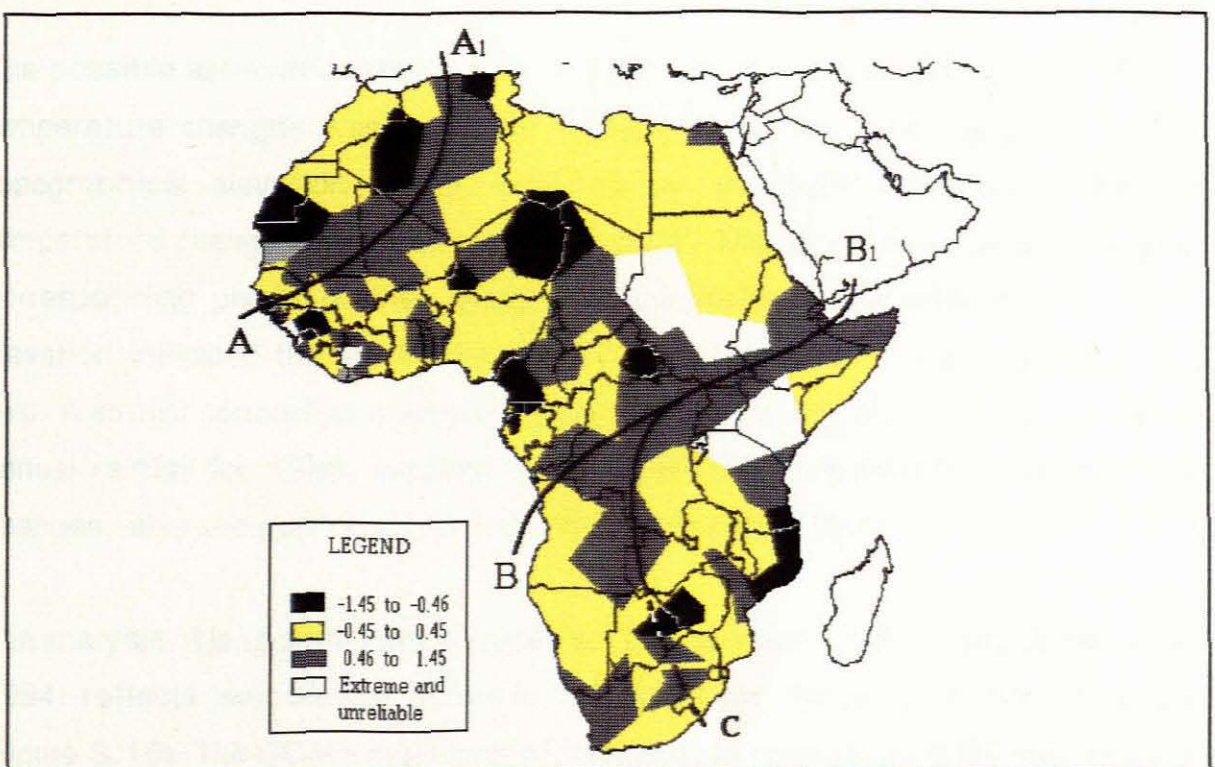

Figure 6.2: Temperature changes (°C/decade) in relation to zones of moisture discontinuity, AA_1, BB_1 and B_1C.

A comparison of Figure 6.1 and 6.2 may suggest that the warm dry stable air mass associated with the North-East Monsoon may invade further into the Sahara to induce increased temperature trends over the Central regions of Africa. Similarly, the decreasing temperature trends occur on the North-West (Atlas) region which is predominantly under the influence of the cool unstable air mass from the North (Europe). The convergence of these two air masses show a very strong association with increasing temperatures and could be due to increased North-East Monsoon activity along the Atlas Mountain ranges.

The convergence of moist warm air from the Indian Ocean and the warm moist unstable air from the Atlantic Ocean seem to be the causal factor behind the observed temperature increase along the Ethiopian and East African Highlands. Similarly, the occurrence of increasing temperature trends further south in central Africa can be due to a strong invasion of hot unstable and cool moist unstable air from the South-West region of Africa. Prolonged July air circulation patterns may greatly influence increasing temperature trends over the regions of influence.

The possible association that mountains and plateaux may have with predicted temperature changes was examined through linear correlation analysis of the topographical elevation image, supplied by the IGBP, and the predicted temperature change image derived in this study. The test of association between corresponding pixels of the images of predicted temperature changes and elevation indicated that no significant (30%) correlation (0.3) exist between the two. A similar correlation analysis between corresponding pixels of the images of annual rainfall for 1989, supplied by the IGBP, and the predicted temperature changes, also showed no significant (30%) correlation (0.2).

The analysis of long-term temperature data for the entire world coverage (Roberts, 1994) reflects temperature decrease in Africa over the recent historical period (Figure 3.10). The GCM simulations of temperature changes indicate temperature increase which ranges from 0.25° to 0.75°C/decade over the African continent (Figure 3.11). The predicted increasing temperature trends are confirmed in this

study for many regions. However, there are regions which experience decreasing temperature trends in contrast to the GCM predictions.

6.3. CONCLUSION

The association of predicted temperature changes with some of the predominant meteorological features, discussed in this chapter, is indicative of the influence that atmospheric global circulation have on the long-term temperature changes over the African continent. It must also be noted that reclassification of predicted temperature changes may produce a completely different spatial pattern which may have association with other meteorological features.

CHAPTER 7

CONCLUSIONS AND RECOMMENDATIONS

7.1. CONCLUSIONS

The results of this study have indicated that the surface air temperatures for most parts of the African continent will not change considerable (-0.45° to 0.45°C) by the year 2000. However, there are some areas where a temperature change greater than 0.46°C may occur. When considering the possible cyclic nature of climatic changes occurring or evident in data series, the validity of linear models predicting extreme temperature changes which have been noted from some stations with limited or short data records, must be viewed with extreme caution. Extrapolation over long term periods greater than the cyclic period is inappropriate.

This study has indicated that 66% of the African continent may experience increase in annual surface air temperatures, except for regions along the north western coast, the South Equatorial Divide, and the southern parts of Chad Basin through the Libyan desert to the Southern coast of Egypt. The increasing trend of surface air temperatures in most parts of the continent are evident in the analysis of palaeotemperature series from the Holocene time to the present.

The predicted temperature change which range from 0.45° to 1.45°C/decade was found related to the zones of moisture discontinuity (front zones) during July over the African continent. The bands of this range of temperture change, also identify with leeward sides of mountain ranges. The question of the magnitude of lee and frontal effects on these temperature changes, not accommodated in this study, is a challenge to all concerned.

7.2. RECOMMENDATIONS

* It is possible that the quadratic model is not the most appropriate despite the lower mean square error when compared to the linear model. Those stations with short records and large cyclic variability should be re-modelled with more appropriate harmonic functions to improve the general prediction. This could change the spatial pattern considerably and would therefore have a profound effect on this attempt to link changes with any forcing mechanisms.

* There are numerous other meteorological stations. An attempt to supplement the database would certainly help in spatial assessment of climatic change.

REFERENCES

ABRAHAMSON, D.E. 1989: *The Challenge of Global Warming.* California, Island Press.

BACH, W. CRANE, A.J., BEGER, A.L., AND LONGHETTO, A. 1983: *Carbon Dioxide: Current Views and Developments in Energy/Climate Research.* Boston, D. Reidel Publishing Co..

BLOOMFIELD, P. 1992: Trends in Global temperature. *Climatic Change,* Vol. 21 (1) 1-16.

BOLIN, B., DOOS, B.R., JAGER, J. AND WARRICK, R.A. (ed) 1989: *The greenhouse Effect, Climatic Change and Ecosystem.* Toronto, John Wiley and Sons.

BOYLE, S. AND ARDILL, J. 1989: *The Greenhouse Effect: A practical Guide to the World's Changing Climate (2nd).* London, New English Library.

CROSSON, P. 1989: Climatic change and mid-latitude Agriculture: Perspective on consequences and Policy responses. *Climatic change,* Vol.15, 51-73.

EASTMAN, R., KINEMAN, J., DODSON, R., LIVINGSTON, M., and AZIMI, N. 1990: *Global Change Database Project: Pilot Project for Africa.* Massachusetts, Clark University.

GLEIK, P.H. 1989: The Implications of Global Climatic Change for International Security. *Climatic Change,* Vol. 15 (1) 309-327.

GREGORY, S. (ed) 1988: *Recent Climatic Change.* London, Belhaven Press.

GRIFFITTS, J.F. (ed) 1972: *World Survey of Climatology Vol. 10: Climates of Africa.* Amsterdam, Elsevier Scientific Publishing Co..

HENDERSON-SELLERS, G AND McGUFFIE, K.A. 1988: *Climate Modelling Premier.* Toronto, John Wiley and Sons.

HEUSSER, C. J. 1989: Climate and Chronology of Antarctica and Adjacent South America over the past 30 000yr. *Palaeogeography, Palaeoclimatology and Palaeoecology,* Vol. 76, 31-37.

LAMB, H.H. 1985 (a): *Climate History and the Future.* Princeton, Princeton University Press.

LAMB, H.H. 1985 (b): *Climate, History and Modern World.* London, Methuen and Co. Ltd.

LAURMANN, J.A. 1989: Emissions Control and Reduction. *Climatic Change*, Vol. 15, 271-298.

LEE-THROP, J.A. AND BEAUMONT, P.B. 1990: Environmental Shifts in the last 20 000 years: Isotopic evidence from Equus Cave. *South African Journal of Science*, Vol. 86, 452-453.

LEGGETT, J. (ed) 1990: *Global Warming: The Greenpeace Report.* Oxford, Oxford University Press.

LEWIS, L.A. AND BERRY, L. 1988: *African Environments and Resources.* London, Unwin Hyman.

LEZINE, A. AND CASANOVA, J. 1989: Pollen and Hydrological evidence for the Interpretation of Past Climates in Tropical West Africa during the Holocene. *Quaternary Science Reviews*, Vol. 8, 45-55.

MABBUTT, J.A. 1989: Impacts of Carbon Dioxide Warming on Climate and Man in the Semi-Arid Tropics. *Climatic Change*, Vol. 15, 191-221.

McBOYLE, G. (ed) 1973: *Climate in Review.* Boston, Houghton Mifflin Co.

MAGUIRE, D.J. 1989: *Computers in Geography.* New York, Longman Scientific & Technical.

MONEY, D.C. 1988: *Climate and Environmental Systems.* London, Hayman Ltd.

NEWLL, R.E. AND KIDSON, J.W. 1984: African Mean Wind Changes between Sahelian Wet and Dry Periods. *Journal of Climatology*, Vol. 4, 27-33.

PARTRIDGE, T.C. 1990: Cainozoic Environmental Changes in Southern Africa. *South African Journal of Science*, Vol.86, 315-317.

PARTRIDGE, T.C. AVERY, D.M., BOTHA, G.A., BRINK, J.S., DEACON, J., HERBERT, R.S., MAUD, R.R., SCHOLTZ, A., TALMA, A.S., and VOGEL, J.C. 1990: Late Pleistocene and Holocene Climatic Change in Southern Africa. *South African Journal of Science*, Vol. 86, 302-306.

PETIT-MAIRE, N., COMMELIN, D., FABRE, J., and FONTUGNE, M. 1990: First Evidence for Holocene Rainfall in the Tanezrouft Hyperdesert

and its Margins. *Palaeogeography, Palaeoclimatology and Palaeoecology*, Vol. 79, 333-338.

PETIT-MAIRE, N., FOTUGNE, M. and ROULAND, C. 1991: Atmospheric Methane ratio and Environmental Changes in the Sahara and Sahel during the Last 130 kyrs. *Palaeogeography, Palaeoclimatology, and Palaeoecology*, Vol. 86,197-204.

PRESTON-WHYTE, R.A. and TYSON, P.D. 1988: *The Atmosphere and Weather of Southern Africa*. Oxford, Oxford University Press.

ROBERTS, N. (ed) 1994: *The changing global environment*. Oxford, Blackwell.

SCHULZE, R.E. 1990: Climate change and Hydrological response in Southern Africa: Heading towards the future. *South African Journal of Science*, Vol. 86, 373-381.

SCOTT, L. 1990: Environmental Changes Reflected by Pollen in some Holocene Sediments from Transvaal, South Africa, and Marion Island, Southern Ocean. *South African Journal of Science*, Vol. 86, 464-467.

SCOTT, L. AND VOGEL, J.C. 1983: Late Quaternary Pollen Profile from Transvaal Highveld, South Africa. *South African Journal of Science*, Vol. 79, 266-272.

SEBAGENZI, M.N., VASSEUR, G. and LOUIS, P. 1992: Recent Warming in Southern Zaire (Central Africa) Infered from Disturbed Geothermal gradients. *Palaeogeography, Palaeoclimatology Palaeoecology (Global and Planetary Change Section)*, Vol. 98, 209-217.

SINGER, S.F. (ed) 1989: *Global Climate Change: Human and Natural influences*. New York, Paragon House Publishers.

SIVAKUMAR, M.V.K. 1989: Climatic Change and Implications for Agriculture in Niger. *Climatic Change*, Vol. 20 (4), 297-312.

SOLOMON, S.I., BERAN, M. AND HOGG, W. (ed) 1987: *The influence of Climatic Change and Climatic Variability on the Hydrologic Regime and Water Resources*. Oxfordshire, IAHS Press.

THACKERAY, J.F. 1990: Temperature Indices from Late Quaternary Sequences in

South Africa: Comparison with the Vostock Core. *The South Africa Geographical Journal*, Vol. 72 (2), 47-49.

TIMBERLAKE, L. 1985: *Africa in Crisis: the causes, the cures of Environmental Bankruptcy*. London, International Institute for Environmental Development.

TYSON, P.D. 1990: Modelling Climatic Change in Southern Africa: a review of available methods. *South African Journal of Science*, Vol. 86, 318-330.

TYSON .P.D. 1991: Climatic Change in Southern Africa: Past and Present conditions and possible future scenarios. *Climatic Change*, Vol. 18, 240-257.

WARD, R.C. 1990: *Principles of Hydrology*. London, McGraw-Hill Book Company (UK) Ltd.

WENGLER, L. AND VERNET, J. 1992: Vegetation, Sedimentary deposits and Climates during the Late Pleistocene and Holocene in Eastern Moroco. *Palaeogeography, Palaeoclimatology, and Palaeoecology*, Vol. 94, 141-167.

WEISS, C. 1989 : Can Market Mechanism Ameliorate the Effects of Long-Term Climatic Change? *Climatic Change*, Vol. 15, 299-307.

WOODWELL, G.M. 1989: The Warming of the Industrialised Middle latitudes 1989 - 2050: Causes and Consequences. *Climatic Change*, Vol. 55, 31-50.

WORLD CLIMATE DISC, 1992: *Global Climate Change Data on CD-ROM*. Cambridge, Chadwyck-Healey Ltd.

WORLD METEOROLOGICAL ORGANISATION, 1983: *Guide to Climatological Practices*. Geneva, Secretatriat of the WMO.

WORLD METEOROLOGICAL ORGANISATION, 1987: *Water*. Geneva, Secretariat of the WMO.

VINCENS, A. 1991: Late Quaternary Vegetation History of the South Tanganyika Basin: Climatic Implications in South Central Africa. *Palaeogeography, Palaeoclimatology, and Palaeoecology*, Vol. 86, 207-226.